TIME-DEPENDENT DENSITY-MATRIX THEORY

By

Minzhuan Gong

A DISSERTATION

Submitted to
Michigan State University
in partial fulfillment of the requirements
for the Degree of

DOCTOR OF PHILOSOPHY

Department of Physics and Astronomy

1990

ABSTRACT

TIME-DEPENDENT DENSITY-MATRIX THEORY

By

Minzhuan Gong

An extended time-dependent Hartree-Fock theory (*TDHF*) is formulated from the BBGKY hierarchy of the equations of motion for density matrices. This theory, called time-dependent density-matrix theory (*TDDM*), consists of coupled equations for the two-body as well as one-body density-matrices. To make numerical calculation feasible, these density-matrices are expanded in a single particle basis which is the solution of a *TDHF* -like equation.

The small amplitude limit of *TDDM* is studied. It is found that *TDDM* reduces to the random phase approximation (*RPA*), second random phase approximation (*SRPA*) and shell model under different approximations. Thus the small amplitude limit of *TDDM* is more general than these existing theories.

TDDM is applied to the small amplitude isoscalar quadrupole motions of ^{16}O and ^{40}Ca. It is found that *TDDM* gives damping widths comparable to experimental data. It is also found that the higher-order correlations are essential to the damping of these isoscalar motions.

The fusion reaction of ^{16}O + ^{16}O is calculated in *TDDM* to study the fusion window problem found in *TDHF*. It is found that *TDDM* gives a threshold energy of 170 MeV for opening the non-fusion window. This energy is much higher than 54

MeV in *TDHF* and is consistent with experiments.

The mass fluctuations in damped reactions of $^{16}O + ^{16}O$ are also studied using *TDDM*. Since *TDDM* determines the time evolution of a two-body density-matrix it provides us with a microscopic way to calculate the fluctuations of one-body quantities. The results of the theory are compared with those obtained in a transport model. It is found that the dispersions in fragment mass calculated in the two models are of the same order of magnitude and much larger than those calculated in the time-dependent Hartree-Fock theory. The differences between the microscopic theory and the transport model are also discussed.

ACKNOWLEDGMENT

There are many people who deserve thanks for help and support during the course of this work and my graduate study. Here I can only list few of them.

I wish to thank my thesis adviser, Prof. Mitsuru Tohyama, for his guidance and help during the last two years of my graduate study. I wish to thank the rest of my guidance committee: Profs. George Bertsch, William Lynch, S. D. Mahanti and Joey Huston. I would like to thank Dr. David Mikolas, Andre Maul and Prof. Wolfgang Bauer for their help in preparing this thesis.

I would like to thank Prof. J. S. Kovacs for the help I received in my pursuit of graduate study in Michigan State University. Thanks are due to Prof. Laszlo Csernai for the help I get from him. I would like to thank Prof. Aurel Bulgac with whom I had many fruitful conversations. I would like to thank Liang Zhao, with whom I share an office for three years, for the help I received and many interesting discussions. Thanks are also due to Wenguang Gong, Dr. Yongsheng Li, Fan Zhu, Bao-an Li and many others for the help I get.

Finally, I would like to thank my wife, Shuang Li, for her love.

Contents

List of Tables

List of Figures

Chapter 1

Introduction

In physics, precisely solving the many-body problem is impossible if the number of constituents is larger than two. Therefore, many techniques have been developed to approximately solve the many-body system. In the one-body level, mean-field approximation has been found to be a good method if the interaction between constituents has certain structure. This method has been used in many areas of physics. For example, our solar system is assumed to move in a mean field generated by the Galaxy and mean-field approximation is used to treat the electron gas.

In nuclear physics, mean-field theories have been widely and successfully applied to various phenomena [Neg 82]. In these theories the nucleons are assumed to move freely within a mean field generated by the other nucleons. The validity of this assumption is based on the fact that the mean free path of nucleon is rather long. The long mean free path is due to the Pauli blocking effect.

Hartree theory was first used to treat the electrons in atoms [Har 27]. After taking into account the antisymmetrization of electron wave function, this theory becomes the Hartree-Fock theory [Foc 30]. The Hartree-Fock (*HF*) theory using the Skyrme-type interaction [Vau 72] is found to be quite successful in reproducing the nuclear ground-state properties such as radius and binding energy. In the mean-field theories the occupation probabilities of single particle states are unity below the Fermi level

and zero above it. However, recent experimental data show that this picture of nuclear ground states is too naive; It is found that the occupation number for level near the Fermi energy is about 0.7 [Pap 89]. To explain this fractional occupation, one has to go beyond the mean-field theory, i.e. to include the effects of nucleon correlations.

The extension of *HF* to time-dependent problem is the time-dependent Hartree-Fock theory (*TDHF*). This theory has extensively been applied to the deep-inelastic heavy-ion collisions (*DIC*) and fusion reactions [Dav 85]. It is found that expectation values of quantities which are of one-body nature, such as the dissipation of translational energy and deflection angle, are well reproduced. However, *TDHF* fails to give fluctuations of one-body observables. It is believed that this defect of *TDHF* is caused by its single Slater determinant assumption. *TDHF* is a one-body theory which is inappropriate for calculating two-body quantities. Futhermore, the application of *TDHF* is limited to low-energy collisions. This is because the *NN* collision effects, neglected in *TDHF*, become more important as the incident energy increases.

TDHF has also been applied to small amplitude collective motions in two ways. The first method is to evolve the system according to the *TDHF* equation [Blo 79]. The second method is to use random phase approximation (*RPA*), which has been shown to be the small amplitude limit of *TDHF* [Ber 75]. In both cases, the centroid energies of giant resonances are well predicted but their damping widths are not produced.

From the above discussions it is clear that to get a realistic description of dissipation and fluctuation in nuclear phenomena, we must go beyond the *TDHF*. Thus, the extension of *TDHF* is a basic problem in nuclear physics. Much work has been done in this direction [Goe 82].

The efforts to extend the *TDHF* at present are divided into two main categories: the first is to improve the mean field theory itself and the second is to incorporate the

NN collision effects into the mean field. The work by Balian and Vénéroni [Bal 81] belongs into the first category. They proposed a variational method which optimizes the size of fluctuation for one-body operators. Numerical calculations [Mar 85, Bon 85] based on this method show that the fluctuations are much larger than those given in *TDHF*. In this category also fall the framework of a mean-field theory proposed by Griffin et al [Gri 80] and theory by other authors [Kle 80, Alh 81]. These theories aim at calculating the reaction S-matrix in the mean-field approximation.

In the second category, many theories have been formulated to incorporate the *NN* collision effects into the mean-field. In Refs. [Ayi 80, Gra 81, Buc 83, Rei 84, Nem 86] quantum statistical methods are used to derived the collision term. In Refs. [Orl 79, Won 78, Won 79, Toh 85] Green function method [Kad 62] is used. A formalism based on the time-dependent density-matrix (*TDDM*) has also been proposed by Wang and Cassing [Wan 85].

Although many models have been proposed to include the *NN* collision effects, because of numerical difficulties only a few applications have been made (except numerical simulations based on semi-classical models [Ber 84] which incorporate the *NN* collisions into mean-field). Köhler [Goe 82] used a relaxation time method to simulate the *NN* collision effects. Wong and Davies [Won 80, Won 83] applied an extended *TDHF* derived from Green's function formalism to the fusion and intermediate energy heavy-ion reactions. Their results, however, are quite unphysical as will be discussed in Chapt. 5. Therefore, there exits a gap between the theoretical formulation of extended *TDHF* and its real understanding. More realistic applications of extended *TDHF* are needed.

In this work we formulate an extended *TDHF* using the time-dependent density-matrix formalism [Wan 85]. The main ingredient of this formalism is the BBGKY hierarchy [Bog 68]. It can be shown that truncation of this hierarchy at the two-body density-matrix level gives *TDHF* [Wan 85]. Therefore, it provides us a con-

venient way to include the higher-order terms. We derive our model by truncating BBGKY hierarchy at the level of three-body density-matrix. We call it time-dependent density-matrix theory (*TDDM*). In *TDDM*, the two-body density-matrix is expressed as the sum of an antisymmetrized product of one-body density-matrices and a correlation function. The two-body correlation function as well as one-body density-matrix are expanded with finite number of single particle orbits; the coefficients are called the two-body correlation matrix and the one-body occupation matrix respectively. *TDDM* consists of three equations: an equation of motion for occupation matrix; an equation of motion for two-body correlation matrix and a *TDHF* -like equation providing the single particle orbits. The equation for single particle orbit is a *TDHF* -like equation in the sense that the density which appears in the self-consistent potential now depends on the time-dependent occupation matrix. We study the small amplitude limit of *TDDM* and compare it with other existing small amplitude theories like *RPA*, second *RPA* and the interacting shell model. In this way we explore the physical meaning of the coupled equations for the occupation matrix and correlation matrix. Two applications of *TDDM* are made. The first is to the isoscalar quadrupole motion, the second is to the fusion and deep-inelastic heavy-ion collisions. In these calculations the Skyrme-type interaction is used. In the first application, we focus on the damping of isoscalar quadrupole motion and compare *TDDM* results with those of *TDHF*. In the second one, we investigate the small impact parameter non-fusion threshold energy of heavy-ion reactions and the mass dispersion of deep-inelastic heavy-ion collisions. Since *TDDM* calculates the two-body density-matrix explicitly, it is an appropriate model to calculate the fluctuations of one-body quantities. We compare the mass dispersion calculated in *TDDM* with those calculated in *TDHF*. We also compare *TDDM* results with those given by a transport model [Ran 78, Ran 79, Ran 82] and discuss the differences between them.

This thesis is organized as follows. In chapter 2 we derive our model from the time-dependent density-matrix theory. In chapter 3 the small amplitude limit of this theory is derived and compared with other theories of small amplitude motion. *TDDM* is applied to the problem of isoscalar in chapter 4, and to heavy-ion reactions in chapter 5. A summary of this work, followed by a discussion of its limitations and potential extensions are given in the final chapter.

Chapter 2

Time dependent density-matrix formalism

In this chapter we briefly present the time-dependent density-matrix formalism. We then derive the model used in this work from this formalism.

2.1 Density-matrix description of many-body systems

We consider a closed N-body fermion system whose hamiltonian is as follows,

$$H = \sum_{i=1}^{N} h_0(i) + \sum_{i<j}^{N} v(ij) \tag{2.1}$$

where $h_0(i)$ is the kinetic energy of the ith particle and $v(ij)$ is a two-body interaction. The time evolution of the system is completely described by the total wave function $|\Psi(t)>$ which satisfies the time-dependent Schrödinger equation

$$i\hbar\frac{\partial}{\partial t}|\Psi(t)>= H|\Psi(t)> . \tag{2.2}$$

To solve this Schrödinger equation for $|\Psi(t)>$ is impossible except for some few-body systems. In most cases it is also not necessary to do so since $|\Psi(t)>$ contains more information than we need. There are many ways to separate out the quantities which are of interest without solving the Schrödinger equation completely. Here we present

a time-dependent density-matrix formalism [Wan 85] which provides a truncation scheme to separate out the density-matrices of different ranks.

We start with the N-body density-matrix defined as

$$\rho_N(t) = |\Psi(t) >< \Psi(t)|. \tag{2.3}$$

The time development of this density-matrix is given by the von Neumann equation

$$i\hbar\dot{\rho}_N = [H, \rho_N], \tag{2.4}$$

which is equivalent to Eq. 2.2. It is convenient to define the reduced density-matrix

$$\rho_n(1,\ldots,n;1',\ldots,n',t) = \frac{1}{(N-n)!} Tr_{(n+1,\ldots,N)}\rho_N, \tag{2.5}$$

where $Tr_{(n+1,\ldots,N)}$ is the trace over particles $n+1,\ldots,N$. The numbers "$1,\ldots,n$" used as arguments mean particle coordinates. ρ_n thus defined is symmetric with respect to any exchange of pairs (ii') and (jj') and antisymmetric with respect to any exchange of i' and j'. The equations of motion for these reduced density-matrices can be deduced from Eq. 2.4. The resulting equations form a set of coupled equations: [Bog 68]

$$\begin{aligned}
i\hbar\dot{\rho}_1 &= [h_0, \rho_1] + Tr_{(2)}\{[v, \rho_2]\}, \\
i\hbar\dot{\rho}_2 &= \left[\sum_{i=1}^{2} h_0(i), \rho_2\right] + [v, \rho_2] + Tr_{(3)}\left\{\left[\sum_{i=1}^{2} v(i3), \rho_3\right]\right\}, \\
&\vdots \\
i\hbar\dot{\rho}_n &= \left[\sum_{i=1}^{n} h_0(i), \rho_n\right] + \left[\sum_{j>i}^{n-1} v(ij), \rho_n\right] \\
&\quad + Tr_{(n+1)}\left\{\left[\sum_{i=1}^{n} v(i, n+1), \rho_{n+1}\right]\right\}, \\
&\vdots
\end{aligned} \tag{2.6}$$

This set of coupled equations is called the *BBGKY hierarchy* (named after Born, Bogoliubov, Green, Kirkwood and Yvon).

These coupled equations are fully equivalent to equation 2.4 and therefore can not be easily solved either. In order to solve equation 2.6, it must be truncated at a certain level. In practice one keeps only the first few reduced density-matrices, usually the one-body and two-body density-matrices. In this work we follow the truncation scheme proposed by Wang and Cassing [Wan 85]. They separate the reduced density-matrix into correlated and uncorrelated terms,

$$\rho_2 = AS_{(2)}(\rho\rho) + c_2, \tag{2.7}$$

$$\rho_3 = AS_{(3)}(\rho\rho\rho + \rho c_2) + c_3, \tag{2.8}$$

and generally

$$\rho_n = AS_{(n)} \sum_{p=1}^{n-1} \rho_{n-p} c_p + c_n. \tag{2.9}$$

In the above equations c_n is called the n-body *correlation function* and $c_1 = \rho_1 = \rho$. The operator S symmetrizes a product of density matrices with respect to exchange of all pair indices (ii') and (jj') whereas A antisymmetrizes it with respect to exchange of single indices i' and j'. The subscript (n) indicates that the operations are carried out among n particles. The n-body correlation c_n has the same symmetry properties as ρ_n. Using the identity [Wan 85]

$$\rho_n - c_n = AS_{(n)} \sum_{p=1}^{n-1} \rho_{n-p} c_p = AS_{(n)} \sum_{p=1}^{n-1} \rho_{n-p} \rho_p, \tag{2.10}$$

Wang and Cassing [Wan 85] derived the equation of motion for the correlation functions from Eq. 2.6. For later use we list the first two equations:

$$\begin{aligned} i\hbar\dot{\rho}(11') = & [h_0(1) - h_0(1')]\rho(11') \\ & + Tr_{(2)}\{[v(12) - v(1'2')][\rho(11')\rho(22') \\ & - \rho(12')\rho(21') + c_2(12, 1'2')]\}_{2=2'}, \end{aligned} \tag{2.11}$$

$$
\begin{aligned}
i\hbar\dot{c}_2(12,1'2') \;=\; & [h_0(1)+h_0(2)-h_0(1')-h_0(2')]c_2(12,1'2') \\
& +[v(12)-v(1'2')]c_2(12,1'2') \\
& +[v(12)-v(1'2')][\rho(11')\rho(22')-\rho(12')\rho(21')] \\
& -Tr_{(3)}\{[v(13)-v(1'3')]\rho(11')\rho(23')\rho(32') \\
& +[v(23)-v(2'3')]\rho(13')\rho(22')\rho(31') \\
& -[v(13)-v(2'3')]\rho(12')\rho(23')\rho(31') \\
& -[v(23)-v(1'3')]\rho(13')\rho(21')\rho(32') \\
& -[v(13)-v(1'3')][\rho(11')c_2(23,2'3')+\rho(33')c_2(12,1'2') \\
& \qquad -\rho(13')c_2(23,2'1')-\rho(23')c_2(13,1'2') \\
& \qquad -\rho(31')c_2(12,3'2')-\rho(32')c_2(12,1'3')] \\
& -[v(23)-v(2'3')][\rho(22')c_2(13,1'3')+\rho(33')c_2(12,1'2') \\
& \qquad -\rho(13')c_2(23,2'1')-\rho(23')c_2(13,1'2') \\
& \qquad -\rho(31')c_2(12,3'2')-\rho(32')c_2(12,1'3')] \\
& +[v(13)-v(2'3')]\rho(12')c_2(23,1'3') \\
& +[v(23)-v(1'3')]\rho(21')c_2(13,2'3')\}_{3=3'} \\
& +Tr_{(3)}\{[\sum_{i=1}^{2}v(i3),c_3]\}. \qquad (2.12)
\end{aligned}
$$

In the above equation the time dependences of ρ, c_2 and c_3 are implicit. Wang and Cassing suggested truncating this hierarchy by neglecting the 3-body correlation function. The resulting equations, Eq. 2.11 and Eq. 2.12 without the last term, form a closed set of equations for ρ and c_2. It will be shown later that this truncation scheme preserves principal conservation laws such as energy and momentum conservation. In general, truncation at the level of three-body correlation is compatible with the conservation laws for two-body quantities as was discussed by Wang and Cassing.

In the following sections we will discuss a further reduction of Eqs. 2.11 and 2.12 and clarify the physical meaning of the truncation by comparing it with other existing

theories.

2.2 Time dependent Hartree-Fock theory

In this section we show that the time-dependent Hartree-Fock theory (*TDHF*) can be obtained from a further truncation of the density-matrix hierarchy i.e.

$$c_2 = c_3 = \ldots = 0. \tag{2.13}$$

We get a closed equation for the single-particle density-matrix

$$\begin{aligned} i\hbar\dot{\rho}(11') &= [h_0(1) - h_0(1')]\rho(11') \\ &\quad + Tr_{(2)}\{[v(12) - v(1'2)][\rho(11')\rho(22) - \rho(12)\rho(21')]\}. \end{aligned} \tag{2.14}$$

This equation can be written as

$$i\hbar\dot{\rho} - [h, \rho] = 0, \tag{2.15}$$

where

$$h = -\frac{\hbar^2\nabla^2}{2m} + U[\rho] \tag{2.16}$$

and

$$U[\rho]\rho(11') = \int d2\, v(12)[\rho(2,2)\rho(1,1') - \rho(1,2)\rho(2,1')]. \tag{2.17}$$

Eq. 2.15 is the *TDHF* expressed using the density-matrix.

2.3 Time dependent density-matrix theory

In this section we will present the framework of the model which is used in this thesis. We call this model "time-dependent density-matrix theory" (*TDDM*). Because of the limit of computer capability it is impractical to solve the coupled equations 2.11 and 2.12 in the three-dimension coordinate space. Therefore, we expand ρ and c_2 using a truncated single-particle basis $\{\psi_\lambda\}$. A convenient basis is the solution of

a *TDHF* -like equation. That is to say that the differential equation for the s.p. wave function has the same form as that of *TDHF* but the one-body density-matrix used to calculate the mean-field is that of *TDDM*. The one-body density-matrix and two-body correlation function are expanded as

$$\rho(11') = \sum_{\alpha,\beta} n_{\alpha\beta}\psi_\alpha(1)\psi^*_\beta(1'), \tag{2.18}$$

$$c_2(12,1'2') = \sum_{\alpha\beta\alpha'\beta'} C_{\alpha\beta\alpha'\beta'}\psi_\alpha(1)\psi_\beta(2)\psi^*_{\alpha'}(1')\psi^*_{\beta'}(2'). \tag{2.19}$$

Here we call $n_{\alpha\beta}$ the occupation matrix and $C_{\alpha\beta\alpha'\beta'}$ the correlation matrix. In the above equations all the quantities are time-dependent.

Due to the symmetry properties of ρ and c_2, $n_{\alpha\beta}$ and $C_{\alpha\beta\alpha'\beta'}$ satisfy

$$n_{\alpha\beta} = n^*_{\beta\alpha}. \tag{2.20}$$

$$C_{\alpha\beta\alpha'\beta'} = C_{\beta\alpha\beta'\alpha'} = C^*_{\alpha'\beta'\alpha\beta} = -C_{\alpha\beta\beta'\alpha'}. \tag{2.21}$$

The time evolution of n and C is determined from the equation of motions for ρ and c_2, i.e. Eq. 2.11 and 2.12,

$$i\hbar\dot{n}_{\alpha\beta} = \sum_{\gamma\delta\sigma}\{C_{\gamma\delta\beta\sigma} < \alpha\sigma|v|\gamma\delta > -C_{\alpha\delta\gamma\sigma} < \gamma\sigma|v|\beta\delta >\}, \tag{2.22}$$

and

$$i\hbar\dot{C}_{\alpha\beta\alpha'\beta'} = B_{\alpha\beta\alpha'\beta'}(t) + H_{\alpha\beta\alpha'\beta'}(t) + P_{\alpha\beta\alpha'\beta'}(t), \tag{2.23}$$

where

$$\begin{aligned} B_{\alpha\beta\alpha'\beta'} = & \sum_{\lambda_1\lambda_2\lambda_3\lambda_4} < \lambda_1\lambda_2|v|\lambda_3\lambda_4 >_A \\ & \{(\delta_{\alpha\lambda_1} - n_{\alpha\lambda_1})(\delta_{\beta\lambda_2} - n_{\beta\lambda_2})n_{\lambda_3\alpha'}n_{\lambda_4\beta'} \\ & -n_{\alpha\lambda_1}n_{\beta\lambda_2}(\delta_{\lambda_3\alpha'} - n_{\lambda_3\alpha'})(\delta_{\lambda_4\beta'} - n_{\lambda_4\beta'})\}, \end{aligned} \tag{2.24}$$

$$
\begin{aligned}
H_{\alpha\beta\alpha'\beta'} \;=\; & \sum_{\lambda_1\lambda_2\lambda_3\lambda_4} < \lambda_1\lambda_2|v|\lambda_3\lambda_4 > \\
& \{\delta_{\alpha\lambda_1}(n_{\lambda_3\alpha'}C_{\beta\lambda_4\beta'\lambda_2} - n_{\lambda_3\beta'}C_{\beta\lambda_4\alpha'\lambda_2} \\
& \quad - n_{\lambda_4\alpha'}C_{\lambda_3\beta\lambda_2\beta'} - n_{\lambda_4\beta'}C_{\lambda_3\beta\alpha'\lambda_2}) \\
& +\delta_{\beta\lambda_2}(n_{\lambda_4\beta'}C_{\alpha\lambda_3\alpha'\lambda_1} - n_{\lambda_4\alpha'}C_{\alpha\lambda_3\beta'\lambda_1} \\
& \quad - n_{\lambda_3\beta'}C_{\alpha\lambda_4\alpha'\lambda_1} - n_{\lambda_3\alpha'}C_{\alpha\lambda_4\lambda_1\beta'}) \\
& -\delta_{\lambda_3\alpha'}(n_{\alpha\lambda_1}C_{\beta\lambda_4\beta'\lambda_2} - n_{\beta\lambda_1}C_{\alpha\lambda_4\beta'\lambda_2} \\
& \quad - n_{\alpha\lambda_2}C_{\beta\lambda_4\beta'\lambda_1} - n_{\beta\lambda_2}C_{\alpha\lambda_4\lambda_1\beta'}) \\
& -\delta_{\lambda_4\beta'}(n_{\beta\lambda_2}C_{\alpha\lambda_3\alpha'\lambda_1} - n_{\alpha\lambda_2}C_{\beta\lambda_3\alpha'\lambda_1} \\
& \quad - n_{\beta\lambda_1}C_{\alpha\lambda_3\alpha'\lambda_2} - n_{\alpha\lambda_1}C_{\beta\lambda_3\lambda_2\alpha'})\}, \qquad (2.25)
\end{aligned}
$$

$$
\begin{aligned}
P_{\alpha\beta\alpha'\beta'} \;=\; & \sum_{\lambda_1\lambda_2\lambda_3\lambda_4} < \lambda_1\lambda_2|v|\lambda_3\lambda_4 > \\
& \{\delta_{\alpha\lambda_1}\delta_{\beta\lambda_2}C_{\lambda_3\lambda_4\alpha'\beta'} - C_{\alpha\beta\lambda_1\lambda_2}\delta_{\lambda_3\alpha'}\delta_{\lambda_4\beta'} \\
& -\delta_{\alpha\lambda_1}n_{\beta\lambda_2}C_{\lambda_3\lambda_4\alpha'\beta'} - \delta_{\beta\lambda_2}n_{\alpha\lambda_1}C_{\lambda_4\lambda_3\beta'\alpha'} \\
& +\delta_{\lambda_3\alpha'}n_{\lambda_4\beta'}C_{\alpha\beta\lambda_1\lambda_2} + \delta_{\lambda_4\beta'}n_{\lambda_3\alpha'}C_{\alpha\beta\lambda_1\lambda_2}\}. \qquad (2.26)
\end{aligned}
$$

In Eq. 2.24 "A" means that the matrix element of the two-body interaction is antisymmetrized. In perturbative expansion with respect to v, B is the first-order particle-particle (p-p) interaction (Born term), H the higher-order particle-hole (p-h) interaction and P the higher-order p-p interaction. In Fig. 2.1, typical diagrams from each term are shown. In the following section we will show that the basic conservation rules are conserved in *TDDM*.

2.4 Conservation laws

A general discussion of the consistency between truncation and conservation laws is given by Wang and Cassing [Wan 85], which expresses the density-matrix in coordinate space. Here we show that the *TDDM* equations also conserve the total number

$B_{\alpha\beta\alpha'\beta'}$:(Born term, first-order p-p correlation)

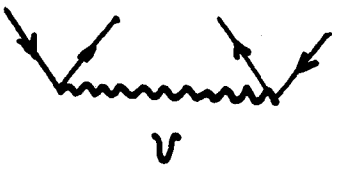

$P_{\alpha\beta\alpha'\beta'}$:(higher-order p-p correlation)

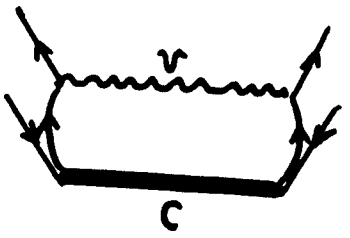

$H_{\alpha\beta\alpha'\beta'}$:(higher-order p-h correlation)

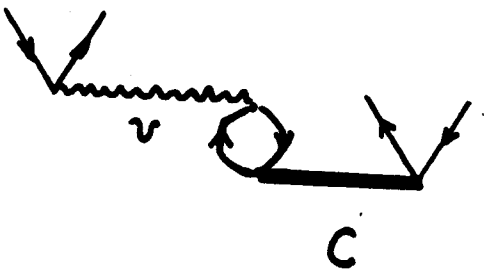

Figure 2.1: Typical diagrams in each term of Eq. 2.23; the wavy lines are interactions and the thick lines are two-body correlations.

of particles, total momentum and energy.

2.4.1 Particle number conservation

The total particle number N is given by

$$N = Tr[\rho(11')]_{1=1'} = \sum_{\lambda} n_{\lambda\lambda}. \tag{2.27}$$

From equation 2.22 we have the time derivative of N

$$\frac{dN}{dt} = \frac{1}{i\hbar} \sum_{\alpha\beta\gamma\lambda} \{C_{\alpha\beta\gamma\lambda} < \lambda\gamma|v|\alpha\beta > -C_{\lambda\beta\alpha\gamma} < \alpha\gamma|v|\lambda\beta >\} = 0. \tag{2.28}$$

Thus the total particle number is conserved.

2.4.2 Momentum conservation

The linear momentum for an A-body system is given by

$$\mathbf{P} = \frac{1}{A!} Tr(\hat{\rho}_A \hat{p}). \tag{2.29}$$

Because momentum $\hat{p}$ is a one-body operator the above equation reduces to

$$\mathbf{P} = Tr(\rho\hat{p}) = \sum_{\lambda\lambda'} n_{\lambda\lambda'} < \lambda'|\hat{p}|\lambda > . \tag{2.30}$$

The time derivative of $\mathbf{P}$ is

$$\frac{d\mathbf{P}}{dt} = \frac{i}{\hbar} \sum_{\lambda\lambda'} n_{\lambda\lambda'} < \lambda'|[h, \hat{p}]|\lambda > + \sum_{\lambda\lambda'} \dot{n}_{\lambda\lambda'} < \lambda'|\hat{p}|\lambda >, \tag{2.31}$$

where h is the mean field hamiltonian. The first term in the above equation can be written as

$$\frac{i}{\hbar} \sum_{\lambda\lambda'} n_{\lambda\lambda'} < \lambda'|[h, \hat{p}]|\lambda >= -\int d1d2 \{[\rho(11)\rho(22) - \rho(12)\rho(21)]\nabla_1 v(12)\}, \tag{2.32}$$

where ∇_1 means that differential operator only acts on $\mathbf{r_1}$. It is easy to see by exchanging the integral variables that if the two-body potential only depends on the

relative coordinate then the integral vanishes. Inserting Eq. 2.22 into the second term of Eq. 2.31 and using the completeness of single particle basis and relation 2.21, the second term reads

$$\begin{aligned}\sum_{\lambda\lambda'} \dot{n}_{\lambda\lambda'} < \lambda'|\hat{p}|\lambda > &= \frac{1}{i\hbar}\sum_{\alpha\beta\gamma\delta} C_{\alpha\beta\gamma\delta} < \gamma\delta|[-i\hbar\nabla_1, v(12)]|\alpha\beta >, \\ &= -\int d1d2\ c(12,12)[\nabla_1 v(12)].\end{aligned}$$

Again we can apply the same argument as above to this equation and show the integral vanishes, therefore the total linear momentum is conserved.

2.4.3 Energy conservation

The total energy can be expressed as

$$E = \frac{1}{A!}Tr[\rho_A H] = Tr[\rho t] + \frac{1}{2}Tr[\rho_2 v]. \tag{2.33}$$

We divide this equation into two parts: one contains the correlation function only and the other has the form of the Hartree-Fock energy. We call them correlation energy and Hartree-Fock energy, respectively. Eq. 2.33 can be written as

$$E = E_{HF} + E_{corr}. \tag{2.34}$$

The expressions for E_{HF} and E_{corr} are as follows:

$$\begin{aligned}E_{HF} &= Tr(\hat{\rho}\hat{t}) + \frac{1}{2}Tr[AS(\rho\rho)v] \\ &= \sum_{\lambda\lambda'}\{< \lambda'|\hat{t}|\lambda > + \frac{1}{2} < \lambda'|U(\rho)|\lambda >\} n_{\lambda\lambda'}; \qquad (2.35) \\ E_{cor} &= \frac{1}{2}Tr(vc_2) \\ &= \frac{1}{2}\sum_{\alpha\beta\gamma\delta} C_{\alpha\beta\gamma\delta} < \gamma\delta|v|\alpha\beta > . \qquad (2.36)\end{aligned}$$

With Eq. 2.22, the time derivative of E_{HF} is

$$\begin{aligned}\dot{E}_{HF} &= \sum_{\lambda\lambda'}\frac{1}{i\hbar}\{<\lambda'|[\hat{t},h]|\lambda> + \frac{1}{2}<\lambda'|[U[\rho],h]|\lambda>\}n_{\lambda\lambda'} \\ &+\frac{1}{2}\sum_{\lambda\lambda'}<\lambda'|\dot{U}[\rho]|\lambda> n_{\lambda\lambda'} \\ &+\sum_{\lambda\lambda'}\{<\lambda'|\hat{t}|\lambda> + \frac{1}{2}<\lambda'|U[\rho]|\lambda>\}\dot{n}_{\lambda\lambda'} \\ &= \sum_{\lambda\lambda'}\epsilon_{\lambda\lambda'}\dot{n}_{\lambda'\lambda}, \end{aligned} \tag{2.37}$$

where $\epsilon_{\lambda\lambda'} =< \lambda|h|\lambda' >$ and $h = \hat{t} + U[\rho]$. The time derivative of E_{corr} is

$$\dot{E}_{corr} = \frac{1}{2}\sum_{\alpha\beta\gamma\delta}\dot{C}_{\alpha\beta\gamma\delta} < \gamma\delta|v|\alpha\beta > + \frac{1}{2}\sum_{\alpha\beta\gamma\delta} C_{\alpha\beta\gamma\delta}\frac{d}{dt} < \gamma\delta|v|\alpha\beta > . \tag{2.38}$$

In the above equation, the first term is zero after inserting the equation of motion for $C_{\alpha\beta\gamma\delta}$ (Eq. 2.23). In order to evaluate the second term we use the completeness of the single particle basis and its equation of motion

$$i\hbar\frac{\partial\psi_\lambda}{\partial t} = h\psi_\lambda = \sum_\alpha \epsilon_{\alpha\lambda}\psi_\alpha, \tag{2.39}$$

where $\epsilon_{\alpha\lambda} =< \alpha|h|\lambda >$. The resulting equation is

$$\begin{aligned}\frac{1}{2i\hbar}\sum_{\alpha\beta\gamma\lambda} \quad & C_{\alpha\beta\gamma\delta}(-\epsilon_{\gamma\lambda} < \lambda\delta|v|\alpha\beta > -\epsilon_{\delta\lambda} < \gamma\lambda|v|\alpha\beta > + \epsilon_{\lambda\alpha} < \gamma\delta|v|\lambda\beta > \\ & + \epsilon_{\lambda\beta} < \gamma\delta|v|\alpha\lambda >).\end{aligned}$$

After re-arranging terms and using Eq. 2.22 we obtain

$$-\sum_{\lambda\lambda'}\epsilon_{\lambda\lambda'}\dot{n}_{\lambda'\lambda}. \tag{2.40}$$

The total energy is therefore conserved. Since we have used the completeness property of the single particle basis, the above derivation is not strict if the single particle space is truncated. In the numerical calculations shown later energy conservation is violated.

Chapter 3

Small amplitude limit

3.1 Introduction

In small amplitude limit, the equations of motion can be linearized according the small deviation of relevant quantities (e.g. density-matrix) from their equilibrium values (or ground state value). The excitation of the system is then the eigenmode of these linear coupled equations. In this chapter we linearize the *TDDM* according to the small deviation of the density-matrix and correlation function, and call the resulting theory small amplitude *TDDM* (*STDDM*). The purpose of this chapter is to explore the physical meaning of the coupled-equations for ρ and c_2. To this end, we compare *STDDM* with the existing small amplitude motion theories such as the random phase approximation (*RPA*), the second *RPA* and the shell model.

3.2 *TDDM* in small amplitude limit

3.2.1 Ground state density-matrix

First we discuss how to determine the ground state density-matrix ρ^0 and correlation function C_2^0 from the *TDDM* equations. We expand ρ^0 and C_2^0 in terms of a *HF* -like

single particle basis

$$\rho^0(11') = \sum_{\alpha\beta} n^0_{\alpha\beta}\psi_\alpha(1)\psi^*_\beta(1'), \tag{3.1}$$

$$C^0_2(12,1'2') = \sum_{\alpha\beta\gamma\delta} C^0_{\alpha\beta\gamma\delta}\psi_\alpha(1)\psi_\beta(2)\psi^*_\gamma(1')\psi^*_\delta(2'), \tag{3.2}$$

where ψ_α is the solution of *HF* equation

$$h[\rho_0]\psi_\alpha = \varepsilon_\alpha\psi_\alpha. \tag{3.3}$$

In the above equations all the quantities are time-independent. In the time independent case, it is obvious that the left hand sides of Eq. 2.11 and 2.12 are equal to zero (i.e. $\dot{\rho} = 0$ and $\dot{C}_2 = 0$). We then substitute the density-matrix and the correlation function with the expansions Eq. 3.1 and Eq. 3.2. Using the fact that the single particle basis is the solution of Eq. 3.3, we obtain the following results:

$$(\varepsilon_\beta - \varepsilon_\alpha)n^0_{\alpha\beta} = \text{r.h.s. of Eq. 2.22}, \tag{3.4}$$

$$(\varepsilon_{\alpha'} + \varepsilon_{\beta'} - \varepsilon_\alpha - \varepsilon_\beta)C^0_{\alpha\beta\alpha'\beta'} = \text{r.h.s. of Eq. 2.23}, \tag{3.5}$$

where the time-dependent coefficients n and C on the right hand side of equations 2.22 and 2.23 should be replaced by the stationary ones n^0 and C^0. Eq. 3.4 and 3.5 are not sufficient to determine all the elements of $n^0_{\alpha\beta}$ and $C^0_{\alpha\beta\alpha'\beta'}$, e.g. the diagonal elements can not be determined by the above equations. We, therefore, need additional conditions. By the definition of reduced density-matrix, we have following four relations which may provide such conditions,

$$N = \int d1\rho(11), \tag{3.6}$$

$$\rho(11') = \frac{1}{N-1}\int d2\rho_2(12,1'2), \tag{3.7}$$

$$\rho_2(12,1'2') = \frac{1}{N-2}\int d3\rho_3(123,1'2'3), \tag{3.8}$$

and

$$\rho_3(123,1'2'3') = \frac{1}{(N-3)}\int d4\rho_4(1234,1'2'3'4), \tag{3.9}$$

where ρ_2, ρ_3 and ρ_4 are expressed in terms of the one-body density-matrix and two-body correlation function using Eq. 2.10. It can be proven that Eqs. 3.7–3.9 are sufficient to satisfy the general relation

$$\rho_n = \frac{1}{N-n} Tr_{n+1}\{\rho_{n+1}\}, \tag{3.10}$$

as long as ρ_n and ρ_{n+1} are expressed with ρ and c_2 according to Eq. 2.10. Eqs. 3.7–3.9 can be written explicitly:

$$\rho(11') = \int d2\{\rho(12)\rho(21') - c_2(12,1'2)\}, \tag{3.11}$$

$$\begin{aligned} c_2(12,1'2') = \frac{1}{2}\int d3\{&\rho(13)c_2(32,1'2') + \rho(23)c_2(13,1'2') \\ &+ c_2(12,32')\rho(31') + c_2(12,1'3)\rho(32')\}, \end{aligned} \tag{3.12}$$

$$\begin{aligned} 0 = \int d4\{&c_2(12,1'4)c_2(34,2'3') - c_2(12,2'4)c_2(34,1'3') \\ &+ c_2(12,3'4)c_2(34,1'2') - c_2(13,1'4)c_2(24,2'3') \\ &+ c_2(13,2'4)c_2(24,1'3') - c_2(13,3'4)c_2(24,1'2') \\ &- c_2(14,1'3')c_2(23,2'4) + c_2(14,2'3')c_2(23,1'4) \\ &+ c_2(14,1'2')c_2(23,3'4)\}. \end{aligned} \tag{3.13}$$

The above equations hold for both time-dependent and time-independent cases.

The expressions of these equations in the single particle basis (either time-dependent or time-independent) are straightforward, so we do not show them here. It is shown by Tohyama[1] that Eq. 3.4–3.5 supplemented by Eqs. 3.7–3.9 give the approximate solution of the ground state of Lipkin model [Rin 80]. He points out that the condition that the solution is the energy eigenstate should also be used. Since solving the Eqs. 3.4–3.9 for a general case is very difficult, we assume in the following discussion that such a solution exists.

[1] Private communication.

3.2.2 Formalism of the small amplitude limit

In the small amplitude limit ρ and c_2 can be expanded as

$$\rho(11';t) = \rho^0(11') + \eta(11',t), \tag{3.14}$$

$$c_2(12,1'2';t) = c_2^0(12,1'2') + g(12,1'2';t), \tag{3.15}$$

where η and g denote small deviation from the ground state. Substituting the above equations into Eq. 2.22-2.23 and keeping only those terms which are linear in η and g, we obtain the following equations for η and g:

$$\begin{aligned} i\hbar\dot{\eta}(11') &= [h_0(1) - h_0(1')]\eta(11') \\ &\quad + Tr_{(2)}\{[v(12) - v(1'2')][\rho^0(11')\eta(22') + \eta(11')\rho^0(22') \\ &\quad - \rho^0(12')\eta(21') - \eta(12')\rho^0(21') + g(12,1'2')]\}_{2=2'}, \end{aligned} \tag{3.16}$$

$$\begin{aligned} i\hbar\dot{g}(12,1'2') &= [h_0(1) + h_0(2) - h_0(1') - h_0(2')]g(12,1'2') \\ &\quad + [v(12) - v(1'2')]g(12,1'2') \\ &\quad + [v(12) - v(1'2')][\rho^0(11')\eta(22') + \eta(11')\rho^0(22') \\ &\qquad - \rho^0(12')\eta(21') - \eta(12')\rho^0(21')] \\ &\quad - Tr_{(3)}\{[v(13) - v(1'3')][\eta(11')\rho^0(23')\rho^0(32') \\ &\qquad + \rho^0(11')\eta(23')\rho^0(32') + \rho^0(11')\rho^0(23')\eta(32')] \\ &\quad + [v(23) - v(2'3')][\eta(13')\rho^0(22')\rho^0(31') \\ &\qquad + \rho^0(13')\eta(22')\rho^0(31') + \rho^0(13')\rho^0(22')\eta(31')] \\ &\quad - [v(13) - v(2'3')][\eta(12')\rho^0(23')\rho^0(31') \\ &\qquad + \rho^0(12')\eta(23')\rho^0(31') + \rho^0(12')\rho^0(23')\eta(31')] \\ &\quad - [v(23) - v(1'3')][\eta(13')\rho^0(21')\rho^0(32') \\ &\qquad + \rho^0(13')\eta(21')\rho^0(32') + \rho^0(13')\rho^0(21')\eta(32')] \\ &\quad - [v(13) - v(1'3')][\eta(11')c_2^0(23,2'3') + \eta(33')c_2^0(12,1'2') \end{aligned}$$

$$
\begin{aligned}
&- \eta(13')c_2^0(23,2'1') - \eta(23')c_2^0(13,1'2') \\
&- \eta(31')c_2^0(12,3'2') - \eta(32')c_2^0(12,1'3') \\
&+ \rho^0(11')g(23,2'3') + \rho^0(33')g(12,1'2') \\
&- \rho^0(13')g(23,2'1') - \rho^0(23')g(13,1'2') \\
&- \rho^0(31')g(12,3'2') - \rho^0(32')g(12,1'3')] \\
&- [v(23) - v(2'3')][\eta(22')c_2^0(13,1'3') + \eta(33')c_2^0(12,1'2') \\
&- \eta(13')c_2^0(23,2'1') - \eta(23')c_2^0(13,1'2') \\
&- \eta(31')c_2^0(12,3'2') - \eta(32')c_2^0(12,1'3') \\
&+ \rho^0(22')g(13,1'3') + \rho^0(33')g(12,1'2') \\
&- \rho^0(13')g(23,2'1') - \rho^0(23')g(13,1'2') \\
&- \rho^0(31')g(12,3'2') - \rho^0(32')g(12,1'3')] \\
&+ [v(13) - v(2'3')][\eta(12')c_2^0(23,1'3') + \rho^0(12')g(23,1'3')] \\
&+ [v(23) - v(1'3')][\eta(21')c_2^0(13,2'3') + \rho^0(21')g(13,2'3')]\}_{3=3'}.
\end{aligned}
\tag{3.17}
$$

In the same way as we did in Eqs. 3.1-3.2 we expand η and g in terms of the single particle basis Eq. 3.3:

$$
\eta(11';t) = \sum_{\alpha\beta} m_{\alpha\beta}(t)\psi_\alpha(1)\psi^*_\beta(1'), \tag{3.18}
$$

$$
g(12,1'2';t) = \sum_{\alpha\beta\gamma\delta} G_{\alpha\beta\gamma\delta}(t)\psi_\alpha(1)\psi_\beta(2)\psi^*_\gamma(1')\psi^*_\delta(2'). \tag{3.19}
$$

We further make a Fourier transformation with respect to time and denote the Fourier amplitude with the same symbol, i.e. m and G. Inserting Eqs. 3.1-3.2 and 3.18-3.19 into Eqs. 3.16-3.17 we reach the final expression for m and G:

$$
\begin{aligned}
(w - \epsilon_\alpha + \epsilon_\beta)m_{\alpha\beta} = \sum_{\gamma\delta\sigma}\{&G_{\gamma\delta\beta\sigma} < \alpha\sigma|v|\gamma\delta > - G_{\alpha\delta\gamma\sigma} < \gamma\sigma|v|\beta\delta > \\
&[< \gamma\delta|v|\sigma\beta >_A n^0_{\alpha\gamma} - < \alpha\delta|v|\sigma\gamma >_A n^0_{\gamma\beta}]m_{\sigma\delta}\},
\end{aligned}
$$

(3.20)

$$(w - \varepsilon_\alpha - \varepsilon_\beta + \varepsilon_{\alpha'} + \varepsilon_{\beta'})G_{\alpha\beta\alpha'\beta'} =$$

$$A_{\alpha\beta\alpha'\beta'}(t) + B_{\alpha\beta\alpha'\beta'}(t) + H_{\alpha\beta\alpha'\beta'}(t) + P_{\alpha\beta\alpha'\beta'}(t),$$

(3.21)

where

$$\begin{aligned} A_{\alpha\beta\alpha'\beta'} &= \sum_{\lambda_1\lambda_2\lambda_3} \{< \alpha\lambda_1|v|\lambda_2\lambda_3 >_A C^0_{\lambda_2\beta\alpha'\beta'} \\ &\quad + < \beta\lambda_1|v|\lambda_2\lambda_3 >_A C^0_{\alpha\lambda_2\alpha'\beta'} \\ &\quad - < \lambda_2\lambda_1|v|\alpha'\lambda_3 >_A C^0_{\alpha\beta\lambda_2\beta'} \\ &\quad - < \lambda_2\lambda_1|v|\beta'\lambda_3 >_A C^0_{\alpha\beta\alpha'\lambda_2}\} m_{\lambda_1\lambda_3}, \end{aligned} \tag{3.22}$$

$$\begin{aligned} B_{\alpha\beta\alpha'\beta'} &= -\sum_{\lambda_1\lambda_2\lambda_3\lambda_4} < \lambda_1\lambda_2|v|\lambda_3\lambda_4 >_A \\ &\quad \{m_{\alpha\lambda_1}(\delta_{\beta\lambda_2} - n^0_{\beta\lambda_2}) n^0_{\lambda_3\alpha'} n^0_{\lambda_4\beta'} \\ &\quad + (\delta_{\alpha\lambda_1} - n^0_{\alpha\lambda_1}) m_{\beta\lambda_2} n^0_{\lambda_3\alpha'} n^0_{\lambda_4\beta'} \\ &\quad - (\delta_{\alpha\lambda_1} - n^0_{\alpha\lambda_1})(\delta_{\beta\lambda_2} - n^0_{\beta\lambda_2}) m_{\lambda_3\alpha'} n^0_{\lambda_4\beta'} \\ &\quad - (\delta_{\alpha\lambda_1} - n^0_{\alpha\lambda_1})(\delta_{\beta\lambda_2} - n^0_{\beta\lambda_2}) n^0_{\lambda_3\alpha'} m_{\lambda_4\beta'} \\ &\quad + m_{\alpha\lambda_1} n^0_{\beta\lambda_2}(\delta_{\lambda_3\alpha'} - n^0_{\lambda_3\alpha'})(\delta_{\lambda_4\beta'} - n^0_{\lambda_4\beta'}) \\ &\quad + n^0_{\alpha\lambda_1} m_{\beta\lambda_2}(\delta_{\lambda_3\alpha'} - n^0_{\lambda_3\alpha'})(\delta_{\lambda_4\beta'} - n^0_{\lambda_4\beta'}) \\ &\quad - n^0_{\alpha\lambda_1} n^0_{\beta\lambda_2} m_{\lambda_3\alpha'}(\delta_{\lambda_4\beta'} - n^0_{\lambda_4\beta'}) \\ &\quad - n^0_{\alpha\lambda_1} n^0_{\beta\lambda_2}(\delta_{\lambda_3\alpha'} - n^0_{\lambda_3\alpha'}) m_{\lambda_4\beta'}\}, \end{aligned} \tag{3.23}$$

$$H_{\alpha\beta\alpha'\beta'} = \sum_{\lambda_1\lambda_2\lambda_3\lambda_4} < \lambda_1\lambda_2|v|\lambda_3\lambda_4 >$$

$$
\begin{aligned}
&\{\delta_{\alpha\lambda_1}(m_{\lambda_3\alpha'}C^0_{\beta\lambda_4\beta'\lambda_2} - m_{\lambda_3\beta'}C^0_{\beta\lambda_4\alpha'\lambda_2} \\
&\quad - m_{\lambda_4\alpha'}C^0_{\lambda_3\beta\lambda_2\beta'} - m_{\lambda_4\beta'}C^0_{\lambda_3\beta\alpha'\lambda_2} \\
&\quad + n^0_{\lambda_3\alpha'}G_{\beta\lambda_4\beta'\lambda_2} - n^0_{\lambda_3\beta'}G_{\beta\lambda_4\alpha'\lambda_2} \\
&\quad - n^0_{\lambda_4\alpha'}G_{\lambda_3\beta\lambda_2\beta'} - n^0_{\lambda_4\beta'}G_{\lambda_3\beta\alpha'\lambda_2}) \\
&+ \delta_{\beta\lambda_2}(m_{\lambda_4\beta'}C^0_{\alpha\lambda_3\alpha'\lambda_1} - m_{\lambda_4\alpha'}C^0_{\alpha\lambda_3\beta'\lambda_1} \\
&\quad - m_{\lambda_3\beta'}C^0_{\alpha\lambda_4\alpha'\lambda_1} - m_{\lambda_3\alpha'}C^0_{\alpha\lambda_4\lambda_1\beta'} \\
&\quad + n^0_{\lambda_4\beta'}G_{\alpha\lambda_3\alpha'\lambda_1} - n^0_{\lambda_4\alpha'}G_{\alpha\lambda_3\beta'\lambda_1} \\
&\quad - n^0_{\lambda_3\beta'}G_{\alpha\lambda_4\alpha'\lambda_1} - n^0_{\lambda_3\alpha'}G_{\alpha\lambda_4\lambda_1\beta'}) \\
&- \delta_{\lambda_3\alpha'}(m_{\alpha\lambda_1}C^0_{\beta\lambda_4\beta'\lambda_2} - m_{\beta\lambda_1}C^0_{\alpha\lambda_4\beta'\lambda_2} \\
&\quad - m_{\alpha\lambda_2}C^0_{\beta\lambda_4\beta'\lambda_1} - m_{\beta\lambda_2}C^0_{\alpha\lambda_4\lambda_1\beta'} \\
&\quad + n^0_{\alpha\lambda_1}G_{\beta\lambda_4\beta'\lambda_2} - n^0_{\beta\lambda_1}G_{\alpha\lambda_4\beta'\lambda_2} \\
&\quad - n^0_{\alpha\lambda_2}G_{\beta\lambda_4\beta'\lambda_1} - n^0_{\beta\lambda_2}G_{\alpha\lambda_4\lambda_1\beta'}) \\
&- \delta_{\lambda_4\beta'}(m_{\beta\lambda_2}C^0_{\alpha\lambda_3\alpha'\lambda_1} - m_{\alpha\lambda_2}C^0_{\beta\lambda_3\alpha'\lambda_1} \\
&\quad - m_{\beta\lambda_1}C^0_{\alpha\lambda_3\alpha'\lambda_2} - m_{\alpha\lambda_1}C^0_{\beta\lambda_3\lambda_2\alpha'} \\
&\quad + n^0_{\beta\lambda_2}G_{\alpha\lambda_3\alpha'\lambda_1} - n^0_{\alpha\lambda_2}G_{\beta\lambda_3\alpha'\lambda_1} \\
&\quad - n^0_{\beta\lambda_1}G_{\alpha\lambda_3\alpha'\lambda_2} - n^0_{\alpha\lambda_1}G_{\beta\lambda_3\lambda_2\alpha'})\}, \qquad (3.24)
\end{aligned}
$$

and

$$
\begin{aligned}
P_{\alpha\beta\alpha'\beta'} \;=\; &\sum_{\lambda_1\lambda_2\lambda_3\lambda_4} < \lambda_1\lambda_2|v|\lambda_3\lambda_4 > \\
&\{\delta_{\alpha\lambda_1}\delta_{\beta\lambda_2}G_{\lambda_3\lambda_4\alpha'\beta'} - G_{\alpha\beta\lambda_1\lambda_2}\delta_{\lambda_3\alpha'}\delta_{\lambda_4\beta'} \\
&- \delta_{\alpha\lambda_1}m_{\beta\lambda_2}C^0_{\lambda_3\lambda_4\alpha'\beta'} - \delta_{\beta\lambda_2}m_{\alpha\lambda_1}C^0_{\lambda_4\lambda_3\beta'\alpha'} \\
&+ \delta_{\lambda_3\alpha'}m_{\lambda_4\beta'}C^0_{\alpha\beta\lambda_1\lambda_2} + \delta_{\lambda_4\beta'}m_{\lambda_3\alpha'}C^0_{\alpha\beta\lambda_1\lambda_2} \\
&- \delta_{\alpha\lambda_1}n^0_{\beta\lambda_2}G_{\lambda_3\lambda_4\alpha'\beta'} - \delta_{\beta\lambda_2}n^0_{\alpha\lambda_1}G_{\lambda_4\lambda_3\beta'\alpha'} \\
&+ \delta_{\lambda_3\alpha'}n^0_{\lambda_4\beta'}G_{\alpha\beta\lambda_1\lambda_2} + \delta_{\lambda_4\beta'}n^0_{\lambda_3\alpha'}G_{\alpha\beta\lambda_1\lambda_2}\}. \qquad (3.25)
\end{aligned}
$$

$A_{\alpha\beta\alpha'\beta'}$ comes from the linearization of the mean-field hamiltonian on the right-hand side of Eq. 2.12. To make the physical meaning of the linearized equations 3.20 and 3.21 transparent, we use the *HF* approximation for the ground state in the following discussion. In the *HF* approximation $n^0_{\alpha\beta}$ and $C^0_{\alpha\beta\gamma\delta}$ take the following values:

$$n^0_{\alpha\beta} = a_\alpha \delta_{\alpha\beta};\ \ a_\alpha = (1, \text{ for hole states; } 0, \text{ for particle states}), \tag{3.26}$$

$$C^0_{\alpha\beta\gamma\delta} = 0. \tag{3.27}$$

Substituting the above values into Eq. 3.20–3.25, we get following equations:

$$\begin{aligned}(w - \varepsilon_\alpha + \varepsilon_\beta) m_{\alpha\beta} &= \sum_{\gamma\delta\sigma} [G_{\gamma\delta\beta\sigma} < \alpha\sigma|v|\gamma\delta > - G_{\alpha\delta\gamma\sigma} < \gamma\sigma|v|\beta\delta >] \\ &\quad + \sum_{\delta\sigma} [< \alpha\delta|v|\sigma\beta >_A a_\alpha - < \alpha\delta|v|\sigma\beta >_A a_\beta] m_{\sigma\delta},\end{aligned} \tag{3.28}$$

and

$$\begin{aligned}(w - \varepsilon_\alpha - \varepsilon_\beta + \varepsilon_{\alpha'} + \varepsilon_{\beta'}) G_{\alpha\beta\alpha'\beta'} = \\ [b_\alpha b_\beta a_{\alpha'} a_{\beta'} - a_\alpha a_\beta b_{\alpha'} b_{\beta'}] < \alpha\beta|v|\alpha'\beta' >_A (w = 0) \\ - \sum_\lambda \{ [b_\beta a_{\alpha'} a_{\beta'} + a_\beta b_{\alpha'} b_{\beta'}] < \lambda\beta|v|\alpha'\beta' >_A m_{\alpha\lambda} \\ + [b_\alpha a_{\alpha'} a_{\beta'} + a_\alpha b_{\alpha'} b_{\beta'}] < \alpha\lambda|v|\alpha'\beta' >_A m_{\beta\lambda} \\ - [b_\alpha b_\beta a_{\beta'} + a_\alpha a_\beta b_{\beta'}] < \alpha\beta|v|\lambda\beta' >_A m_{\lambda\alpha'} \\ - [b_\alpha b_\beta a_{\alpha'} + a_\alpha a_\beta b_{\alpha'}] < \alpha\beta|v|\alpha'\lambda >_A m_{\lambda\beta'} \} \\ + \sum_{\lambda\lambda'} \{ [1 - a_\alpha - a_\beta] < \alpha\beta|v|\lambda\lambda' > G_{\lambda\lambda'\alpha'\beta'} \\ - [1 - a_{\alpha'} - a_{\beta'}] < \lambda\lambda'|v|\alpha'\beta' > G_{\alpha\beta\lambda\lambda'} \} \\ + \sum_{\lambda\lambda'} \{ [b_\alpha a_{\alpha'} - a_\alpha b_{\alpha'}] < \alpha\lambda|v|\alpha'\lambda' >_A G_{\lambda'\beta\lambda\beta'}\end{aligned}$$

$$- [b_\alpha a_{\beta'} - a_\alpha b_{\beta'}] < \alpha\lambda|v|\lambda'\beta' >_A G_{\lambda'\beta\alpha'\lambda}$$

$$+ [b_\beta a_{\beta'} - a_\beta b_{\beta'}] < \lambda\beta|v|\lambda'\beta' >_A G_{\alpha\lambda'\alpha'\lambda}$$

$$- [b_\beta a_{\alpha'} - a_\beta b_{\alpha'}] < \lambda\beta|v|\alpha'\lambda' >_A G_{\alpha\lambda'\lambda\beta'}\}, \qquad (3.29)$$

where the first term is for $w = 0$ only. Eq. 3.28 and 3.29 are the basic formalism of *STDDM* based on the *HF* ground state.

In the following sections we discuss the relation of the *STDDM* to other existing theories.

3.3 Random phase approximation

In this section we will show that under certain conditions *STDDM* can be reduced to *RPA*. Before we do that we first present the *RPA* equations[2]. In *RPA* a collective state is assumed to be the coherent superposition of 1p-1h excitations. Therefore the excited state can be generated by

$$|n> = Q_n^\dagger|0>, \qquad (3.30)$$

$$Q_n^\dagger = \sum_{\rho\nu}(X_{\rho\nu}^n a_\rho^\dagger a_\nu - Y_{\rho\nu}^n a_\nu^\dagger a_\rho), \qquad (3.31)$$

where ν and μ (ρ and σ) denote the occupied (unoccupied) s.p. states, $a^\dagger$ (a) is the creation (annihilation) operator and $|0>$ is the ground state. The coefficients $X_{\rho\nu}^n$ and $Y_{\rho\nu}^n$ are the transition amplitudes. The equation of motion is written as

$$[H, Q_n^\dagger]|0> = (E_n - E_0)Q_n^\dagger|0> . \qquad (3.32)$$

In the space spanned by 1-*ph* excitations, we get two equations:[3]

$$< 0|[a_\nu^\dagger a_\rho, [H, Q_n^\dagger]]|0> = w_n < 0|[a_\nu^\dagger a_\rho, Q_n^\dagger]|0>,$$

$$< 0|[a_\rho^\dagger a_\nu, [H, Q_n^\dagger]]|0> = w_n < 0|[a_\rho^\dagger a_\nu, Q_n^\dagger]|0>, \qquad (3.33)$$

[2]There are many ways to derive it. Here we use the so called equation of motion method discussed by Ring and Schuck [Rin 80].

[3]We multiply Eq. 3.32 with $< 0|a_\nu^\dagger a_\rho$ and $< 0|a_\rho^\dagger a_\nu$, and use the relation $< 0|Q_n^\dagger = 0$.

where $w_n = E_n - E_0$. Since the ground state $|0>$ is difficult to obtain, it is usually approximated by $|HF>$. Under this approximation the above equation can be written in a matrix form:

$$\begin{pmatrix} A_{11} & B_{11} \\ A_{11}^* & B_{11}^* \end{pmatrix} \begin{pmatrix} X_1 \\ Y_1 \end{pmatrix} = w \begin{pmatrix} 1 & 0 \\ 0 & -1 \end{pmatrix} \begin{pmatrix} X_1 \\ Y_1 \end{pmatrix}, \tag{3.34}$$

where

$$(X_1)_{\rho\nu} = X_{\rho\nu}, \ (Y_1)_{\rho\nu} = Y_{\nu\rho}, \tag{3.35}$$

$$(A_{11})_{\rho\nu,\sigma\mu} = (\varepsilon_\rho - \varepsilon_\nu)\delta_{\rho\sigma}\delta_{\nu\mu} + < \rho\mu|v|\nu\sigma >_A, \tag{3.36}$$

$$(B_{11})_{\rho\nu,\sigma\mu} = < \rho\sigma|v|\nu\mu >_A . \tag{3.37}$$

Eq. 3.34 is the usual form of *RPA*. In the following we will see that the same equations can be derived from *STDDM* if we neglect all of the two-body correlation coefficients in *STDDM*. This can be understood from the fact that *RPA* only takes into account the 1p-1h excitations. Neglecting the two-body correlation matrix in Eq. 3.28, we obtain

$$(w - \varepsilon_\alpha + \varepsilon_\beta)m_{\alpha\beta} = (a_\alpha - a_\beta)\sum_{\delta\sigma} < \alpha\delta|v|\sigma\beta >_A m_{\sigma\delta}. \tag{3.38}$$

The above equation immediately yields that $m_{\rho\sigma} = m_{\mu\nu} = 0$ and

$$(w - \varepsilon_\rho + \varepsilon_\nu)m_{\rho\nu} = \sum_{\sigma\mu}\{< \rho\mu|v|\nu\sigma >_A m_{\sigma\mu} + < \rho\sigma|v|\nu\mu >_A m_{\mu\sigma}\}, \tag{3.39}$$

$$(w - \varepsilon_\nu + \varepsilon_\rho)m_{\nu\rho} = \sum_{\sigma\mu}\{< \nu\sigma|v|\mu\rho >_A m_{\mu\sigma} + < \nu\mu|v|\sigma\rho >_A m_{\sigma\mu}\}. \tag{3.40}$$

Now it is easy to see that Eq. 3.40 is equivalent to Eq. 3.34. To understand the relations between (X_1, Y_1) and $(m_{\rho\nu}, m_{\nu\rho})$, let us make the following discussion. Let $|\Psi(t)>$ be the time-dependent many-body wave function, i.e. a wave packet, which is the mixture of the ground state $|0>$ and excited states $|n>$, and let us assume that

the components of the excited states are small. The wave function can be written as

$$|\Psi(t)>= e^{-iE_0t}\left(|0>+\sum_n c_n|n>e^{-iw_nt}\right), \tag{3.41}$$

where $\{c_n\}$ are small quantities and $\{w_n\}$ the excitation energies. To the first order of the c-coefficients we have

$$\begin{aligned} m_{\rho\nu}(t) &= <\Psi(t)|a_\nu^\dagger a_\rho|\Psi(t)> \\ &= \sum_n\{c_n<0|a_\nu^\dagger a_\rho|n>e^{-iw_nt}+c_n^*<n|a_\nu^\dagger a_\rho|0>e^{iw_nt}\}, \qquad (3.42) \\ m_{\nu\rho}(t) &= <\Psi(t)|a_\rho^\dagger a_\nu|\Psi(t)> \\ &= \sum_n\{c_n<0|a_\rho^\dagger a_\nu|n>e^{-iw_nt}+c_n^*<n|a_\rho^\dagger a_\nu|0>e^{iw_nt}\}. \qquad (3.43) \end{aligned}$$

The fourier transformation of both quantities are

$$m_{\rho\nu}(w) = c_n<0|a_\nu^\dagger a_\rho|n>, \tag{3.44}$$

$$m_{\nu\rho}(w) = c_n<0|a_\rho^\dagger a_\nu|n>. \tag{3.45}$$

So $m_{\rho\nu}$ and $m_{\nu\rho}$ have the meaning of a transition amplitude. As discussed by Ring and Schuck [Rin 80], X_1 and Y_1 also have the meaning of a transition amplitude. The relation between (X_1, Y_1) and $(m_{\rho\nu}, m_{\nu\rho})$ is now

$$(X_1)_{\rho\nu} = m_{\rho\nu}/c_n, \quad (Y_1)_{\rho\nu} = m_{\nu\rho}/c_n. \tag{3.46}$$

3.4 Second random phase approximation

In the second random phase approximation (*SRPA*) [Saw 62] $2p-2h$ as well as $1p-1h$ excitations are taken into account. The derivation of *SRPA* is tedious, so we only outline one of the derivations, i.e. the equation of motion method [Yan 83].

In the equation of motion method, a collective excitation is still generated by Eq. 3.32, but the operator $Q_n^\dagger$ has been extended to include two-ph pair excitations. In the way similar to Eq. 3.33, $Q_n^\dagger$ is defined as

$$Q_n^\dagger = \sum_{\rho\nu}(X^n_{\rho\nu}a_\rho^\dagger a_\nu - Y^n_{\rho\nu}a_\nu^\dagger a_\rho) + \sum_{\rho\sigma\nu\mu}(X^n_{\rho\sigma\nu\mu}a_\rho^\dagger a_\sigma^\dagger a_\mu a_\nu - Y^n_{\rho\sigma\nu\mu}a_\nu^\dagger a_\mu^\dagger a_\sigma a_\rho), \tag{3.47}$$

where μ and ν denote the hole states, and σ and ρ the particle states.

As in the case of *RPA* the exact solution of the ground state is very difficult to obtain, so it is approximated by the *HF* state when the ground state expectation values are calculated. Under this approximation the expectation values of some useful commutations can be quite simply evaluated. The following are a few useful examples,

$$< 0|[a^\dagger_\mu a_\rho, a^\dagger_\alpha a_{\alpha'}]|0 > \approx \delta_{\mu\alpha'}\delta_{\alpha\rho}, \tag{3.48}$$

$$< 0|[a^\dagger_\rho a_\mu, a^\dagger_\alpha a_{\alpha'}]|0 > \approx -\delta_{\rho\alpha'}\delta_{\alpha\mu}; \tag{3.49}$$

$$< 0|[a^\dagger_\mu a^\dagger_\nu a_\rho a_\sigma, a^\dagger_\alpha a^\dagger_\beta a_\gamma a_\delta]|0 > \approx A_{(\gamma\delta)}(\delta_{\mu\delta}\delta_{\nu\gamma})A_{(\alpha\beta)}(\delta_{\sigma\alpha}\delta_{\rho\beta}), \tag{3.50}$$

$$< 0|[a^\dagger_\rho a^\dagger_\sigma a_\mu a_\nu, a^\dagger_\alpha a^\dagger_\beta a_\gamma a_\delta]|0 > \approx A_{(\mu\nu)}(\delta_{\alpha\nu}\delta_{\beta\mu})A_{(\delta\gamma)}(\delta_{\rho\gamma}\delta_{\sigma\delta}), \tag{3.51}$$

$$< 0|[a^\dagger_\rho a^\dagger_\mu a_\sigma a_\nu, a^\dagger_\alpha a^\dagger_\beta a_\gamma a_\delta]|0 > \approx 0, \tag{3.52}$$

where operator $A_{(\alpha\beta)}$ antisymmetrize the product with respect to α and β. For the expectation values of the commutators between a one-*ph* pair operator and a two-*ph* pair operator we have

$$< 0|[a^\dagger_\alpha a_{\alpha'}, a^\dagger_\beta a^\dagger_\gamma a_{\beta'} a_{\gamma'}]|0 >= 0, \tag{3.53}$$

if $\beta \neq \beta', \gamma'$ and $\gamma \neq \beta', \gamma'$.

With the above expectation values we can derive *SRPA* equations in a way similar to *RPA*. Since the final result is the same as that from *STDDM*, we give the final expression at the end of this section. In the following we derive *SRPA* from *STDDM*.

If we keep only the one-*ph* amplitude ($m_{\rho\nu}$ and $m_{\nu\rho}$) and the two-*ph* amplitude ($G_{\rho\rho'\nu\nu'}$ and $G_{\nu\nu'\rho\rho'}$), the basic equations of *STDDM* will become

$$\begin{aligned}(w - \varepsilon_\rho + \varepsilon_\nu)m_{\rho\nu} &= \sum_{\sigma\mu}\{< \rho\mu|v|\nu\sigma >_A m_{\sigma\mu} + < \rho\sigma|v|\nu\mu >_A m_{\mu\sigma}\} \\ &\quad + \sum_{\sigma\sigma'\mu} < \rho\mu|v|\sigma\sigma' > G_{\sigma\sigma'\nu\mu} \\ &\quad - \sum_{\sigma\mu\mu'} < \mu\mu'|v|\nu\sigma > G_{\rho\sigma\mu\mu'},\end{aligned} \tag{3.54}$$

$$(w-\varepsilon_\nu+\varepsilon_\rho)m_{\nu\rho} = \sum_{\sigma\mu}\{<\mu\nu|v|\rho\sigma>_A m_{\sigma\mu}+<\sigma\nu|v|\rho\mu>_A m_{\mu\sigma}\}$$

$$+\sum_{\sigma\mu\mu'}<\nu\sigma|v|\mu\mu'>G_{\mu\mu'\rho\sigma}$$

$$-\sum_{\sigma\sigma'\mu}<\sigma\sigma'|v|\rho\mu>G_{\nu\mu\sigma\sigma'}, \qquad (3.55)$$

$$(w-\varepsilon_\rho-\varepsilon_{\rho'}+\varepsilon_\nu+\varepsilon_{\nu'})G_{\rho\rho'\nu\nu'} =$$

$$-\sum_{\mu}\{<\mu\rho'|v|\nu\nu'>_A m_{\rho\mu}+<\rho\mu|v|\nu\nu'>_A m_{\rho'\mu}\}$$

$$+\sum_{\sigma}\{<\rho\rho'|v|\sigma\nu'>_A m_{\sigma\nu}+<\rho\rho'|v|\nu\sigma>_A m_{\sigma\nu'}\}$$

$$+\sum_{\sigma\sigma'}<\rho\rho'|v|\sigma\sigma'>G_{\sigma\sigma'\nu\nu'}$$

$$+\sum_{\mu\mu'}<\mu\mu'|v|\nu\nu'>G_{\rho\rho'\mu\mu'}$$

$$+\sum_{\mu\sigma}\{<\rho\mu|v|\nu\sigma>_A G_{\sigma\rho'\mu\nu'}-<\rho\mu|v|\sigma\nu'>_A G_{\sigma\rho'\nu\mu}$$

$$+<\mu\rho'|v|\sigma\nu'>_A G_{\rho\sigma\nu\mu}-<\mu\rho'|v|\nu\sigma>_A G_{\rho\sigma\mu\nu'}\}, \qquad (3.56)$$

and

$$(w-\varepsilon_\nu-\varepsilon_{\nu'}+\varepsilon_\rho+\varepsilon_{\rho'})G_{\nu\nu'\rho\rho'} =$$

$$-\sum_{\sigma}\{<\sigma\nu'|v|\rho\rho'>_A m_{\nu\sigma}+<\nu\sigma|v|\rho\rho'>_A m_{\nu'\sigma}\}$$

$$+\sum_{\mu}\{<\nu\nu'|v|\mu\rho'>_A m_{\mu\rho}+<\nu\nu'|v|\rho\mu>_A m_{\mu\rho'}\}$$

$$-\sum_{\mu\mu'}<\nu\nu'|v|\mu\mu'>G_{\mu\mu'\rho\rho'}$$

$$-\sum_{\sigma\sigma'}<\sigma\sigma'|v|\rho\rho'>G_{\nu\nu'\sigma\sigma'}$$

$$-\sum_{\sigma\mu}\{<\nu\sigma|v|\rho\mu>_A G_{\mu\nu'\sigma\rho'}-<\nu\sigma|v|\mu\rho'>_A G_{\mu\nu'\rho\sigma}$$

$$+ < \sigma\nu'|v|\mu\rho' >_A G_{\nu\mu\rho\sigma} - < \sigma\nu'|v|\rho\mu >_A G_{\nu\mu\sigma\rho'}\}. \tag{3.57}$$

In the last section we found that the m-coefficient has the meaning of a transition amplitude. In the same way as for the one-body amplitude we can easily show that to the first order in the c-coefficient, the G-coefficients are

$$G_{\rho\rho'\nu\nu'} = c_n < 0|a^\dagger_{\nu'}a^\dagger_\nu a_\rho a_{\rho'}|n >, \tag{3.58}$$

$$G_{\nu\nu'\rho\rho'} = c_n < 0|a^\dagger_{\rho'}a^\dagger_\rho a_\nu a_{\nu'}|n > . \tag{3.59}$$

(For the meaning of c_n and $|n >$ refer to the previous section). The relations between (X, Y) and G are similar to Eq. 3.46. The full expression of *STDDM* Eqs. 3.54–3.57 can also be written in a matrix form using Eq. 3.36, 3.37, 3.46 and the following notions,

$$X_2 = G_{\rho\rho'\nu\nu'}/c_n, \quad Y_2 = G_{\nu\nu'\rho\rho'}/c_n, \ (\rho < \rho', \ \nu < \nu') \tag{3.60}$$

$$\begin{aligned} A_{12} &= A_{\rho\nu,\sigma\sigma'\mu\mu'} \\ &= A_{(\mu\mu')}(< \rho\mu'|v|\sigma\sigma' >_A \delta_{\mu\nu}) - A_{(\sigma\sigma')}(< \mu\mu'|v|\nu\sigma' >_A \delta_{\rho\sigma}), \end{aligned} \tag{3.61}$$

$$\begin{aligned} A_{21} &= A_{\rho\rho'\nu\nu',\sigma\mu} \\ &= A_{(\nu\nu')}(< \rho\rho'|v|\sigma\nu' >_A \delta_{\nu\mu}) - A_{(\rho\rho')}(< \mu\rho'|v|\nu\nu' >_A \delta_{\sigma\rho}), \end{aligned} \tag{3.62}$$

and

$$\begin{aligned} C_{22} &= C_{\rho\rho'\nu\nu',\sigma\sigma'\mu\mu'} \\ &= (\varepsilon_\rho + \varepsilon_{\rho'} - \varepsilon_\nu - \varepsilon_{\nu'})\delta_{\rho\sigma}\delta_{\rho'\sigma'}\delta_{\nu\mu}\delta_{\nu'\mu'} \\ &\quad + < \rho\rho'|v|\sigma\sigma' >_A \delta_{\nu\mu}\delta_{\nu'\mu'} + < \mu\mu'|v|\nu\nu' >_A \delta_{\rho\sigma}\delta_{\rho'\sigma'} \\ &\quad - A_{(\rho\rho')}A_{(\nu\nu')}A_{(\sigma\sigma')}A_{(\mu\mu')}(< \rho\mu'|v|\sigma\nu' >_A \delta_{\sigma'\rho'}\delta_{\mu\nu}). \end{aligned} \tag{3.63}$$

The final expression is

$$\begin{vmatrix} A_{11} & B_{11} & A_{12} & 0 \\ -B_{11}^* & -A_{11}^* & 0 & -A_{12}^* \\ A_{21} & 0 & C_{22} & 0 \\ 0 & -A_{21}^* & 0 & -C_{22}^* \end{vmatrix} \begin{vmatrix} X_1 \\ Y_1 \\ X_2 \\ Y_2 \end{vmatrix} = w \begin{vmatrix} X_1 \\ Y_1 \\ X_2 \\ Y_2 \end{vmatrix}. \tag{3.64}$$

This form is equivalent to the second *RPA* of Sawicki [Saw 62], [Dap 65] and also that of Yannouleas et al. [Yan 83]. The neglect of the interaction in C_{22} corresponds to the Born approximation, and this limit was studied by Ayik [Ayi 85].

3.5 Shell Model

If we keep only the forward one-ph ($m_{\rho\nu}$) and two-ph ($G_{\rho\rho'\nu\nu'}$) amplitudes, we can reduce *STDDM* to the shell model in the $1p-1h$ and $2p-2h$ space. The equation for $m_{\rho\nu}$ is

$$\begin{aligned} (w-\varepsilon_\rho+\varepsilon_\nu)m_{\rho\nu} &= \sum_{\sigma\mu} < \rho\mu|v|\nu\sigma >_A m_{\sigma\mu} \\ &\quad + \sum_{\sigma\sigma'\mu} < \rho\mu|v|\sigma\sigma' > G_{\sigma\sigma'\nu\mu} \\ &\quad - \sum_{\sigma\mu\mu'} < \mu\mu'|v|\nu\sigma > G_{\rho\sigma\mu\mu'}, \end{aligned} \tag{3.65}$$

and the equation for $G_{\rho\rho'\nu\nu'}$ remains the same as Eq. 3.56. So Eq. 3.65, together with Eq. 3.56, can be expressed in the matrix form

$$\begin{vmatrix} A_{11} & A_{12} \\ A_{21} & C_{22} \end{vmatrix} \begin{vmatrix} X_1 \\ X_2 \end{vmatrix} = w \begin{vmatrix} X_1 \\ X_2 \end{vmatrix}. \tag{3.66}$$

3.6 Summary

In this chapter, we discussed the time-independent form of *TDDM* and derived the small amplitude limit of *TDDM* by expanding ρ and C_2 about their ground state

values. The small amplitude limit of *TDDM* based on the *HF* state was compared with existing models. We found that *STDDM* reduces to

a) *RPA* if all the two-body correlation coefficients are neglected;

b) *SRPA* if we keep only $m_{\rho\nu}$, $m_{\nu\rho}$, $G_{\rho\sigma\nu\mu}$ and $G_{\nu\mu\rho\sigma}$;

c) and the shell model formalism in $1p-1h$ and $2p-2h$ space if we keep only the forward amplitudes $m_{\rho\nu}$ and $G_{\rho\sigma\nu\mu}$.

Thus *STDDM* is a more general theory than the above mentioned theories for small amplitude motions.

Chapter 4

Isoscalar quadrupole resonance

4.1 Introduction

Experimentally, a giant resonance is identified with a broad peak in inelastic scattering. The giant resonance can decay via particle emission as well as coupling to other complicated states. The width associated with the particle emission is often denoted as $\Gamma^{\uparrow}$ (called the escape width) and that associated with the coupling to complicated states is denoted as $\Gamma^{\downarrow}$ (called the spreading width).

The most commonly used microscopic theory in the study of giant resonance is the *RPA*. This theory predicts correctly the centroid energy of giant resonance. However *RPA* fails to give a width comparable with experimental value. *TDHF* has also been used in isoscaler giant resonance in light nuclei [Eng 75, Blo 79, Str 79, Cho 87]. The *TDHF* results are found to be the same as those of *RPA*. This is expected because *RPA* is the small amplitude limit of *TDHF*. *TDHF* as well as *RPA* are one-body theories. Therefore, they are not the appropriate tools to treat quantities of two-body nature like the spreading widths. In this chapter we are going to apply *TDDM*, which takes into account the two-particle correlations, to the isoscalar giant quadrupole resonance. We compare *TDDM* results with those given by *TDHF*. Because of the limitation of computational power, we can only apply *TDDM* to the light doubly-closed shell nuclei ^{16}O and ^{40}Ca.

The isoscalar giant quadrupole resonance (GQR), which is the subject of this chapter, has a positive parity, angular momentum $J = 2$ and is usually denoted as $E2^+$. The experimental centroid energies of the GQR are well described by [Spe 81]

$$E_c^{2+} = 65A^{-1/3}. \tag{4.1}$$

The strength of the resonance in medium- and heavy-mass nuclei exhausts 50-100% of the energy weighted sum rule limit. In light nuclei the strength is strongly fragmented.

The hydrodynamic picture of the quadrupole resonance is that of an an oscillating spherid changing back and forth from prolate to oblate shape. If the excitation has $\Delta T = 0$ (isoscalar), then the protons and neutrons oscillate in phase, i.e. they are compressed and expanded simultaneously. If $\Delta T = 1$ (isovector), then the protons and neutrons oscillate out of phase. This picture is illustrated by Fig. 4.1.

Microscopically the giant resonances are often described by the coherent superposition of single-*ph* excitations. For example the isoscalar GQR can be described as the superposition of those 1p-1h excitations which have the same parity and angular momentum assignment as the GQR. Fig. 4.2 illustrates this situation in a harmonic shell model. Since the uncorrelated *ph* transition crosses two major shells, GQR is a $2\hbar w$ excitation. This simple picture gives the correct A-dependent of the excitation energy, i.e. $E_c \sim A^{-1/3}$.

4.2 Small amplitude isoscalar quadrupole motions of ^{16}O and ^{40}Ca

4.2.1 Description of numerical method

As was discussed in chapter 3, solving the ground state in *TDDM* is a difficult task. In the following applications of *TDDM* we approximate the initial configuration by the *HF* ground state. Fig. 4.3 and Fig. 4.4 show the single particle levels used in

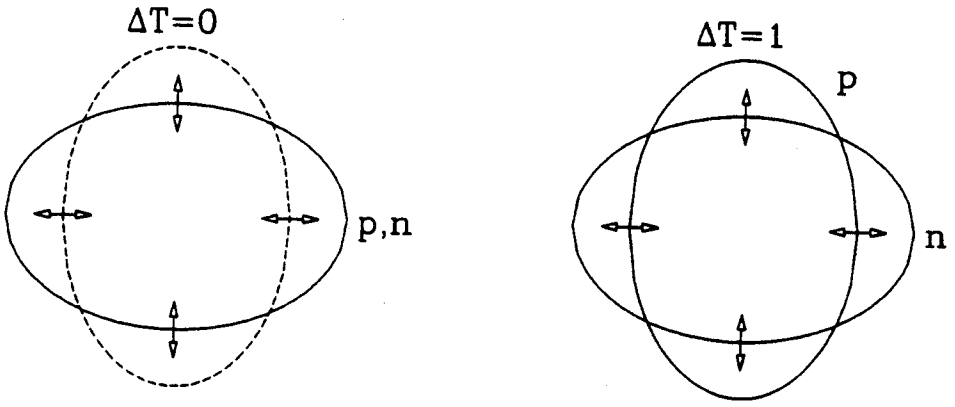

Figure 4.1: Schematic illustration of giant quadrupole resonance.

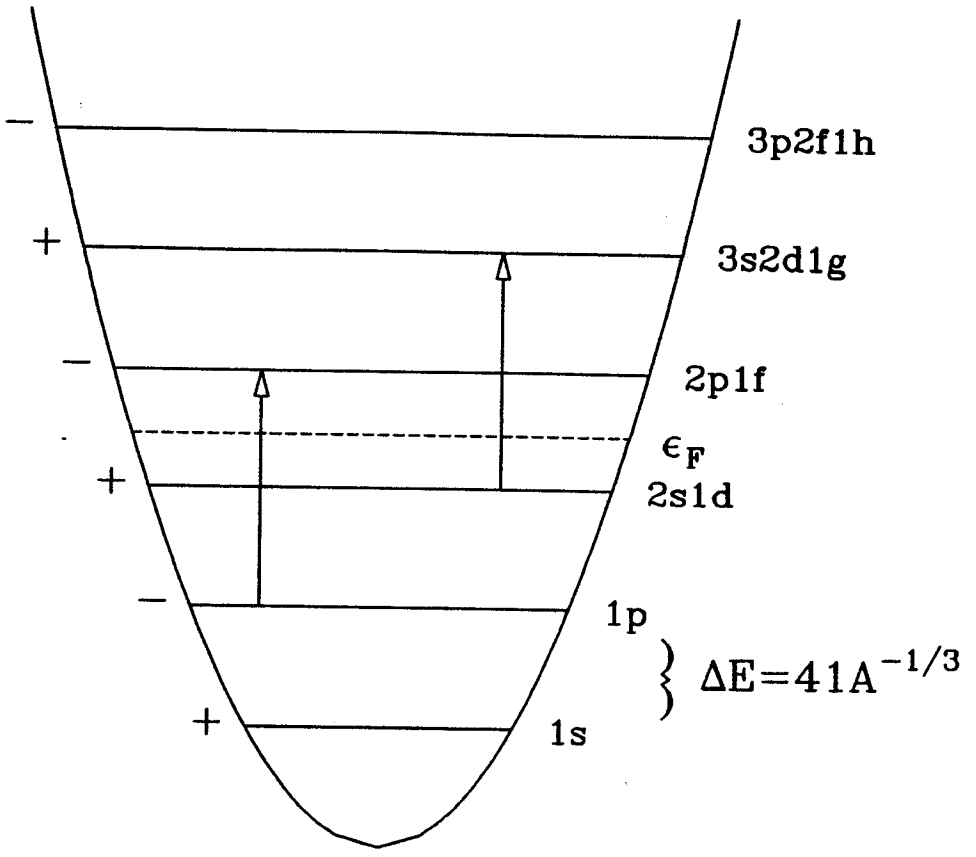

Figure 4.2: Quadrupole resonance in the harmonic oscillator shell model.

the calculation and their initial occupation. The static Hartree-Fock s.p. states are calculated with the imaginary time step method [Dav 80]. Since we assume complete spin-isospin degeneracy, each single particle level can be occupied by 4 particles. The quadrupole excitation is excited in a way similar to *TDHF* calculation i.e. by boosting each single particle wave function with a phase factor

$$\psi_\lambda(\vec{r}, t=0) = e^{i\alpha r^2 Y_{20}(\theta)}\phi_\lambda(\vec{r}), \tag{4.2}$$

where coefficient α (with dimension $[L^{-2}]$) is a parameter determining the amplitude of the motion and ϕ_λ is the *HF* single particle state. This phase factor provides a quadrupole velocity field as can be seen from the nucleon-current density

$$\begin{aligned} \vec{J}(\vec{r}) &= \frac{i\hbar}{2m}\sum_{\lambda=1}^{A}\{(\nabla\psi_\lambda^*)\psi_\lambda - \psi_\lambda^*\nabla\psi_\lambda\} \\ &= \frac{\alpha\hbar}{m}\rho(r)\nabla(r^2Y_{20}(\theta)), \end{aligned} \tag{4.3}$$

where we assume that the *HF* ground state has no current density. If the *HF* mean-field doesn't contain a non-local part, the excitation energy is contained in the kinetic energy part. Since the total current of *HF* configuration is zero, we have the excitation energy corresponding to the boosting as

$$\Delta E = \frac{\alpha^2\hbar^2}{2m}\int d^3r\rho(\vec{r})[\nabla r^2 Y_{20}(\theta)]^2. \tag{4.4}$$

To the first order of α, ansatz of Eq. 4.2 corresponds to a sudden acceleration by a quadrupole field. This can be shown by the following argument. Let h be the mean field hamiltonian and let us assume that the system is under an impulsive perturbation

$$V(\vec{r}, t) = -\delta(t)\alpha r^2\hbar Y_{20}(\theta). \tag{4.5}$$

The single particle wave function obeys the following equation

$$i\hbar\frac{\partial}{\partial t}\psi_\lambda(\vec{r}, t) = (h + V(\vec{r}, t))\psi_\lambda(\vec{r}, t). \tag{4.6}$$

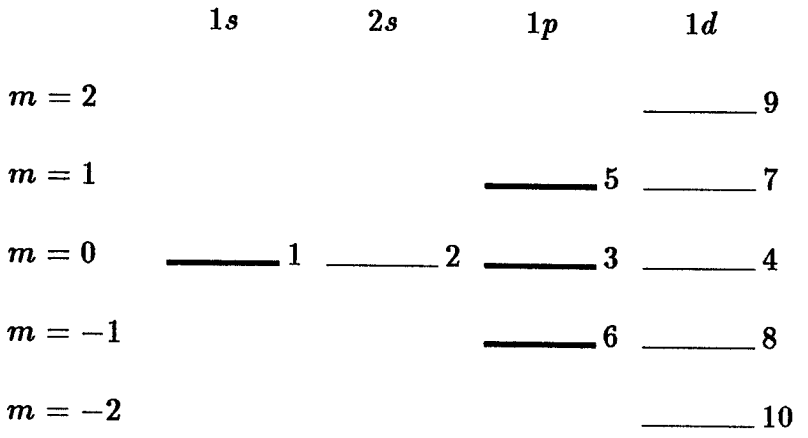

Figure 4.3: The numbering of s.p. levels for ^{16}O, the thick lines represent occupied states and thin lines represent unoccupied states.

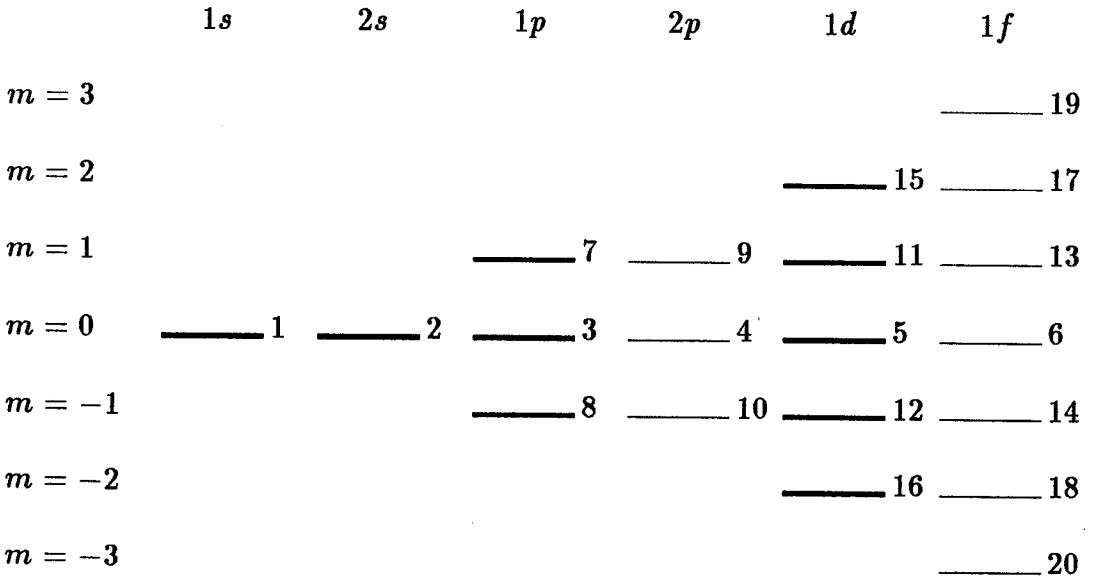

Figure 4.4: The numbering of s.p. levels for ^{40}Ca, the thick lines represent occupied states and thin lines represent unoccupied states.

Integrating the above equation over a small time interval, we obtain

$$\psi_\lambda(\vec{r}, t = 0^+) = (1 + i\alpha r^2 Y_{20}(\theta))\phi_\lambda(\vec{r}). \tag{4.7}$$

Thus Eq. 4.7 is equivalent to Eq. 4.2 to first order in α. In our calculation we choose the value of α in such range that the above derivation is valid.

A detailed general description of the numerical method used in solving *TDHF* equation can be found in Ref. [Bon 76, Dav 81]. In this section we only point out the particular aspect in our calculation. The *TDHF* equation involves coordinates of three dimensions. It is reduced to a two-dimensional one by assuming axial symmetry. In order to reduce the single particle space we assume complete spin-isospin degeneracy. The effective interaction which provides the mean field is the Bonche-Koonin-Negele force [Bon 76]

$$v(\vec{r}, \vec{r'}) = t_0\delta(\vec{r} - \vec{r'}) + \frac{1}{6}t_3\rho\delta(\vec{r} - \vec{r'}) + V_0\frac{e^{-|\vec{r}-\vec{r'}|/a}}{|\vec{r} - \vec{r'}|/a}P + \text{Coulomb}, \tag{4.8}$$

where $t_0 = -497.726$ MeVfm^3, $t_3 = 17270$ MeVfm^6, $aV_0 = -166.9239$ MeV fm, $a_0 = 0.45979$ fm and the operator $P = \frac{16}{15} + \frac{4}{15}P_x$ with P_x as the space exchange operator. In calculating the mean field, the spin-orbit coupling is not taken into account. The most time comsuming part of the numerical calculation is to solve the equations of motion for $n_{\lambda\lambda'}$ and $C_{\alpha\beta\alpha'\beta'}$. To make the calculation feasible we use the residual interaction of a δ-function form $v = v_0\delta^3(r - r')$ with $v_0 = -300$MeV fm^3. This value of the strength is so chosen that it gives a) a free nucleon-nucleon cross section of 40mb in the Born approximation and b) an approximate depth of the nuclear mean field potential for nuclear matter. Later we will see that this interaction strength also gives reasonable widths of the quadrupole strength distribution. Eq. 2.22 and 2.23 are solved with the Runge-Kutta method. The space mesh sizes for both longitudinal and transverse direction are set to be 0.4 fm and the size of time step is 0.25×10^{-23}second. The orthonormal property for s.p. states is well conserved. For example the deviation of total particle numbers is less than 0.2%.

The initial occupation coefficients are assigned according to Fig. 4.3 and Fig. 4.4. To avoid a sudden change in the correlation coefficients during the initial stage, we calculate their initial values using the Born approximation i.e. the static solution of Eq. 2.23 with only the Born term.

For the calculation of quadrupole motion, the two-dimensional *TDHF* program described in Ref. [Dav 81] is modified to calculate only one nucleus. We implement a subroutine which solves the equations of motion for $n(t)$ and $C(t)$ (Eq. 2.22 and Eq. 2.23). Because $C(t)$ is a four-dimension array, this subroutine consumes most of the total CPU. The number of single particle states used is 10 (Fig. 4.3) for ^{16}O and 20 (Fig. 4.4) for ^{40}Ca. In principle, the total number of elements of $C(t)$ is N^4_{orbit}, where N_{orbit} is the number of orbits. Due to symmetries imposed, both $n(t)$ and $C(t)$ are sparse matrices. The number of non-zero matrix elements of $C(t)$ is about $\frac{1}{10}N^4_{orbit}$. The *TDHF* code passes the single particle wave functions to this subroutine at each time step and this subroutine passes the occupation matrix to the *TDHF* code. The one-body density is now calculated with the occupation matrix and single particle wave functions. In the calculations shown later, the number of time steps is about 600. For a calculation which includes all the terms of Eq. 2.23 each time step takes about 1 minute CPU in VAX8530 in case of ^{16}O and 5 minutes in case of ^{40}Ca. These values are about 70 times of those needed for *TDHF* calculation.

4.2.2 Ground state

The initial *HF* ground state evolves in time because it is not a solution of *TDDM*. Here we discuss the time evolution of the *HF* state (before being boosted by Eq. 4.2). The total energy shown in Fig. 4.5 is conserved quite well, indicating the accuracy of numerical calculation. However, the oscillation seen on the correlation and *HF* energies indicates the mixing of various configurations. We call the state as "calculational ground state". In Fig. 4.7 we show the evolution of the r.m.s. radius of

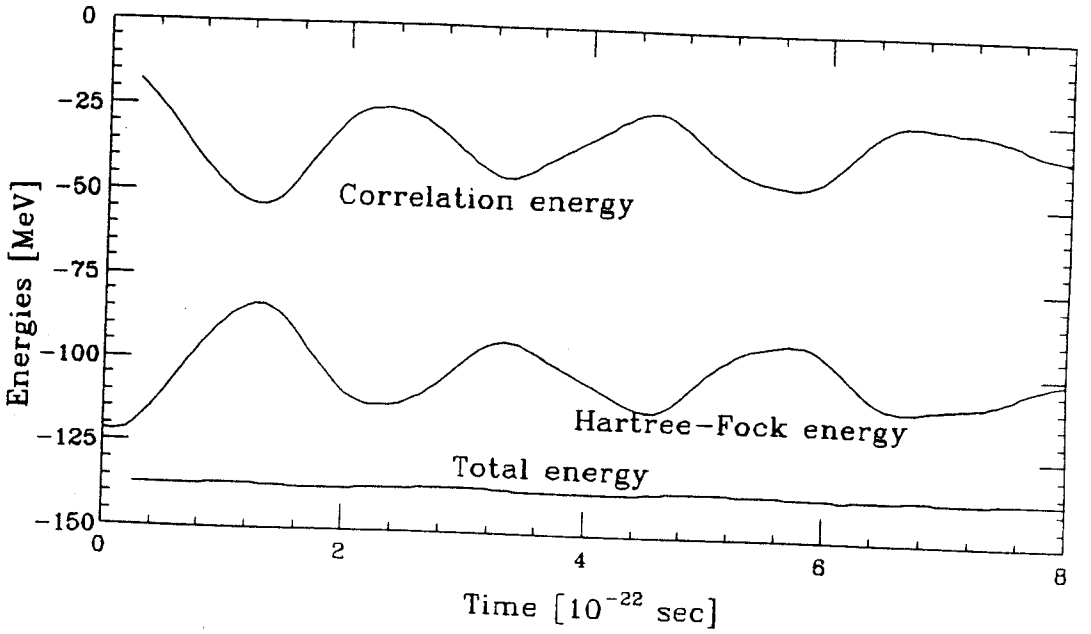

Figure 4.5: "Ground state" energies of ^{16}O starting from a pure *HF* configuration.

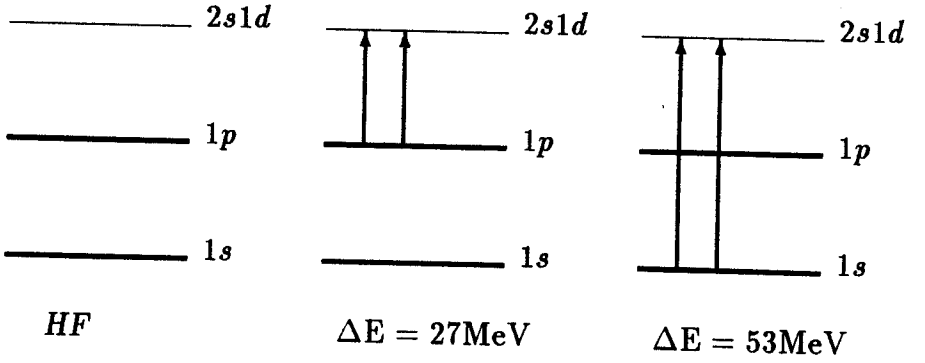

Figure 4.6: Illustration of the three states used to estimate the true ground state of ^{16}O, thick lines represent the occupied levels and thin lines represent the unoccupied levels.

^{16}O from the Hartree-Fock value. The fluctuation is about 4% of the average r.m.s. radius. In Fig. 4.8 we show the time evolution of the quadrupole moment of the same configuration and the fluctuation is very small. The quadrupole motion which will be shown in section 4.3 are excited from this calculational ground state. What we are interested in, however, is the quadrupole resonance built on the true ground state which is a solution of *TDDM*. We therefore need to estimate the mixing rate of the true ground state with the calculational ground state. For this purpose we make a simple estimation of the percentage which the true ground state possesses in the calculational ground state for ^{16}O. First we assume that the calculational ground state consists of the *HF* state and 2p-2h configurations. To make the estimation simple, we further assume that there are two kinds of $2p-2h$ states: 2p-2h states made of the 1p to 2s1d excitations, and those which consist of the 1s to 2s1d excitations. These are illustrated in Fig. 4.6. Because the other kinds of transitions have negative parity they are neglected. Since the 2s1d states are almost degenerate, the problem may be replaced by the three-level problem given by the following 3×3 matrix

$$\begin{vmatrix} 0 & < HF|v|1p \rightarrow 2s1d > & < HF|v|1s \rightarrow 2s1d > \\ < 1p \rightarrow 2s1d|v|HF > & \Delta E(1p \rightarrow 2s1d) & 0 \\ < 1s \rightarrow 2s1d|v|HF > & 0 & \Delta E(1s \rightarrow 2s1d) \end{vmatrix},$$

where we neglect the coupling between 2p-2h states. To calculate these matrix elements, we make use of the initial correlation energy (Eq. 2.36) given in the Born approximation. The initial correlation energy is -16 MeV as shown in Fig. 4.5. The contribution from the $1p \rightarrow 2s1d$ transition is found to be -14 MeV whereas that from $1s \rightarrow 2s1d$ is -2 MeV. Since the initial correlation energy is expressed as the interaction matrix element divided by the single particle energy difference, the average interaction matrix element can be roughly estimated by the known values of correlation energy and the single particle energy difference. The coupling matrix elements

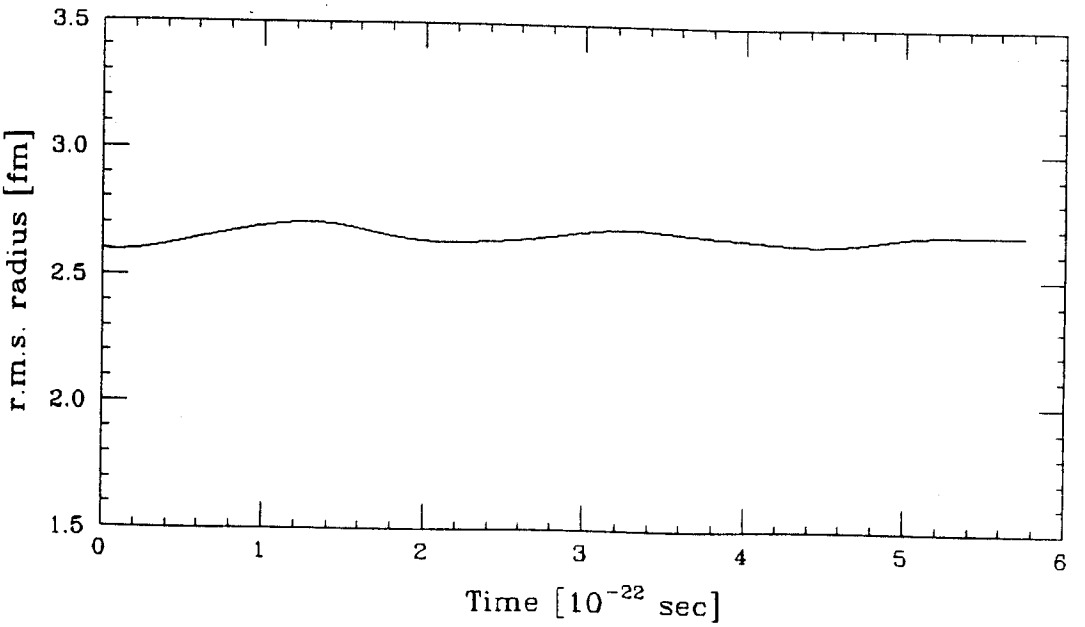

Figure 4.7: Time evolution of the r.m.s. radius of ^{16}O starting from a *HF* configuration.

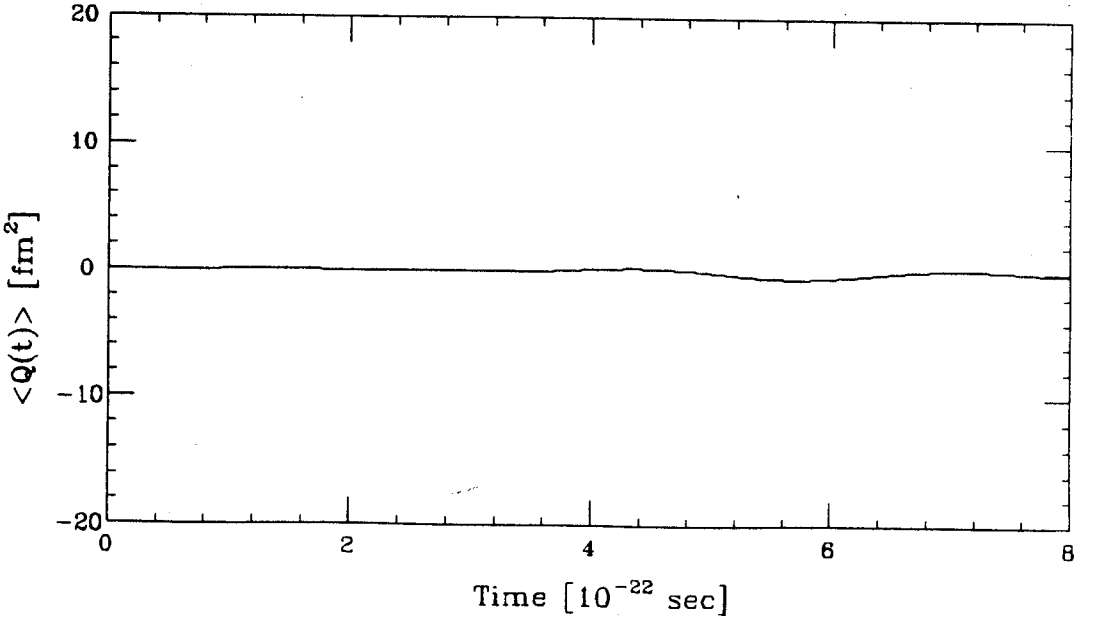

Figure 4.8: Time evolution of the quadrupole moment of ^{16}O starting from a *HF* configuration.

thus estimated are as follows (in MeV):

$$\begin{vmatrix} 0 & 19 & 11 \\ 19 & 27 & 0 \\ 11 & 0 & 53 \end{vmatrix}. \tag{4.9}$$

After diagonalizing the above matrix we found that the component of the true ground state mixed in the *HF* inital state is about 79%. This value is close to a shell model calculation done by Hoshino et al. [Hos 88].

4.3 Results and discussion

We first show the time dependence of the quadrupole moment defined as

$$< Q(t) >= \int d^3r\rho(\vec{r})r^2Y_{20}(\theta). \tag{4.10}$$

We calculate the quadrupole moments of ^{16}O in three different models: *TDDM*, *TDDM'* and *TDHF*. Here *TDDM'* means that only the Born term of Eq. 2.23 is included in the calculation. For ^{40}Ca the moments are calculated only in *TDDM* and *TDHF*. The results are plotted in Fig. 4.9 and Fig. 4.10. The results calculated in *TDDM'* and *TDHF* show very little damping, but those calculated in *TDDM* have oscillation patterns which are quite different. The non-harmonic pattern found in the *TDDM* results indicates that the quadrupole motion is the superposition of several harmonic motions with different frequencies. To discuss the differences between the results of *TDDM* and *TDHF* in more detail, we look at a useful quantity called strength function.

The strength function is defined as

$$S(w) = \sum_n | < n|V|0 > |^2\delta(E - E_n). \tag{4.11}$$

Here V is the operator which causes the excitation and $E_n = \hbar w_n$ is the excitation

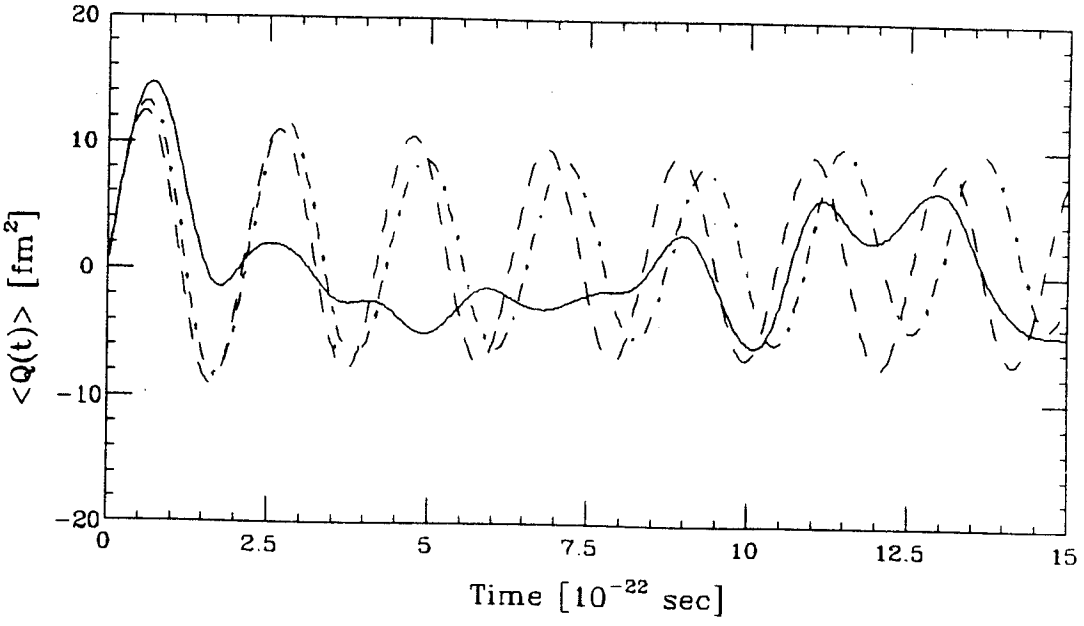

Figure 4.9: Quadrupole moments as function of time for ^{16}O, the solid line is calculated in *TDDM*, dot-dashed line in *TDDM'* and the dashed line in *TDHF*.

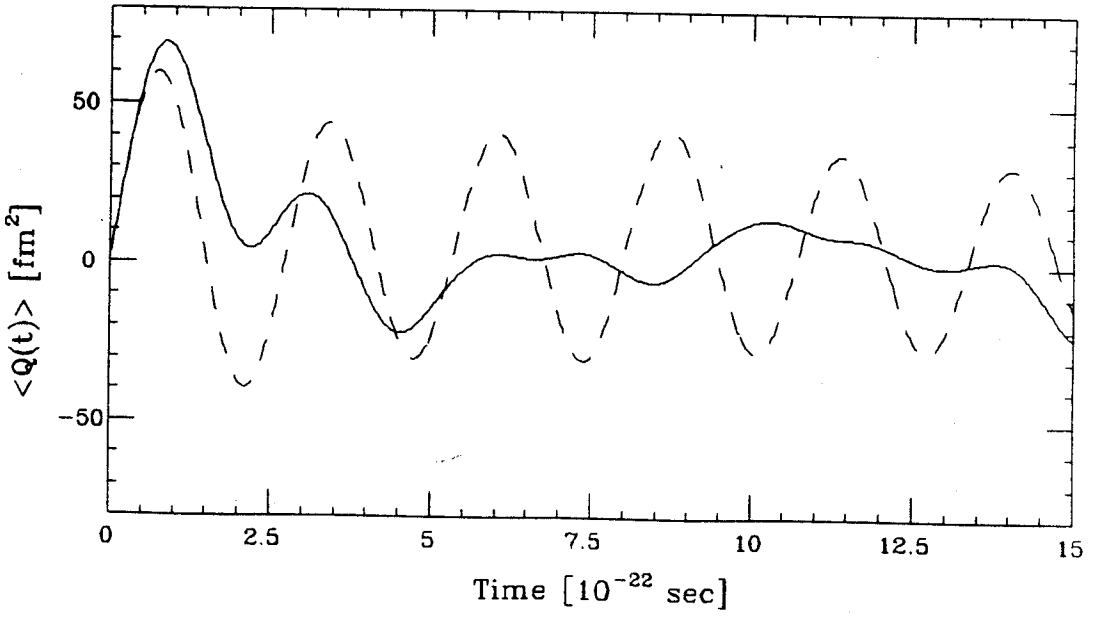

Figure 4.10: Quadrupole moments as function of time for ^{40}Ca, the solid line is calculated in *TDDM* and the dashed line in *TDHF*.

energy of the eigenstate $|n>$. In our calculation

$$V = \sum_{i}^{A} Q(\vec{r}_i), \quad Q(\vec{r}) = r^2 Y_{20}(\theta). \tag{4.12}$$

The relation between the quadrupole moment and strength function is derived in appendix A. Here we only write down the final result (Eq. A.14)

$$S(w) = \frac{1}{\pi\alpha\hbar}\int_0^\infty < Q(t) > \sin wt dt. \tag{4.13}$$

We perform Fourier transformation of the quadrupole moments given in Fig. 4.9 and Fig. 4.10. The calculated strength functions are plotted in Fig. 4.11– 4.14. Since we only have finite numbers of points, the Fourier transformation of the low frequency contains spurious components. So we only present those components whose frequencies are higher than 10 MeV. Of course, this number is rather arbitrary. These *TDDM* strength functions have a broad distribution and the width of ^{16}O is larger than that of ^{40}Ca. If we fit the distributions with Gaussian function, the widths for both strength functions are roughly 8 MeV (^{16}O) and 5 MeV (^{40}Ca). These values are qualitatively in agreement with experiments [Kno 75, Mos 75] and shell model calculations [Hos 76, Hos 88, Knu 76]. In contrast to *TDDM*, the results of *TDHF* are centralized peaks corresponding to the harmonic temporal behaviours. The sharp distributions seen in the *TDHF* strength functions are in coincidence with the *RPA* calculations [Ber 75].

In the following we discuss why *TDDM'* gives small damping widths. In Sec. 3.4 we showed that *SRPA* can be derived from the small amplitude limit of *TDDM*. The neglect of higher-order terms in *TDDM'* corresponds to the neglect of the interaction between $2p-2h$ states in *SRPA*. A numerical calculation based on this version of *SRPA* was done by Drozdz et al. [Dro 86], in which the spreading of strength function is not found either. Therefore, Drozdz's result and *TDDM'* calculation indicate that merely introducing the coupling between 1p-1h space and 2p-2h space does not

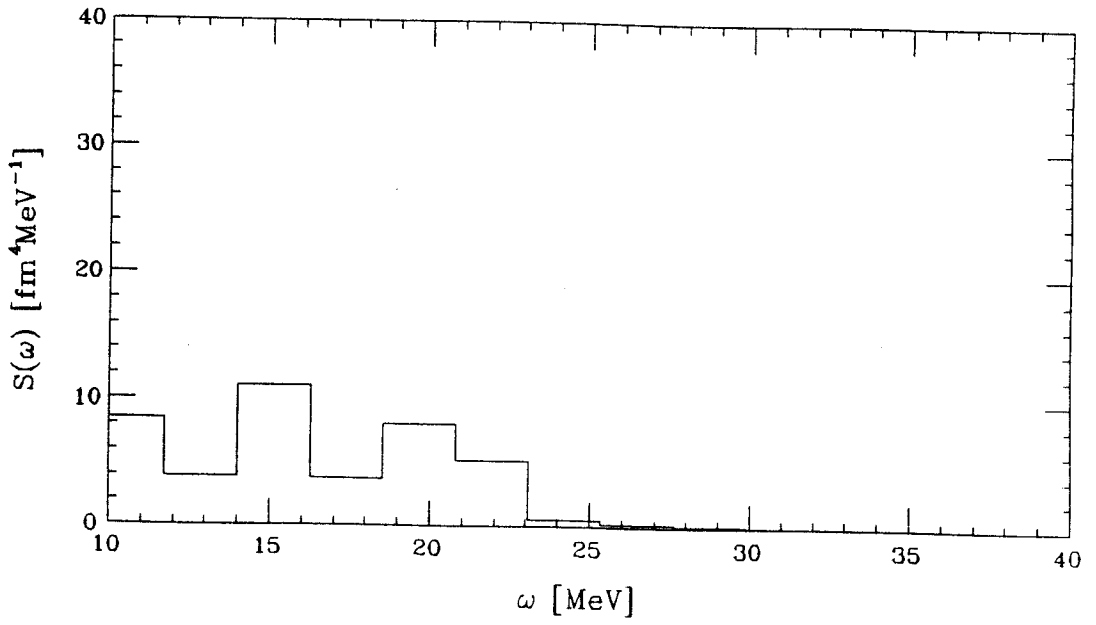

Figure 4.11: Quadrupole strength distribution calculated in *TDDM* for ^{16}O.

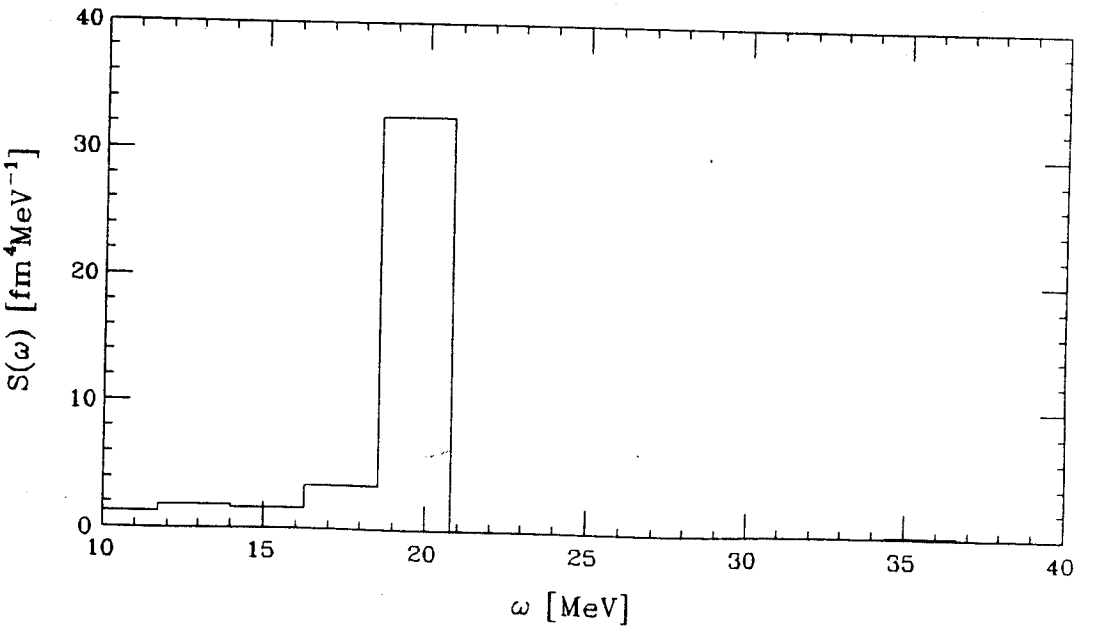

Figure 4.12: Quadrupole strength distribution calculated in *TDHF* for ^{16}O.

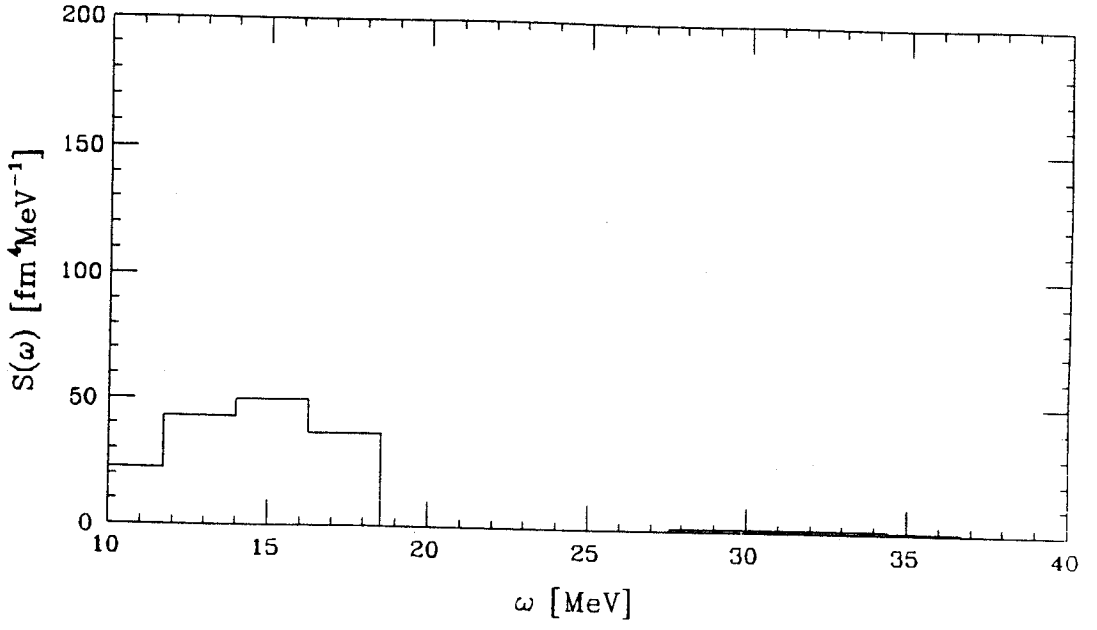

Figure 4.13: Quadrupole strength distribution calculated in *TDDM* for ^{40}Ca.

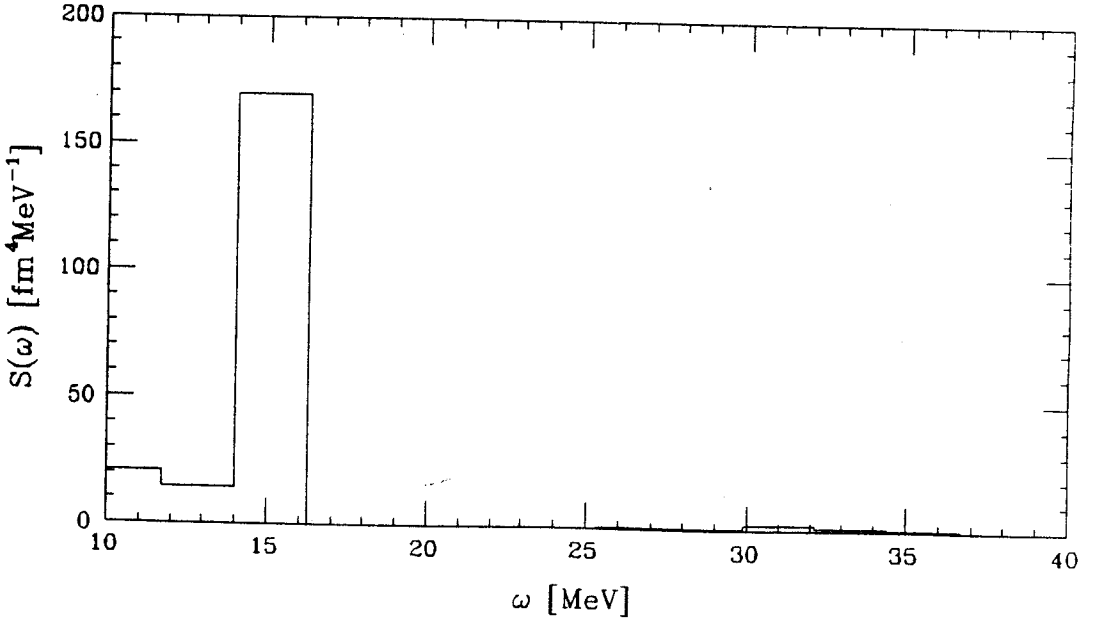

Figure 4.14: Quadrupole strength distribution calculated in *TDHF* for ^{40}Ca.

cause redistribution of strength. Using the single-particle states employed in the shell model calculation done by Knüpfer and Huber [Knu 76], we discuss this point further. Fig. 4.15 shows the energy levels used in their calculation and Fig. 4.16 gives the possible unperturbed states generated by the 1p-1h and 2p-2h excitations. The residual interaction between the $1p-1h$ states produces a coherent state which exhausts most of the strength [Rin 80]. The coherent state found in Ref. [Knu 76] is located at $E_x = 21$ MeV which is much lower than the unperturbed 2p-2h states. Because this $1p-1h$ coherent state is located far away from the unperturbed $2p-2h$ states, the coupling between them does not give any spreading of the strength. The broadening of the strengths in *TDDM* and in the shell model calculations is caused by the residual interaction between the 2p-2h states. This residual interaction redistributes the 2p-2h states.

Here we point out that the spreading of strength function also depends on the strength of residual interaction. In Fig. 4.17 and 4.18 we show the strength functions which are calculated in *TDDM* with $v_0 = -250\text{MeV} \cdot \text{fm}^3$ and $v_0 = -212\text{MeV} \cdot \text{fm}^3$, respectively. The spreading of strength function reduces when the $|v_0|$ becomes small. The centroid energy is also shifted upward when $|v_0|$ becomes small.

Another quantity which can be compared with experiment is the centroid energy of the distributions. All the centroid values given in our calculation are smaller than the empirical values described by Eq. 4.1. Krewald et al [Kre 77] find that the position of the 1p-1h coherent state calculated in *RPA* depends on the effective interaction used to generate the mean field. They use several effective interactions (SkII, SkIII, SkIV, SkV and Sk-LB) in their *RPA* calculation. The position of the coherent state for ^{16}O is found to be always lower than the empirical centroid given by Eq. 4.1. SkIII and Sk-LB give lower excitation energies than the other interactions and the values are similar to our *TDHF* result. The position of the coherent 1p-1h state may be sensitive to the effective mass. SKIII and Sk-LB have larger effective masses than

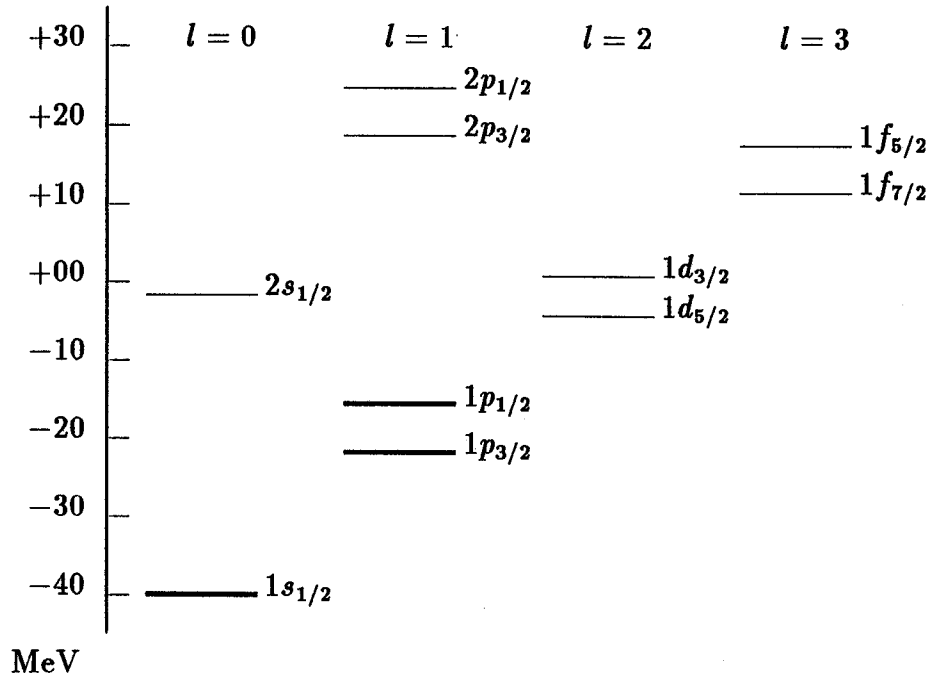

Figure 4.15: The s.p. levels for ^{16}O, thick lines are occupied state, thin lines are empty.

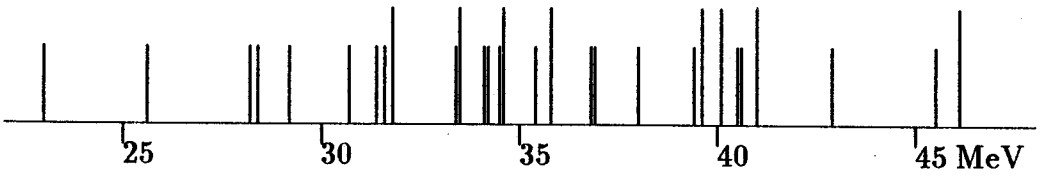

Figure 4.16: The excitation energies at the unperturbed states are shown for the isoscalar $E2^+$ transition in ^{16}O. The long vertical lines are those of $1p-1h$ states and the short lines are those of $2p-2h$ states.

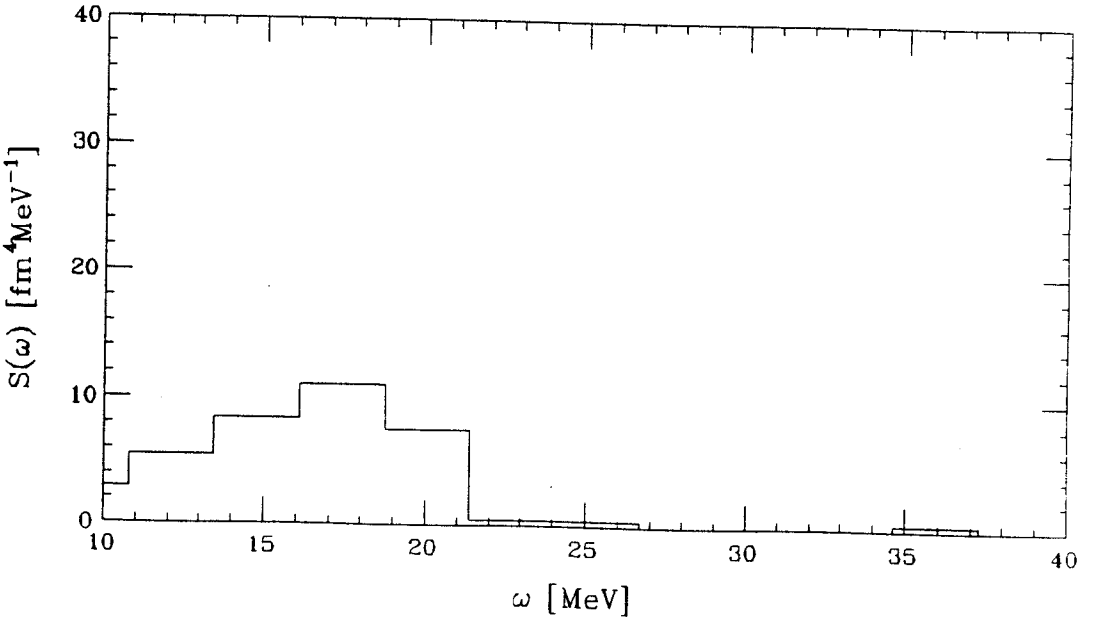

Figure 4.17: Strength function calculated in *TDDM* for ^{16}O with residual interaction $v_0 = -250$ MeV $\cdot$ fm^3.

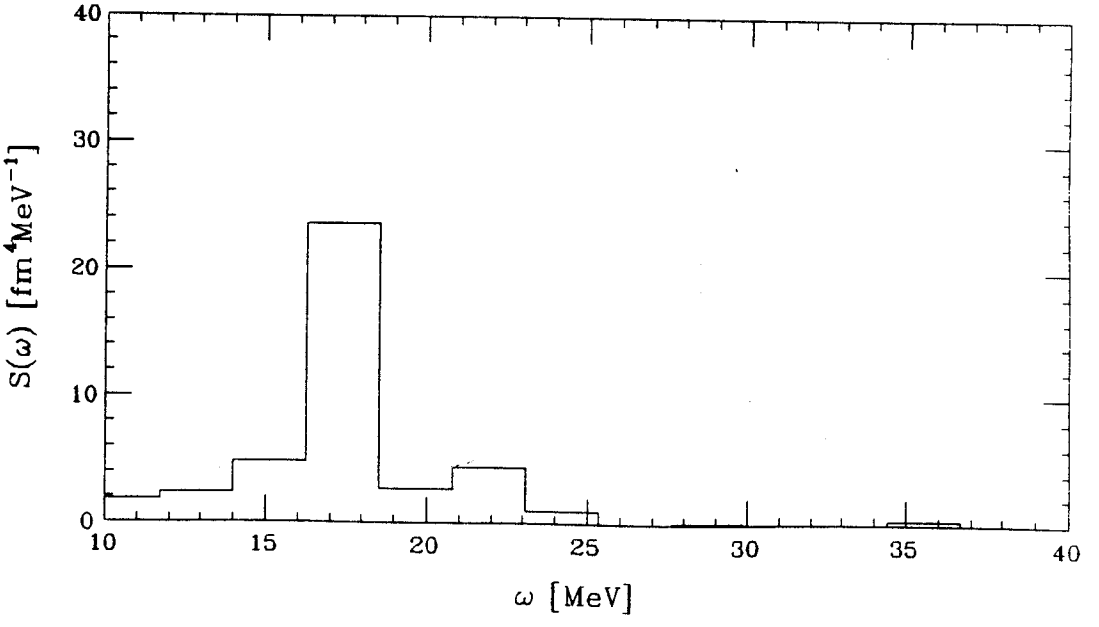

Figure 4.18: Strength function calculated in *TDDM* for ^{16}O with residual interaction $v_0 = -212$ MeV $\cdot$ fm^3.

the other interactions; the values are about 0.75 and 0.8, respectively. The effective interaction used in our calculation has effective mass 1. The difference between the *TDDM* centroid energy and the *TDHF* one is larger in ^{16}O than in ^{40}Ca. We interpret this in the following way. The level density of 2p-2h states is lower in ^{16}O than in ^{40}Ca. For ^{16}O some of the perturbed 2p-2h states are distributed on the lower-energy side of the coherent state. So the centroid of the distribution is down shifted as compared to the *TDHF* result. Since its 2p-2h level density is low, the strength distribution in ^{16}O is sensitive to the location of the perturbed 2p-2h states, i.e. to the residual interaction. The two shell model calculations [Hos 76, Knu 76] use different residual interactions and give quite different strength distributions. Our result is closer to the calculation by [Knu 76]. In case of ^{40}Ca the coherent state is embedded in the denser distribution of the perturbed 2p-2h states, therefore, the centroid of the distribution is hardly shifted.

The sum rule which is most often used to compare the theoretical calculation with experiment is the so called energy-weighted sum rule (*EWSR*)[1]. A general form of *EWSR* is as follows

$$\sum_n (E_n - E_0)| < n|V|0 > |^2 = \int d^3r \rho_0 \frac{(\nabla V)^2}{2m}. \tag{4.14}$$

Here ρ_0 is the ground state density and $V(\vec{r})\delta(t)$ is the impulsive perturbative field. For the quadrupole field used in our calculation we have

$$\sum_n (E_n - E_0)| < n|V|0 > |^2 = \frac{3A < r^2 >}{4\pi m}, \tag{4.15}$$

where A is the mass number. In calculating the sum rule limit (r.h.s of Eq. 4.15) we use $< r^2 >= 6.76\text{fm}^2$ for ^{16}O, and 11.3 fm^2 for ^{40}Ca. These two values of r.m.s. radii are the results of *HF* calculation using the same force as that used in *TDDM*. Using Eq. 4.11, the sum rule is related to the calculated strength as

$$\sum_n (E_n - E_0)| < n|V|0 > |^2 = \int S(w) w dw. \tag{4.16}$$

[1]For a derivation of this sum rule, one can refer to [Ber 83].

Table 4.1: Calculated strength S, expressed as percent of the energy-weighted sum rule limit.

%	TDDM	TDHF	Shell Model	RPA
^{16}O	82	92	91	90
^{40}Ca	68	92	80	

In the r.h.s. of Eq. 4.16 we exclude those whose frequencies are lower than 10 MeV. The ratio of EWSR to the sum rule limit are shown in Table 4.1. The shell model values are taken from Ref. [Hos 76] and the *RPA* values are taken from Ref. [Kre 77] in which the Skyrme II interaction is used. The percentage of EWSR in *TDHF* is comparable with those given by *RPA* calculation with Skyrme interaction [Kre 77], which is about 90% (^{16}O). The *TDDM* values are smaller than those of shell model calculation. In *TDDM* calculation the strength functions disperse over a wide energy range and the exclusion of low frequency components gives some ambiguities to *TDDM* values shown in Table 4.1. The experimental values vary from different probes used[2] and are smaller than the theoretical calculations.

4.4 Summary

In this chapter we studied the isoscalar quadrupole motion in ^{16}O and ^{40}Ca using both *TDDM* and *TDHF*. Similar to the *RPA* calculation, the *TDHF* calculations do not show spread width of the isoscalar motion. In the *TDDM* calculation the spreading widths in both nuclei are well reproduced. It is found that the higher-order terms which describe correlations among the $2p-2h$ excitations are essential to the spreading. Similar results are found in shell model calculations which includes $2p-2h$ correlations.

[2] A summary of experiments is given in table II of ref. [Hos 76].

Chapter 5

Heavy-ion reactions

5.1 Introduction

In chapter 4 we have applied *TDDM* to the small amplitude quadrupole motions. However, as stated in Chapter 1 *TDDM* is devised to treat large amplitude motions e.g. heavy-ion collisions. In this chapter, we apply *TDDM* to fusion reactions and deep-inelastic heavy-ion collisions(*DIC*).

In the low energy heavy-ion collisions, fusion is observed when the colliding energy is near or above the Coulomb barrier. *TDHF* has extensively been applied to fusion reactions above the Coulomb barrier. An interesting finding of such *TDHF* calculations is that a colliding system does not fuse in the low orbital angular momentum region when the incident energy is high enough. The low-l no-fusion threshold energy for $^{16}O+^{16}O$ is found to be about 54 MeV [Dav 85]. However, this prediction of *TDHF* has not been supported by experiments [Kox 80, Laz 81, Tol 81, Ike 86]. One of the attempts trying to solve this problem was given by Umar et al. [Uma 86]. They included the spin-orbit force, which has been neglected in previous *TDHF* calculations, into the mean field calculation and found that the low-l no-fusion window threshold energy was raised to 146 MeV. Tohyama included the nucleon-nucleon (NN) collision effect into the *TDHF* calculation [Toh 87] and found that the no-fusion threshold energy also lay around 145 MeV. His calculation included only the Born term of

Eq. 2.23. In this chapter we re-examine this problem for $^{16}O + ^{16}O$ in *TDDM* which takes into account the higher-order correlations (i.e. H and P terms of Eq. 2.23).

One characteristic aspect of the *DIC* is the broad distributions of observables such as mass and charge [Sch 84]. The most fundamental theory so far applied to *DIC* is *TDHF* [Neg 82, Dav 85]. Although the mean values of one-body observables in *DIC* are reproduced in *TDHF*, their fluctuations predicted in *TDHF* were found to be quite small. For example the mass dispersion calculated in *TDHF* for heavy systems are one order of magnitude smaller than experimental data [Dav 85]. This difficulty is due to the one-body nature of *TDHF* : the total wave function in *TDHF* is restricted to a single Slater determinant which is inadequate to evaluate the expectation values of two-body operators e.g. dispersion of one-body quantities [Das 79]. So far a few microscopic approaches have been proposed to treat the fluctuations better. Yamaji and Tohyama included 2p–2h configurations [Yam 84] in a perturbative way. They found that the mass dispersion in $^{16}O + ^{40}Ca$ are enhanced by a factor of 3 as compared to *TDHF* results. However, the effects of nucleon-nucleon (*NN*) collisions on the dynamics of the heavy-ion collision are neglected in their approach. The other calculations done by Bonche and Flocard [Bon 85] and Marston and Koonin [Mar 85] are based on the variation principle proposed by Balian and Véneroni [Bal 81] which gives a method to calculate the fluctuations in the framework of a mean field theory. The numerical results for $^{16}O + ^{16}O$ and $^{40}Ca + ^{40}Ca$ showed 30% $\sim$ 400% increase in the mass dispersion. The *NN* collision effects on the dynamical development of the colliding system, however, are not included in this approach either.

Since *TDDM* provides us with the two-body density matrix as well as the one-body density matrix, it is straightforward to calculate the fluctuations of one-body observables. In this chapter we also study whether *TDDM* gives large enough fluctuations to overcome the difficulty in *TDHF*.

We study the mass dispersion in $^{16}O + ^{16}O$ which is the largest system we can han-

dle for the present. Since no experimental data are available on the mass dispersion in $^{16}O + ^{16}O$, we compare our results with those calculated in a transport theory called the nucleon exchange transport model (*NET*) [Ran 78, Ran 79, Ran 82]. *NET* has been successful in reproducing experiment data for various systems [Sch 84]. Therefore, the results in *NET* for $^{16}O + ^{16}O$ are considered to be "empirical" values. In the comparison between *NET* and *TDDM*, basic macroscopic parameters in *NET* are obtained from quantities calculated in *TDDM*.

5.2 Mass invariance

In this section we present an expression for the mass dispersion in *DIC*. *DIC* is a binary collision and there are two excited nuclei in the final state. To count the number of the particles in one of the nuclei, we introduce the following number operator

$$\hat{N} = \int_R a^\dagger(\vec{r}) a(\vec{r}) d^3r, \tag{5.1}$$

where the creation and annihilation operators are denoted with $a^\dagger$ and a. and the integral is for half of the space [Dav 85]. The mass dispersion is defined as follows

$$\sigma_R = \sqrt{< \hat{N}^2 > - < \hat{N} >^2}, \tag{5.2}$$

where $< \cdot >$ means the expectation value. Since σ_R^2 contains a two-body operator, the mass dispersion can be expressed with both the one-body and two-body density-matrix,

$$\begin{aligned} \sigma_R^2 &= \int_R d\vec{r} \rho(\vec{r};\vec{r}) - \int_R d\vec{r}_1 d\vec{r}_2 \rho(\vec{r}_1;\vec{r}_2)\rho(\vec{r}_2;\vec{r}_1) \\ &+ \int_R d\vec{r}_1 d\vec{r}_2 c_2(\vec{r}_1\vec{r}_2;\vec{r}_1\vec{r}_2). \end{aligned} \tag{5.3}$$

Here c_2 is the two-body correlation function. Eq. 5.3 can be written in terms of $n_{\alpha\beta}$ and $C_{\alpha\beta\alpha'\beta'}$

$$\sigma_R^2 = \sum_{\alpha\beta} n_{\alpha\beta} < \beta|\alpha >_R$$

$$+ \sum_{\alpha\beta\alpha'\beta'} < \alpha'|\alpha >_R < \beta'|\beta >_R (C_{\alpha\beta\alpha'\beta'} - n_{\alpha\beta'} n_{\beta\alpha'}), \tag{5.4}$$

where $< \alpha|\beta >_R$ is the overlap integral of the two single-particle states α and β in the half space. Since $n_{\alpha\beta} = \delta_{\alpha\beta}$ and $C_{\alpha\beta\alpha'\beta'} = 0$ in *TDHF*, σ_R in *TDHF* simplifies

$$\sigma^2_{RTDHF} = \sum_{\lambda=1}^{A} < \lambda|\lambda >_R - \sum_{\lambda,\lambda'}^{A} < \lambda|\lambda' >_R < \lambda'|\lambda >_R, \tag{5.5}$$

where A is the total number of nucleons.

The experimental mass distribution in *DIC* are well approximated by the gaussian distribution [Sch 84] (Fig. 5.1). For the gaussian distribution the full width at half maximum Γ (*FWHM*) is related to σ_R via

$$\Gamma = \sqrt{8 \ln 2}\ \sigma_R. \tag{5.6}$$

Since the total system is an eigenstate of the total number operator, the dispersion for the entire space must be zero

$$\begin{aligned} \sigma^2_{\text{total}} &= \sum_{\alpha} n_{\alpha\alpha} + \sum_{\alpha\beta} (C_{\alpha\beta\alpha\beta} - n_{\alpha\beta} n_{\beta\alpha}) \\ &= A + \sum_{\alpha\beta} (C_{\alpha\beta\alpha\beta} - n_{\alpha\beta} n_{\beta\alpha}) \\ &= 0. \end{aligned} \tag{5.7}$$

where $< \alpha|\beta >_{\text{total}} = \delta_{\alpha\beta}$ is used. *TDHF* conserves this condition because $C_{\alpha\beta\delta\gamma} = 0$ and $n_{\alpha\beta} = \delta_{\alpha\beta}$.

To show that *TDDM* also satisfies Eq. 5.7, we use the explicit expression for the equation of motion for $C_{\alpha\beta\alpha'\beta'}$ (Eq. 2.23);

$$i\hbar \dot{C}_{\alpha\beta\alpha'\beta'} = B_{\alpha\beta\alpha'\beta'}(t) + H_{\alpha\beta\alpha'\beta'}(t) + P_{\alpha\beta\alpha'\beta'}(t). \tag{5.8}$$

The time derivative of $\sum_{\alpha\beta} C_{\alpha\beta\alpha\beta}$ consists of three terms as can be seen from the above equation. Using the fact that the matrix element of the interaction is antisymmetrized, it is straightforward to show that the Born terms has no contribution;

$$\sum_{\alpha\beta} B_{\alpha\beta\alpha\beta} = 0. \tag{5.9}$$

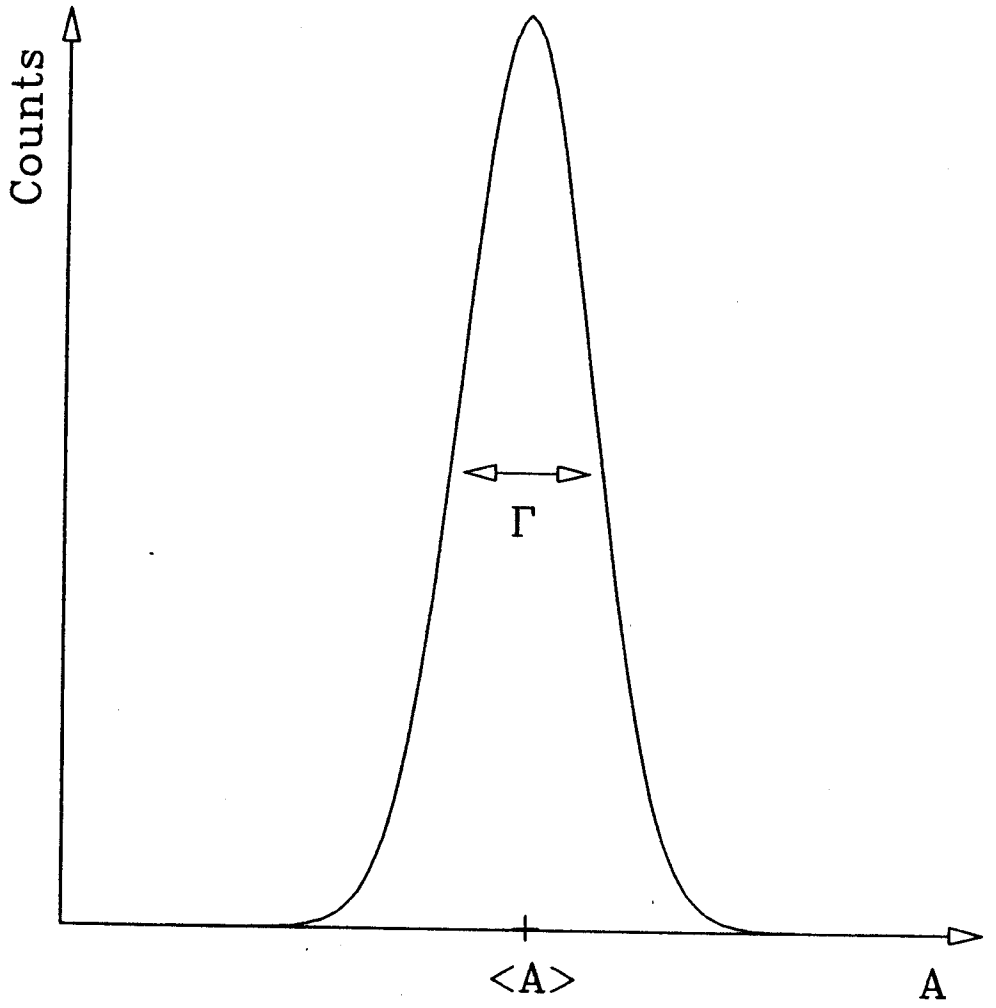

Figure 5.1: A hypothetical mass distribution having the shape of gaussian function

In the sum of the higher-order contributions (H and P) several terms are canceled and remaining terms are summarized as

$$\begin{aligned}\sum_{\alpha\beta} H_{\alpha\beta\alpha\beta} &= -2 \sum_{\alpha\beta\lambda_2\lambda_3\lambda_4} < \alpha\lambda_2|v|\lambda_3\lambda_4 >_A n_{\lambda_3\beta} C_{\beta\lambda_4\alpha\lambda_2} \\ &\quad +2 \sum_{\lambda_1\lambda_2\lambda_4\alpha\beta} < \lambda_1\lambda_2|v|\alpha\lambda_4 >_A n_{\beta\lambda_1} C_{\alpha\lambda_4\beta\lambda_2} \qquad (5.10)\end{aligned}$$

and

$$\begin{aligned}\sum_{\alpha\beta} P_{\alpha\beta\alpha\beta} &= -2 \sum_{\alpha\beta\lambda_2\lambda_3\lambda_4} < \alpha\lambda_2|v|\lambda_3\lambda_4 > n_{\beta\lambda_2} C_{\lambda_3\lambda_4\alpha\beta} \\ &\quad +2 \sum_{\alpha\beta\lambda_1\lambda_2\lambda_4} < \lambda_1\lambda_2|v|\alpha\lambda_4 > n_{\lambda_4\beta} C_{\alpha\beta\lambda_1\lambda_2}. \qquad (5.11)\end{aligned}$$

The derivative of the sum of C finally becomes

$$\begin{aligned}\frac{d}{dt}\sum_{\alpha\beta} C_{\alpha\beta\alpha\beta} &= \frac{2}{i\hbar}\sum_{all}(n_{\lambda_3\beta} < \alpha\lambda_2|v|\lambda_4\lambda_3 > C_{\beta\lambda_4\alpha\lambda_2} \\ &\quad + n_{\beta\lambda_1} < \lambda_1\lambda_2|v|\alpha\lambda_4 > C_{\alpha\lambda_4\beta\lambda_2}) \\ &= 2\sum_{\alpha\beta} n_{\alpha\beta}\dot{n}_{\beta\alpha} \\ &= \frac{d}{dt}\sum_{\alpha\beta} n_{\alpha\beta} n_{\beta\alpha}. \qquad (5.12)\end{aligned}$$

From the first line to second we used the equation of motion for $n_{\alpha\beta}$ (Eq. 2.22). Thus Eq. 5.7 is time-independent. So if $\sigma^2_{\text{total}} = 0$ initially, Eq. 5.7 is always satisfied.

From the above discussion we find whether the condition (Eq. 5.7) is satisfied or not depends on the approximation for the equation of motion for $C_{\alpha\beta\gamma\delta}$. In the Born approximation we always have $\sum_{\alpha\beta} \dot{C}_{\alpha\beta\alpha\beta} = 0$ because of $\sum_{\alpha\beta} B_{\alpha\beta\alpha\beta} = 0$. Since the time derivative of $\sum_{\alpha\beta} n_{\alpha\beta} n_{\beta\alpha}$ is not always zero, the Born approximation does not conserve Eq. 5.7. Therefore we must include all the higher-order terms to assure that the whole space fluctuation vanishes.

We would like to mention that *TDDM* satisfies a relation which is more general

than Eq. 5.7, that is, the relation between the one- and two-body density-matrices

$$\rho(11';t) = \int d2\{\rho(12;t)\rho(21';t) - c(12,1'2;t)\}, \tag{5.13}$$

which is derived from the definition of the reduced density-matrix Eq. 2.5. One can derive Eq. 5.7 from this equation by simply taking trace. The relations Eq. 5.7 and 5.13 indicate that if we want to calculate the time evolution of the two-body density-matrix consistently with one-body density-matrix we should include all the higher-order terms. Therefore, these higher-order terms may be essential not only to the calculation of the mass dispersion but also to other two-body quantities.

5.3 Nucleon exchange transport model

In this section we briefly present how to calculate the mass dispersion in *NET*. The details of *NET* are presented in ref. [Ran 78, Ran 79, Ran 82].

Since we only consider the mass distribution induced by the nucleon transfer, we need a distribution function $P(A,t)$ which is the probability that the projectile-like collision partner has mass number A at time t; and $P(A, t \to -\infty) = \delta(A - A_P)$ where A_P is the mass number of the projectile. The assumption made in this transport theory is that this function satisfies the equation of Fokker-Planck type

$$\frac{\partial}{\partial t}P = -\frac{\partial}{\partial A}V_A P + \frac{\partial^2}{\partial A^2}D_{AA}P. \tag{5.14}$$

where V_A is called drift coefficient and D_{AA} is called diffusion coefficient. If the diffusion and drift coefficients are constants, the solution of Eq. 5.14 will be a Gaussian like function [Nor 74] whose width depends on D and peak drifts with speed V.

Solving Eq. 5.14 for $P(A,t)$ is difficult and often unnecessary, because $P(A,t)$ contains more information than we need to calculate the mass dispersion. We can use a differential equation for the mass dispersion [Ran 82]

$$\frac{d}{dt}\sigma_A^2 = 2D_{AA} + 2\frac{\partial V_A}{\partial A}\sigma_A^2. \tag{5.15}$$

This equation can be derived from Eq. 5.14 using the definition

$$\sigma_A^2 = \int (A - < A >)^2 P(A,t)\, dA. \tag{5.16}$$

Since the derivation of the diffusion and drift coefficients is quite lengthy, we only give the final expressions. In the derivation of these diffusion coefficients some simple assumptions have been made. The nuclei are assumed to be Fermi gases with the same temperature τ and the interaction between the two nuclei is the exchange of nucleons. The geometry of the colliding nuclei assumed in *NET* is illustrated by Fig. 5.2, where both nuclei are spheres connected by an elongate neck. The coefficient D_{AA} is given by

$$D_{AA} = \frac{n_0}{T_F} \pi C_{eff}^2 \tau^*, \tag{5.17}$$

where n_0 is the nucleon current, C_{eff} the neck radius and T_F the Fermi kinetic energy. The values of n_0 and T_F are [Ran 82]: $n_0 = 2.5 \times 10^{21} fm^{-2} s^{-1}$ and $T_F = 37$MeV. τ^* is called the effective temperature and defined by

$$\tau^* = \frac{\omega_{eff}}{2} coth \frac{\omega_{eff}}{2\tau}. \tag{5.18}$$

Here τ is obtained from the dissipated collective energy Q using the relation $Q = \frac{A+B}{8}\tau^2$ where B is the mass number of target nucleus. The effective excitation energy ω_{eff} is given by $\omega_{eff}^2 = \frac{1}{2} p_f^2 (\dot{R}^2 + u_t^2)$ where $\dot{R}$ is the radial velocity, u_t is the tangential velocity and $p_f = 265 MeV/c$ is the Fermi momentum. In the calculations for $^{16}O + ^{16}O$ we use a rotational frame approximation for peripheral collisions. In this approximation u_t =0. The drift coefficient is obtained from the mass formula. Its derivative is expressed as [Ran 82],

$$\begin{aligned} \frac{\partial V_A}{\partial A} &= \frac{2n_0}{T_f} \pi C_{eff}^2 [-\frac{m}{2A}(\dot{R}^2 + \omega^2 R^2) \\ &+ \frac{m}{9A} R^2 \omega^2 + \frac{4}{9} a_2 A^{-\frac{4}{3}} - \frac{5}{9} c_3 A^{-\frac{1}{3}} + \frac{2}{A^2} V_c], \end{aligned} \tag{5.19}$$

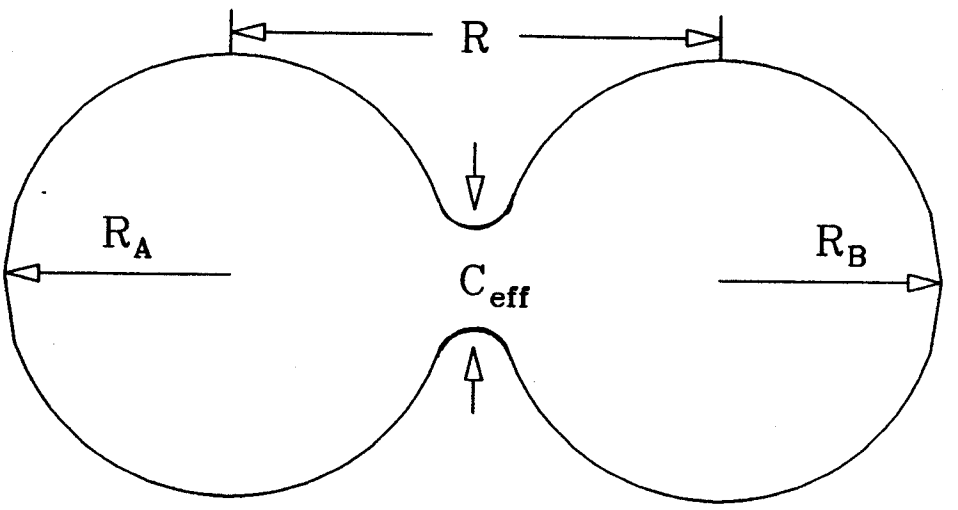

Figure 5.2: Illustration of the spatial relation between two colliding nuclei under the assumption of *NET*.

where

$$V_c = \begin{cases} \frac{e^2A^2}{4R_0}(2 - \frac{R}{R_0}) & R < R_0 \\ \frac{e^2A^2}{4R} & R > R_0 \end{cases} \tag{5.20}$$

Here R is the separation distance between the centers of the two nuclei, R_0 the sum of the radii of the two nuclei, ω the rotational frequency, $a_2 = 17.9437$MeV and $c_3 = 0.7053$MeV.

In this work we use the mean trajectory method [Ran 79] to solve Eq. 5.15. In this method the parameters (R, C_{eff}, w, etc) are determined in a model which describes the mean values well. Such an example can be found in Ref. [Jor 87], where the mean values are calculated in *TDHF*. In this work we will determine the time-dependent parameters with the one-body density distribution given by *TDDM* and integrate Eq. 5.15 for the mass invariant.

In our calculation R and $\dot{R}$ are determined by the one-body density, τ is determined by the kinetic energy loss (KEL) and the angular velocity ω is given by $\omega = L/I(\rho)$ where $I(\rho)$ is the moment of inertia [Dav 81]. The effective neck radius C_{eff} is determined from the one-way current[Jor 87]

$$\begin{aligned} N &= n_0 \pi C_{eff}^2 \\ &= n_0 \int_{window} dxdy \left(\frac{\rho(x, y, z = 0)}{\rho_0} \right)^{4/3}, \end{aligned} \tag{5.21}$$

where N is the total transfer current across the neck and $\rho_0 = 0.17\text{fm}^{-3}$ is the nuclear matter density.

5.4 Numerical detail

The numerical method used for $^{16}O+^{16}O$ is similar to that for the quadrupole motions. In the following we point out some aspect specific to the collisions case.

We use a *TDHF* code on which the axial symmetry is imposed. This symmetry is an exact one for the case of head-on collision. For the case of finite impact parameter collisions the rotational-frame approximation is used [Dav 81]. The colliding ions move toward each other in this frame. The geometry of the colliding system is illustrated in Fig. 5.3. The frame rotates with angular velocity

$$w = \frac{L}{I[\rho]}, \tag{5.22}$$

where L is the conserved total orbital angular momentum and $I[\rho]$ is the moment of inertia. Several prescriptions have been used to calculate the moment of inertia [Dav 81]. In prescription R2 it is assumed that the two ions are point-like objects before they clutched (i.e. the density at the touching point exceeds a certain value, e.g. half of the nuclear matter density) and the moment of inertia is that of rigid body after they clutched. In this prescription there is a jump in the collective energy when two ions clutch or de-clutch. Since we need a continuous change of collective energy, we use prescription R4 which assumes a continuous change of moment of inertia [Dav 78]. R4 is based on R2 but allows for a continuous change in the moment of inertia before clutching.

The initial *HF* s.p. wave function are boosted with a phase factor corresponding to the incident energy. For the left hand side nucleus, we multiply each single particle orbit with a phase factor $\exp(ipz/\hbar)$ and $\exp(-ipz/\hbar)$ for the right hand side one. p is the initial momentum of each nucleus in the C.M. frame.

Due to the axial symmetry, each single-particle state is labeled by quantum number m (magnetic quantum number). For the mass symmetry system like $^{16}O + ^{16}O$ there is another good quantum number, z-parity, due to the z-reflection symmetry. The s.p. wave functions with z-parity are constructed initially in the following way: Let $\{\psi_\alpha^L\}$ ($\{\psi_\alpha^R\}$) be the wave functions which are initially located within the left

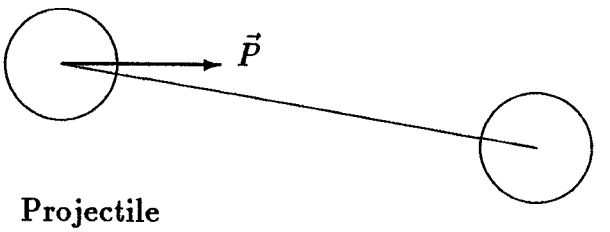

Projectile

Target

L.B.

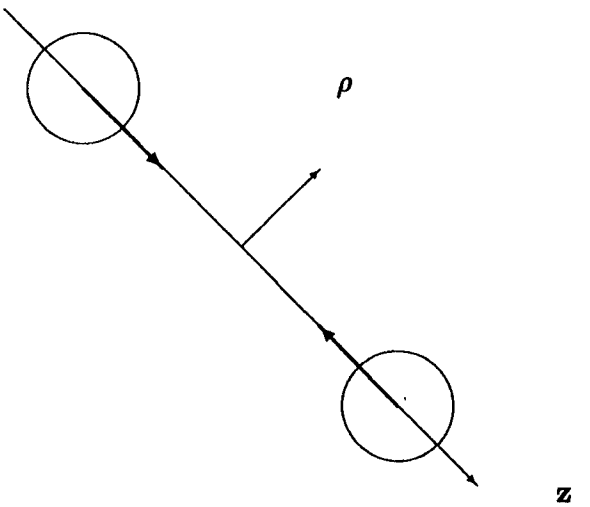

C.M.

Figure 5.3: Illustration of the colliding system viewed in L.B. frame and C.M. frame.

hand (right hand) side nucleus. Due to the reflection symmetry

$$\psi_\alpha^L(\rho,-z) = \psi_\alpha^R(\rho,z). \tag{5.23}$$

The new set of single particle basis which has definite z-parity is given as follows

$$\begin{aligned} \psi_\alpha^+ &= \frac{1}{\sqrt{2}}(\psi_\alpha^R + \psi_\alpha^L), \\ \psi_\alpha^- &= \frac{1}{\sqrt{2}}(\psi_\alpha^R - \psi_\alpha^L). \end{aligned} \tag{5.24}$$

Here the superscript "+" denotes the positive z-parity and "−" denotes the negative z-parity. This prescription is illustrated by Fig. 5.4. The s.p. states used in the calculation are illustrated in Fig. 5.5. With these single particle states having definite z-parity we can suppress those occupation and correlation coefficients with mixed z-parities.

The description of the interface between *TDHF* code and the subroutine solving the equations of motion for $n(t)$ and $C(t)$ (Eq. 2.22 and Eq. 2.23) is given in page 45. The number of single particle states used in the collision case is 20 (Fig. 5.5). In the calculations shown later, the number of time steps is about 500. For a calculation which includes all the terms of Eq. 2.23 each time step takes about 8 minute CPU in VAX8530. These values are about 70 times of those needed for *TDHF* calculation.

5.5 Results and discussion

We first searched the threshold incident energy above which no fusion occurs for a head-on collision and found it to be $E_{\rm lab} \approx 170$MeV. This energy is much higher than that in *TDHF* which is only 54MeV if the spin-orbit force is not included. However, it is not very much higher than the result ($E_{\rm lab} \approx 140$MeV) of the previous *TDDM'* calculation[Toh 87] (which included only the Born term in Eq. 2.23). This indicates that the higher-order terms in Eq. 2.23 are not so important as the Born term, as far

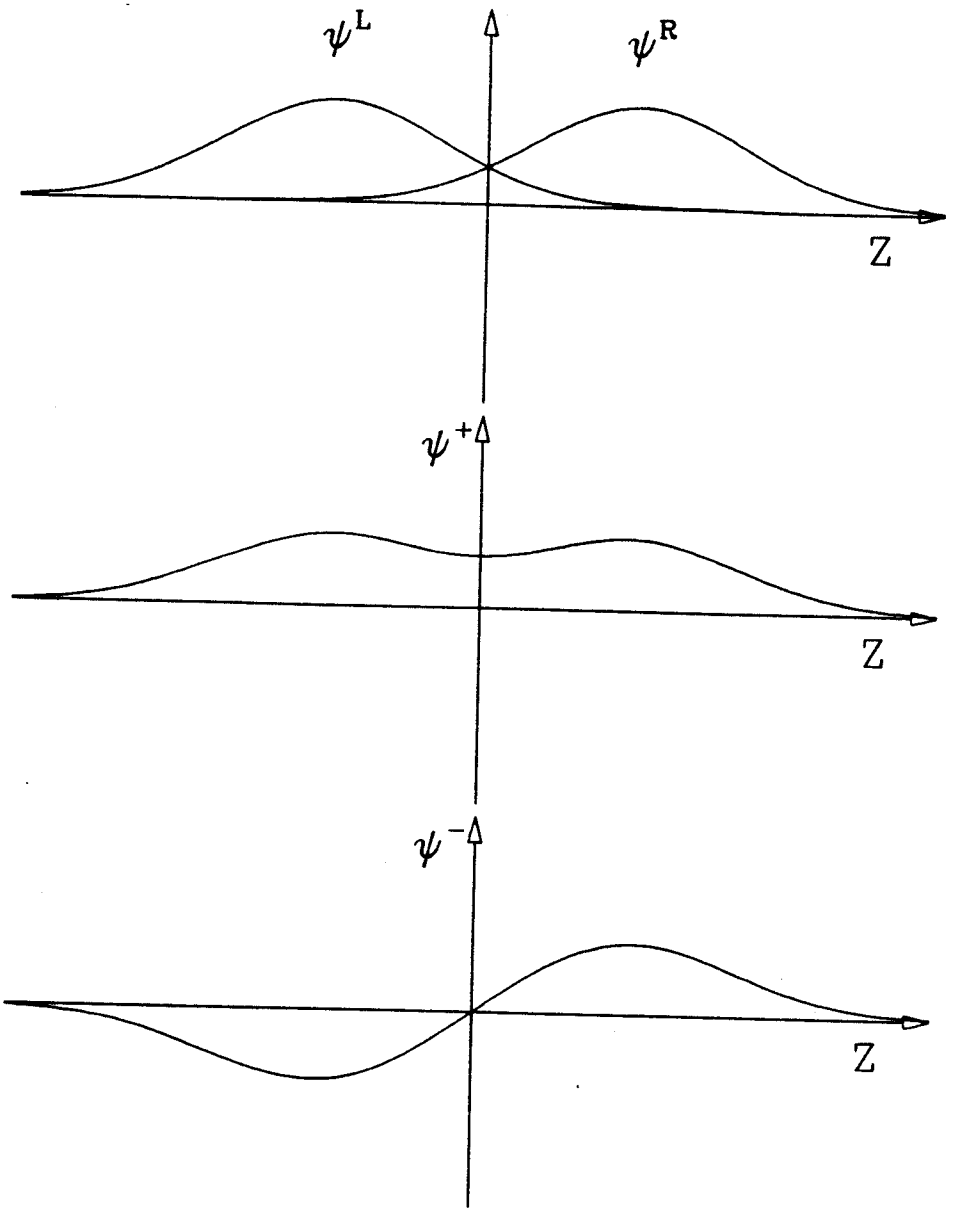

Figure 5.4: Illustration of prescription of constructing wave function having definite z-parity.

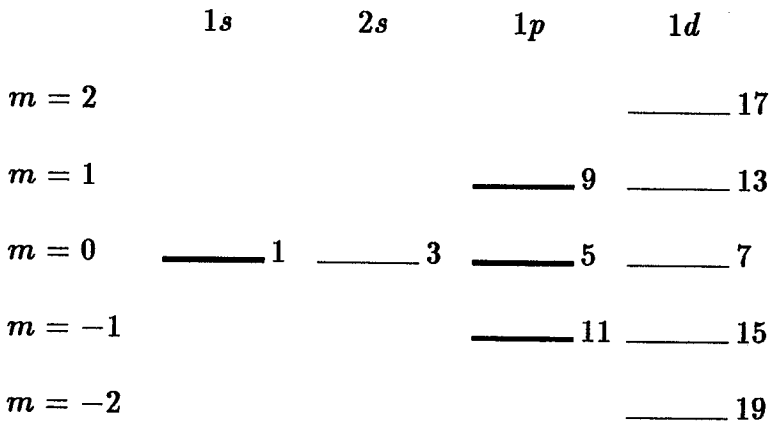

Positive z-parity

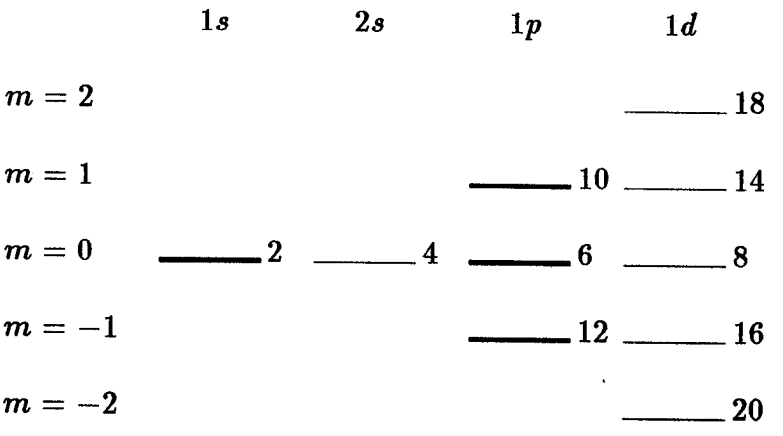

Negative z-parity

Figure 5.5: The numbering of s.p. levels for $^{16}O + ^{16}O$, thick lines are occupied state, thin lines are empty.

as the dissipation in heavy-ion collisions is concerned. As far as fusion is concerned, Umar et al [Uma 86] find that the fusion window problem can be resolved if the spin-orbit coupling is included in the mean field. Their calculation gives 146 MeV of the threshold energy for the same system. The effects of the higher-order correlations were also studied by Cassing and Wang for a one-dimensional system [Cas 87]. They solved the coupled equations for ρ and C_2 in coordinate space using a bare NN interaction with a short range repulsive part. They found that the dissipation due to the NN collisions is weakened by the higher-order terms. Their finding is apparently inconsistent with our result. We interpret the difference in the following way. The higher-order terms may play two different roles; one is to renormalize the bare NN interaction and the other to modify the phase space distribution of two nucleons. The calculation by Cassing and Wang[Cas 87] has no truncation in momentum space; the coupled equations were solved in coordinate space. Therefore, it is likely that they observed the drastic renormalization of the bare interaction when they included the higher-order terms. We believe that this renormalization effect is small in our calculation because of the severe truncation in single-particle space. There still remains the effect of modification of the phase space distribution due to the higher-order correlations. This effect enhances the dissipation as was found in the damping of giant resonances.

The *TDDM* calculation done in this work as well as previous calculations [Toh 87] show that the inclusion of NN collision effects brings about more dissipation as compared to *TDHF*. This is in contradiction with the extended *TDHF* calculations made by Wong and Davies [Won 80, Won 83]. In their application of extended *TDHF* to fusion and intermediate energy heavy-ion collisions, no additional dissipation was found as compared to the *TDHF* calculation. Here we would like to point out the difference between our calculations and theirs. In their model they use the solution of a *TDHF* -like equation as a single-particle basis as we do in *TDDM* but assume

Table 5.1: The total kinetic energy loss (TKL) and reaction time.

	$l = 0\hbar$		$l = 40\hbar$	
	TKL (MeV)	$t_{reac}(10^{-21}s)$	TKL (MeV)	$t_{reac}(10^{-21}s)$
TDDM	82	0.43	37	0.54
TDHF	64	0.25	11	0.25

the occupation matrix to be diagonal. In Ref. [Toh 85] Tohyama points out that the off-diagonal matrix elements are important in bringing about additional dissipation of collective energy. To improve their model Wong and Davies suggest to add to the s.p. basis additional states, which includes the transverse degrees of freedom. In our approach the inclusion of off-diagonal matrix elements plays a role in bringing about such transverse degrees of freedom.

We calculate the mass dispersion for two different reactions i.e. a head-on collision and a peripheral collision ($l = 40\hbar$) at $E_{lab} = 185$MeV. The incident energy is chosen to be above the threshold for a non-fusion event to occur in a head-on collision. In table 5.1 we show the losses of the kinetic energy of the relative motion and the reaction times calculated in *TDHF* and *TDDM*. The reaction time is defined as the period during which two nuclei are clutched [Dav 81] (i.e. the center-of-mass density exceeds half of the nuclear matter density). TDDM gives larger kinetic energy losses and longer reaction times than *TDHF*. In the head-on collision, however, the dissipation of the collective energy is still dominated by one-body mechanisms.

The parameters in *NET* are shown in Fig. 5.6–5.7 (τ and τ^*) and Fig. 5.8 (D_{AA}) as functions of time. Although *NET* is devised to treat peripheral collisions where the overlap between the two nuclei is small, we also apply it to the head-on collision to estimate the order of magnitude of the mass dispersion. The increase in the effective temperature in the final stage of the peripheral collisions is due to an increase in $\dot{R}$. The effective temperature approaches an asymptotic value as the separation between

Table 5.2: σ_A calculated in *TDDM*, *TDHF* and *NET*.

	σ_A (amu)	
	$l = 0\hbar$	$l = 40\hbar$
TDDM	2.0	1.2
TDHF	0.8	0.4
NET	2.7	1.5

the two fragment increases. The peak in τ^* in the head-on collision is due to an increase in the collective energy after many nucleons from one nucleus penetrate into the other nucleus. The temporal behavior of D_{AA} is mainly determined by the one-way current (Eq. 5.21) which is plotted in Fig. 5.9 with solid curves. The double peaks of D_{AA} seen in the head-on collision is caused by peaks of the effective temperature (see Fig. 5.6). In the case of peripheral collision the average value of D_{AA} over the reaction time is $2 \cdot 10^{21}[\text{amu}]^2\text{s}^{-1}$. This value is close to the "empirical" value $D \approx (A + B) \cdot 10^{20}[\text{amu}]^2\text{s}^{-1} = 32 \cdot 10^{20}[\text{amu}]^2 s^{-1}$ which is used in a simple transport model [Sch 77].

The time evolution of the mass dispersion calculated in *TDDM* (Eq. 5.4), *TDHF* (Eq. 5.5) and *NET* are plotted in Fig. 5.10. The mass dispersion in *NET* are dominated by the diffusion term (the first term on the right hand side of Eq. 5.15). All the results of the mass dispersion are quite stable as functions of time after the two ions are well separated. The whole space integral of Eq. 5.7 was calculated to check numerical accuracy and was found to be smaller than $0.02[\text{amu}]^2$. The final-state mass dispersion in *TDDM*, *TDHF* and *NET* are shown in table 5.2. The *TDDM* results are of the same order of magnitude as the NET values, whereas *TDHF* results are much smaller. Since *NET* values are considered as "empirical", the final-state *TDDM* results may be large enough to reproduce experimental mass fluctuations.

There is a noticeable difference between the *TDDM* results and the *NET* ones in the intermediate stage of the collisions. While the transport model yields a monoton-

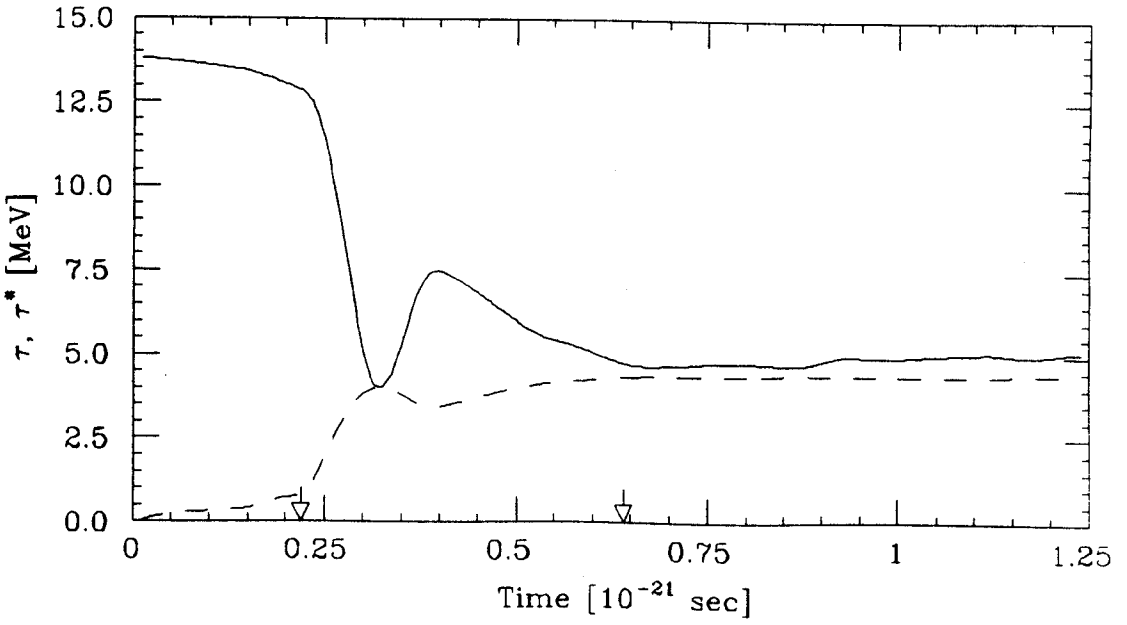

Figure 5.6: For head-on collision τ (solid line) and τ^* (dashed line) in *NET* as functions of time. The arrows indicate the time interval during which two nuclei are clutched.

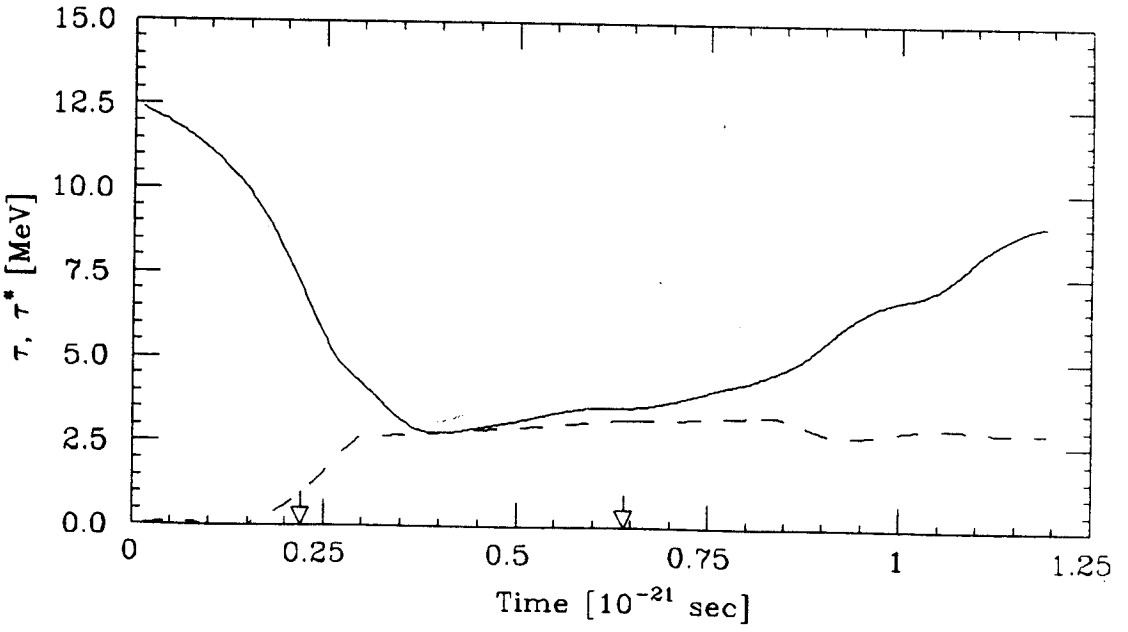

Figure 5.7: Same as Figure 5.6 but for peripheral collision.

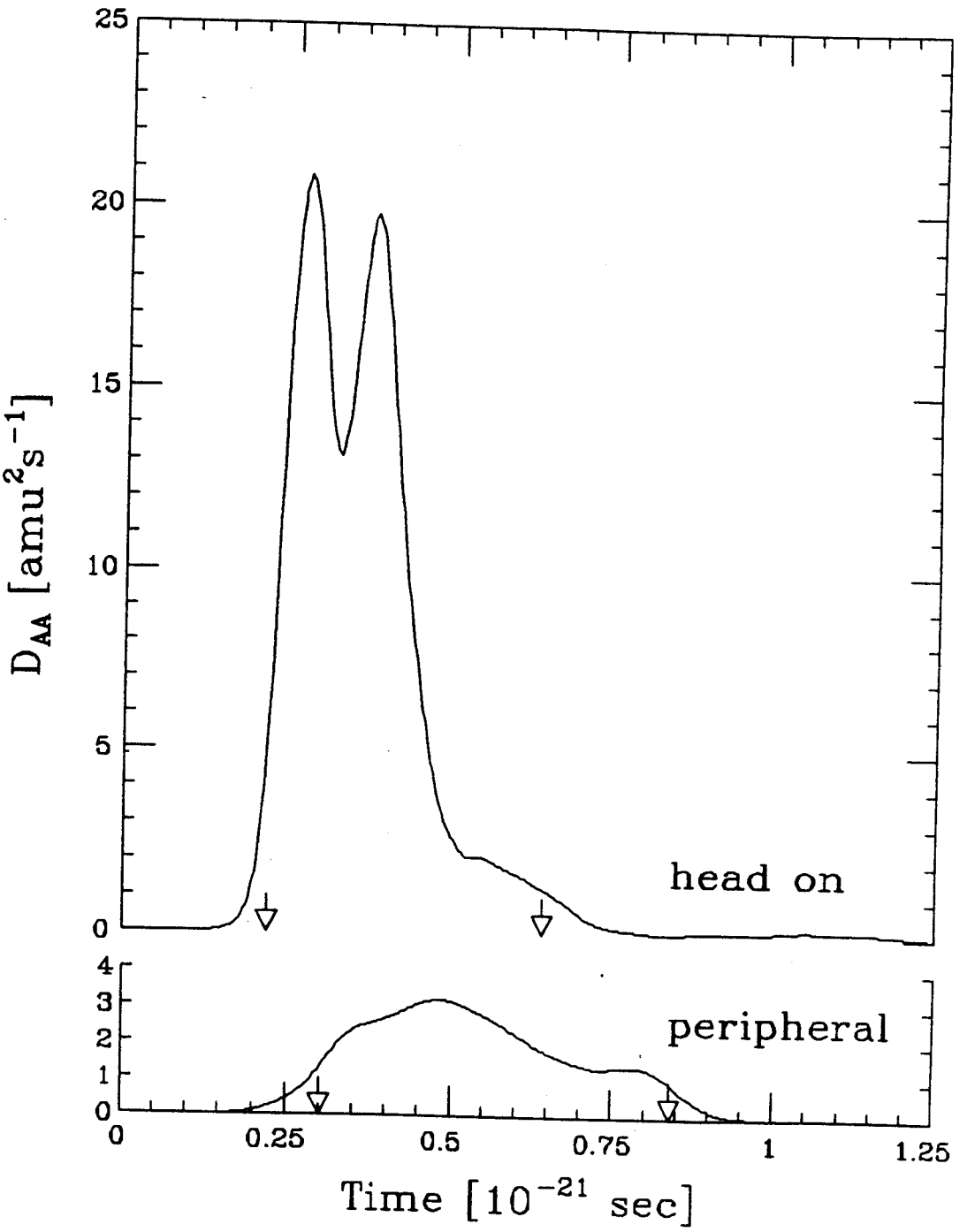

Figure 5.8: Diffusion coefficients in *NET* as functions of time. The arrows indicate the time interval during which two nuclei are clutched.

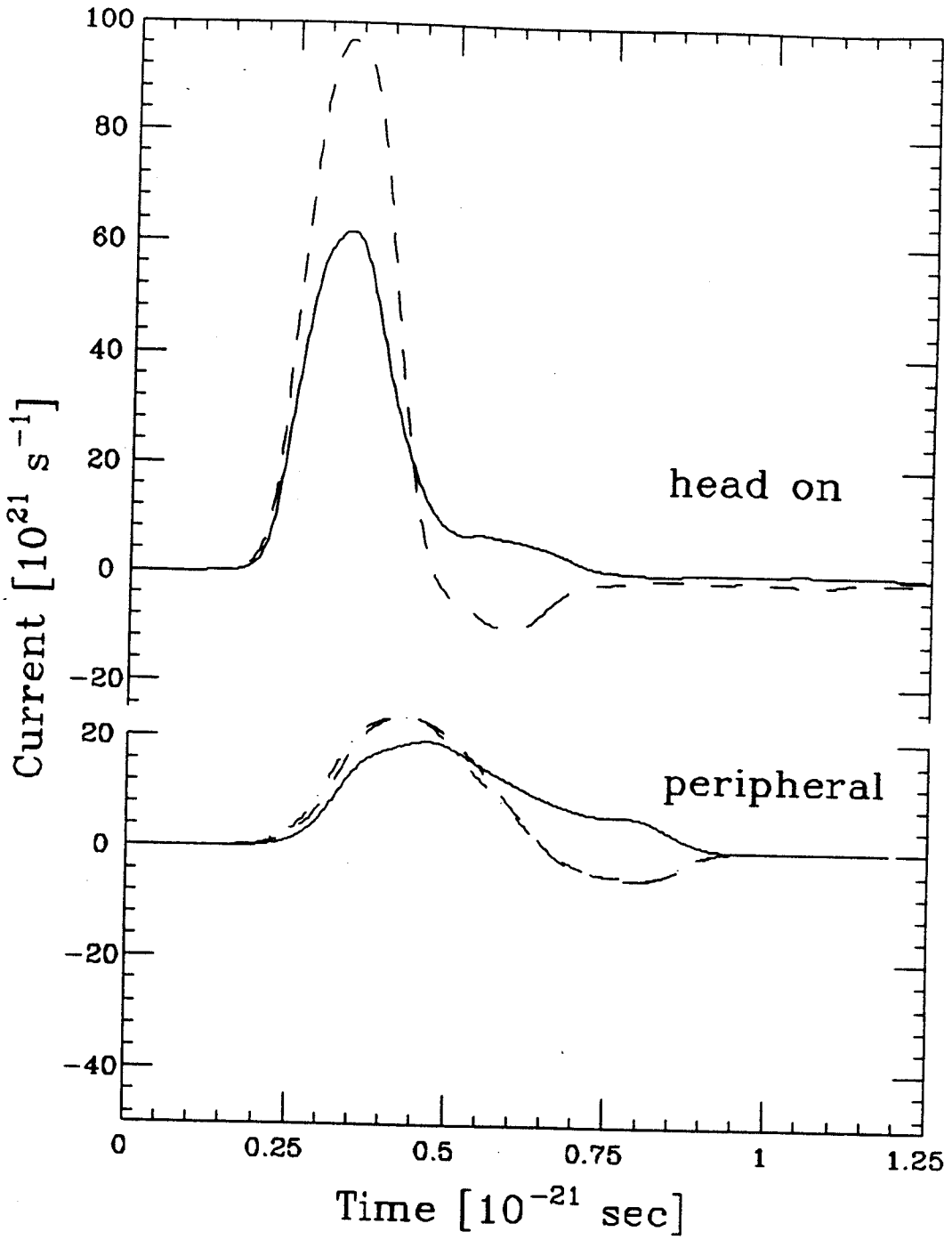

Figure 5.9: One-way currents as functions of time, calculated with Eq. 5.21 (solid lines) and Eq. 5.27 (dashed lines).

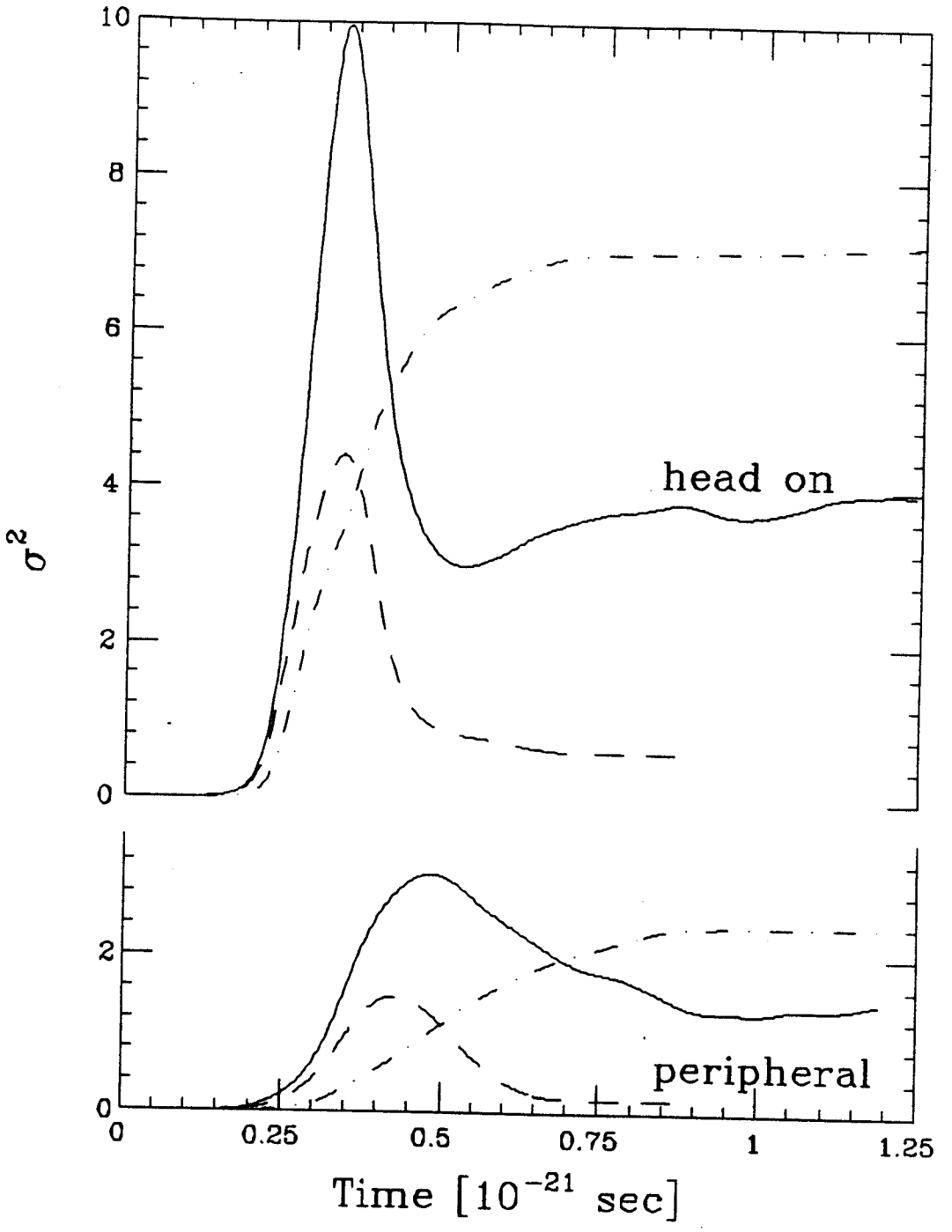

Figure 5.10: σ_R^2 as a function of time. The curves are for TDDM (solid lines), *TDHF* (dashed lines) and *NET* (dot-dashed lines). The unit of σ_R^2 is [amu]^2.

ically increasing mass variance, the quantal results exhibit large peaks at early times, before approaching their respective final values. Before discussing this difference we look at the mass dispersions in *TDDM* in more detail.

We separate the expression for σ_R^2 (Eq. 5.4) into two parts corresponding to a one-body contribution and a two-body correlation contribution,

$$\sigma_R^2 = \sum_{\alpha\beta} n_{\alpha\beta} < \beta|\alpha >_R - \sum_{\alpha\beta\alpha'\beta'} < \alpha'|\alpha >_R < \beta'|\beta >_R n_{\alpha\beta'} n_{\beta\alpha'} \quad (5.25)$$

$$+ \sum_{\alpha\beta\alpha'\beta'} < \alpha'|\alpha >_R < \beta'|\beta >_R C_{\alpha\beta\alpha'\beta'}. \quad (5.26)$$

Each contribution is separately shown in Fig. 5.11. The time when the one-body and two-body contributions start growing is the time when the *NN* collisions were turned on. This time is slightly before the two nuclei start overlapping. The non-zero contribution from each part before the collision of the two nuclei is due to the ground state correlations. The sum of these contributions is equal to zero before the two nuclei overlap, guaranteeing that each nucleus is an eigenstate of the number operator.

For the head-on collision the two-body contribution has a sharp peak (see Fig. 5.11) which is not seen in the peripheral collision. The peak is explained by an increase in the two-body correlation matrix as a result of a decrease in the energy gap between the occupied and unoccupied single-particle states. Fig. 5.12 shows the time evolution of some of the single-particle energies defined by $\epsilon_\lambda =< \lambda|h|\lambda >$. The energy gap between the 1p state and the 2d state becomes very small when the two nuclei strongly overlap. The dominant two-body correlation matrix in the initial stage of the collision i.e. the two-particle two-hole matrix which is inversely proportional to the energy gap is, therefore, enhanced when the energy gap becomes small.

To explain the decrease in the *TDDM* mass dispersion toward the final state of the collision, we introduce the current in *TDDM* which may correspond to the one-way

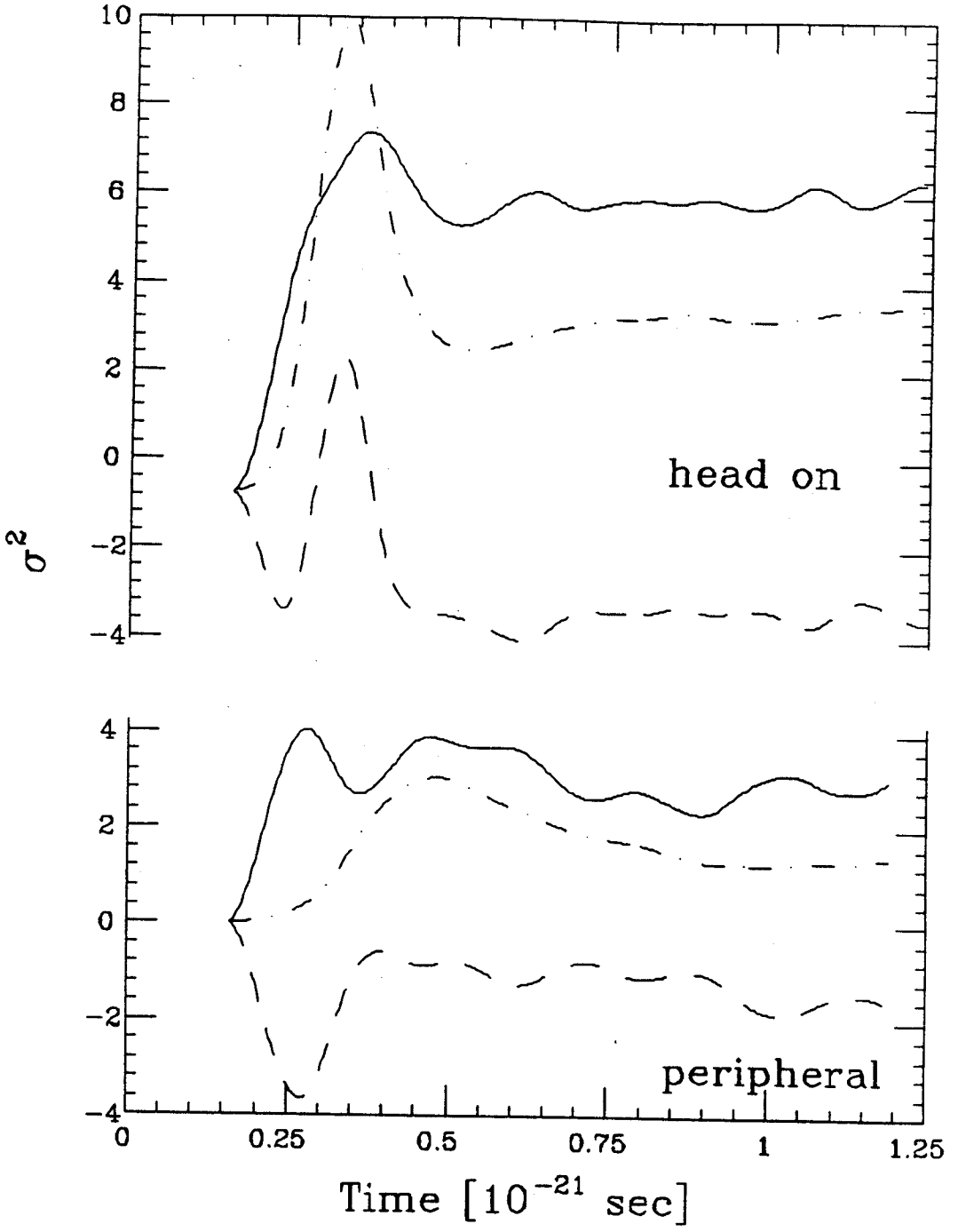

Figure 5.11: σ_R^2 calculated with Eq. 5.25 (dot-dashed line), Eq. 5.26 (dashed line) and the sum of both (solid line). The unit of σ_R^2 is [amu]^2.

current in *NET* ;

$$N = \int dxdyJ_z(z=0). \tag{5.27}$$

where J_z is the z component (beam direction) of the current density

$$\mathbf{J}(\vec{r}) = \sum_{\alpha\beta} n_{\alpha\beta}\frac{i\hbar}{2m}\{\psi_\alpha \nabla\psi^*_\beta - \psi^*_\beta\nabla\psi_\alpha\}. \tag{5.28}$$

The summation in the above equation runs over the single-particle orbits which are initially localized in one of the colliding nuclei. The current thus defined, of course, has little quantitative meaning because the single-particle states from both nuclei mix after the two nuclei overlap. The current is plotted in Fig. 5.9 with dashed curves. The current in *TDDM* is not positive definite and becomes negative in the later stage of the collision. Using Eq. 5.27, we calculated the mass dispersion in *NET*. The results are shown in Fig. 5.13 with dashed curves. The temporal behavior of the mass dispersion is now similar to the *TDDM* result i.e. the decrease of σ_R^2 toward the final state. The above qualitative discussion suggests that the discrepancy between *TDDM* and *NET* originates in the assumption of quick memory loss inherent in the transport treatment. For central collisions of relatively small nuclei, the opportunity for the single-particle motion to become disordered is significantly reduced and the transferred particles may remain coherent beyond the echo time and thus reduce the mass variance when transferred back to their original host nucleus. Clearly, the time local treatment of the *NET* model is inadequate for such a situation.

In the following we point out some ambiguities in our calculation. In the calculations described in previous chapter as well as this chapter, we use effective interaction as the two-body potential in the calculation of mean-field and as residual interaction. Therefore, there exists effect of double counting in our calculation. Some effects of higher-order correlations have been included by using the effective force. Because these effects are static in the sense that the effective force is time-independent, it is not clear which higher-order terms cause the double counting in the dynamic case.

The initial Hartree-Fock ground state is not the true ground state of *TDDM*. Since the ground state correlations grow in time, the mass dispersion may depend on when the *NN* collisions are switched on. For the head-on collision we made two calculations with different starting time of the *NN* collisions; in one calculation the *NN* collisions are turned on when the separation distance of the two nuclei is 5.2fm and in the other the distance is 9fm. The former has practically no ground state correlations grown before the two nuclei overlap, and the latter fully grown correlations. It was found that σ_R^2 vary from $3.6(amu)^2$ to $4.0(amu)^2$ when the separation distance changes from 5.2 fm to 9 fm. The mass dispersion are, therefore, not sensitive to the initial ground state correlations.

In the peripheral collisions the kinetic energy loss and the reaction time depend on how the moment of inertia is calculated. The R4 prescription which gives a continuous change in the moment of inertia [Dav 78] was found to give a larger kinetic energy loss and a longer reaction time than other prescriptions such as R2. As a result of the longer reaction time, the R4 prescription gives a larger mass dispersion than R2.

We also calculated the relative momentum dispersion as was done in Ref. [Mar 85]. Since the initial Hartree-Fock state is not an eigenstate of the relative momentum operator, the initial dispersion of the momentum is non zero ($\sigma_P = 1.17 fm^{-1}$). We calculated the final-state momentum dispersion and found a slight increase in the momentum dispersion. However, it is of the same order of magnitude as the *TDHF* result. This indicates that the s.p. states localizing along one trajectory might not enough to treat the momentum fluctuation.

The total energy for the head-on collision is shown in Fig. 5.14 as a function of time. As was discussed in section 2.4.3, *TDDM* formally preserve energy conservation. The total energy is not conserved in our numerical calculation. The gain in energy is about 60 MeV in the head-on collision. Energy non-conservation is also found in the calculation of isoscalar quadrupole motion but the gain in energy is much less than

that in this case [Gon 88]. The gain in energy occurs during the time when the two nuclei strongly overlap. The violation of the energy conservation is not sensitive to the change in the parameters in the numerical calculations, such as the number of mesh points and mesh sizes. Therefore we conclude that the violation is mainly due to the truncation in the single-particle space.

5.6 Summary

In this chapter we applied *TDDM* to the fusion reaction and the deep-inelastic collision of system $^{16}O + ^{16}O$. First we found that the low-l non-fusion threshold energy is about 170 MeV which is consistent with the experiment [Ike 86]. This value is comparable with that one (140 MeV) which is calculated in *TDDM* without higher-order terms. This indicates that higher-order terms are not so important to the dissipation of translational energy as they are to the spreading of strength function in the case of isoscalar giant quadrupole resonance.

Second we calculate the mass dispersion in two non-fusion *DIC* events; a head-on and a peripheral collision. In both cases the mass dispersion are found to be much larger than the calculation of *TDHF*. We point out that all the higher-order terms must be included in the calculation to assure zero whole space fluctuation. We compare *TDDM* results with that of a phenomenological model called "nucleon exchange transport model" (*NET*). It is found that results from both models have the same order of magnitude. We also discuss the temporal behavior of the mass dispersion in both models. We found that the statistical assumption made in *NET* are not always realized in *TDDM*.

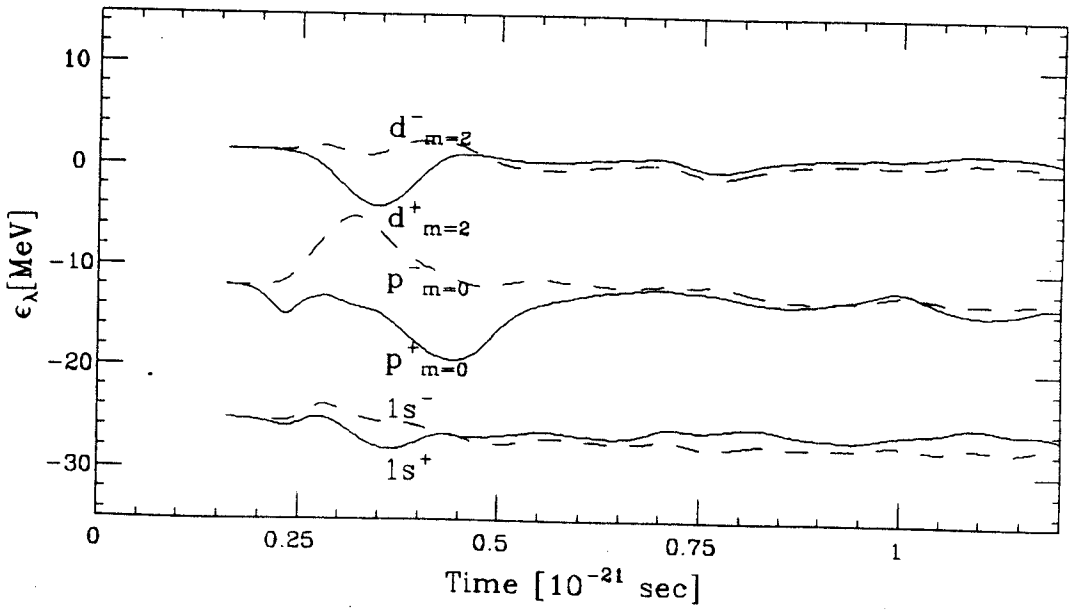

Figure 5.12: Single-particle energies $\epsilon_\lambda =< \lambda|h|\lambda >$ as functions of time for the head-on collision. m is the azimuthal quantum number, + and − denote the z-parity.

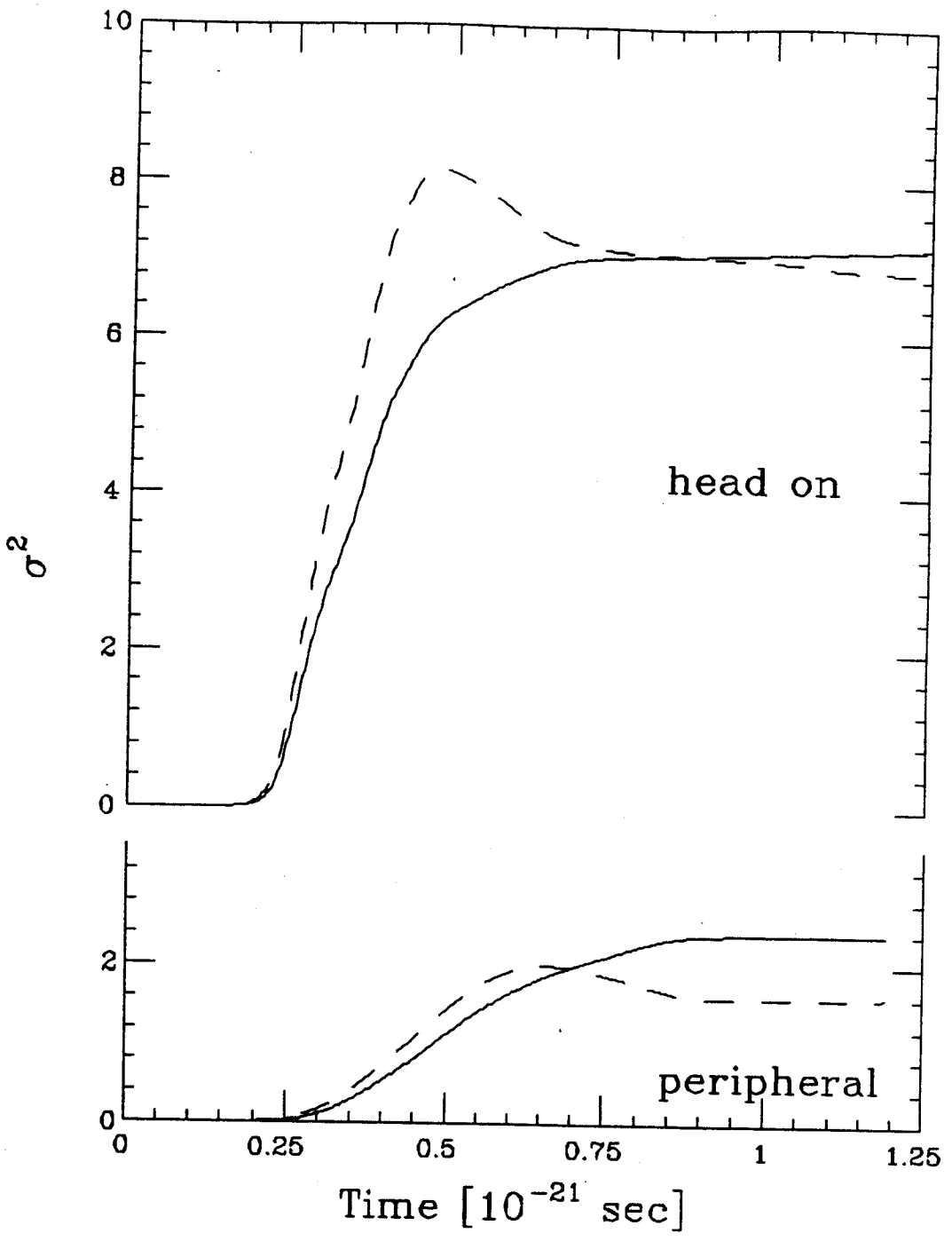

Figure 5.13: The mass dispersion calculated in *NET* with the current Eq. 5.21 (solid line) and with the current Eq. 5.27 (dashed line).

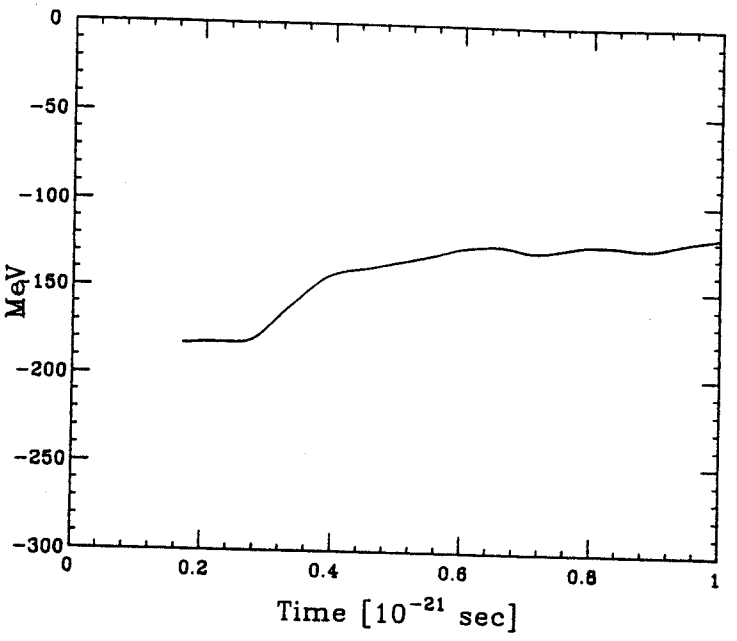

Figure 5.14: The total energy as a function of time for the head-on reaction, as calculated in the *TDDM*.

Chapter 6

Conclusion

We have derived an extended *TDHF* theory, called time-dependent density-matrix theory (*TDDM*), from the time-dependent density formalism of Wang and Cassing. This theory consists of three coupled equations: a *TDHF* -like equation whose solutions are used as single particle basis, an equation of motion for the occupation matrix whose diagonal elements are the probabilities of occupying corresponding single particle orbits, and an equation of motion for the correlation matrix. The equation of motion for the correlation coefficient consists of three terms which reduce to, in a perturbative expansion, a Born term, a particle-hole interaction term and a particle-particle interaction term. This theory formally conserves total energy, momentum and mass.

By taking the small amplitude limit of *TDDM* we have investigated the relation of *TDDM* with other theories. We found that with the ground state approximated by the static Hartree-Fock solution this theory reduces to: a)the random phase approximation (*RPA*) if we neglect all the correlation matrix elements, b)the second random phase approximation (*SRPA*) if we only keep the forward ($G_{\rho\rho'\nu\nu'}$) and backward elements ($G_{\nu\nu'\rho\rho'}$) and c)shell model if we only keep the forward elements.

We have applied *TDDM* to the small amplitude isoscaler quadrupole motion of ^{16}O and ^{40}Ca. *TDDM* gives spread strength distribution which *TDHF* cannot give. The

obtained spreading width is comparable with experiment and shell model calculations which include both $1p-1h$ and $2p-2h$ excitations. *TDDM'*, which excludes higher-order terms but Born term, does not give any damping of the motions. The higher-order terms play an essential role in the damping of quadrupole motion.

We also applied *TDDM* to fusion and deep-inelastic collision of system $^{16}O+^{16}O$. First we found that the low-l non-fusion threshold energy is raised from 54 MeV in *TDHF* calculation to 170 MeV. This value is found to be 140 MeV in *TDDM'* calculation. This indicates that the higher-order terms are not so important in the dissipation of translation energy as they are in the damping of quadrupole motion. These higher-order terms, however, are indispensable in the calculation of the mass dispersion to maintain the condition that the system is an eigenstate of the total number operator. In two deep-inelastic collision events (one head-on and the other peripheral) the mass dispersions are found to be much larger than those calculated in *TDHF* and of the same order of magnitude as those given by a phenomenological transport model.

In the following we discuss limitations and possible extensions of this approach. *TDDM* as well as other extended *TDHF* theories are devised to treat heavy-ion collisions in the intermediate-energy range where there are two competitive processes: the mean-field and nucleon-nucleon (*NN*) collisions. This energy range is roughly from 10 MeV/nucleon to 100 MeV/nucleon. So far, due to the limitation of computational power, we have only solved *TDDM* using a severely truncated single-particle basis. This limits the application of *TDDM* to low energies. Therefore, the future development of this theory requires overcoming of this limitation. It is also necessary to apply *TDDM* to large systems where we can compare the theoretical results with more experimental data. In our calculation there is an ambiguity in the treatment of the ground state. An effort to find a ground state which is consistent with the *TDDM* truncation scheme is necessary. There have been many semi-classical simulations of

heavy-ion collisions. It is interesting to compare the *TDDM* calculations with those calculations, hopefully, to provide some quantal justifications to those semi-classical methods.

Appendix

Appendix A

Strength function

The strength function is defined as Eq. 4.11

$$S(w) = \sum_n | < n|V|0 > |^2 \delta(E - E_n). \tag{A.1}$$

Here V is the operator which causes the excitation and $E_n = \hbar w_n$ is the excitation energy. V is given by Eq. 4.12

$$V = \sum_i^A Q(\vec{r}_i), \quad Q(\vec{r}) = r^2 Y_{20}(\theta). \tag{A.2}$$

To build the relation between $S(w)$ and the quadrupole moment, we consider the following time dependent perturbation induced by an impulse external field Eq. 4.5. As discussed in the text following Eq. 4.5, this is equivalent to the ansatz of boosting each single particle wave function according to Eq. 4.2 in the first order approximation. The exact Schrödinger equation can be written as

$$i\hbar \frac{\partial}{\partial t} \Psi = (H - \alpha \hbar \delta(t) V) \Psi. \tag{A.3}$$

Here H is the unperturbed hamiltonian of the system, V is given by Eq. 4.12 and Ψ is the time-dependent many-body wave function. Let $\{\phi_n\}$ to be the eigenstates of the unperturbed hamiltonian

$$H\phi_n = \varepsilon_n \phi_n. \tag{A.4}$$

We then expand Ψ in terms of $\{e^{-ie_n/\hbar t}\phi_n\}$

$$\Psi = \sum_n a_n(t)\Phi_n(t), \quad \Phi_n(t) = e^{-ie_n/\hbar t}\phi_n. \tag{A.5}$$

Substituting Eq. A.5 into Eq. A.3 and making use of Eq. A.4, we obtain the following equation:

$$i\sum_n \Phi_n \dot{a}_n(t) = -\alpha\delta(t)V\sum_n a_n(t)\Phi_n, \tag{A.6}$$

Assuming $\{\phi_n\}$ to be an orthogonal basis, the above equation can be written as

$$i\frac{da_m(t)}{dt} = -\alpha\delta(t)\sum_n a_n(t)e^{-iw_{nm}t} < m|V|n >, \tag{A.7}$$

where $w_{nm} = \varepsilon_n - \varepsilon_m$. At t=0, the system is at ground state, so

$$a_n(t=0) = \delta_{n0}. \tag{A.8}$$

We always assume that α is a small quantity, so the first order approximation for $a_n(t)$ is (replace $a_n(t)$ at r.h.s with $a_n(0)$)

$$i\frac{da_m(t)}{dt} = -\alpha\delta(t)e^{-iw_{nm}t} < m|V|0 > . \tag{A.9}$$

The solution of the above equation is

$$a_m(t) = i\alpha < m|V|0 > +\delta_{m0}. \tag{A.10}$$

So the first order perturbation wave function is

$$\Psi(t) = \Phi_0(t) + i\alpha\sum_n < n|V|0 > \Phi_n(t). \tag{A.11}$$

Since quantity V defined by Eq. 4.12 is just the quadrupole moment, we hereafter replace it with Q. The quadrupole moment we calculate is the following (to the first order of α)

$$\begin{aligned} < Q(t) > &= < \Psi(t)|Q|\Psi(t) > \\ &= < 0|Q|0 > +2\alpha\sum_n | < n|Q|0 > |^2 \sin w_n t. \end{aligned} \tag{A.12}$$

The quadrupole moment of ground state is zero, so $| < n|Q|0 > |^2$ can be expressed as a Fourier transformation of $< Q(t) >$. Using relation

$$\int_0^\infty \sin wt \sin w_n t dt = \frac{\pi}{2}\delta(w - w_n), \tag{A.13}$$

the strength function Eq. 4.11 can be express as the Fourier transformation of $< Q(t) >$

$$S(w) = \frac{1}{\pi\alpha\hbar}\int_0^\infty < Q(t) > \sin wt dt. \tag{A.14}$$

It is easy to see that $S(w)$ is independent of α in the linear response limit. A strength function of similar form was given in Ref. [Cho 87] for monopole giant resonance.

Appendix B

Calculational form of TDDM

B.1 Spin-isospin saturation

In this section we will derive the *TDDM* formulae used in our numerical calculation which has taken into account the spin-isospin saturation. The residual interaction used here,

$$v = v_0\delta^3(r_1 - r_2), \tag{B.1}$$

does not allow spin or isospin flip. For convenient we write Eqs. 2.23–2.26 in following form

$$\begin{aligned} i\hbar\dot{C}_{\alpha\beta\gamma\delta}(t) &= B_{\alpha\beta\gamma\delta}(t) + \sum_{\nu\tau}(< \alpha\beta|v|\nu\tau > C_{\nu\tau\gamma\delta} - C_{\alpha\beta\nu\tau} < \nu\tau|v|\gamma\delta >) \\ &\quad + F^*_{\gamma\delta\alpha\beta} - F_{\alpha\beta\gamma\delta} + F^*_{\delta\gamma\beta\alpha} - F_{\beta\alpha\delta\gamma}, \end{aligned} \tag{B.2}$$

$$\begin{aligned} F_{\alpha\beta\gamma\delta} &= \sum_{\lambda\mu\tau} < \lambda\mu|v|\gamma\tau > (n_{\alpha\lambda}C_{\beta\tau\delta\mu} - n_{\beta\lambda}C_{\alpha\tau\delta\mu} \\ &\quad - n_{\alpha\mu}C_{\beta\tau\delta\lambda} - n_{\beta\mu}C_{\alpha\tau\lambda\delta} - n_{\tau\delta}C_{\alpha\beta\lambda\mu}). \end{aligned} \tag{B.3}$$

Here $B_{\alpha\beta\gamma\delta}$ is given by Eq. 2.24. Eqs. B.2 and B.3 do not contain any assumption about spin and isospin. In the following discussion let us assume that *a*). Indices α, β, γ and δ are quantum numbers besides spin and isospin; *b*). In the left hand side of each equation there are spin and isospin quantum numbers associating with each indices, but these spin and isospin quantum numbers are not explicitly shown; *c*) In the right hand side of equation the spin and isospin are denoted by symbol

$\Delta(\alpha)$. Since there is no residual interaction between particles having different spin or isospin, the occupation matrix can be written as

$$n_{\alpha\beta} = n_{\alpha\beta}\delta_{\Delta(\alpha)\Delta(\beta)}. \tag{B.4}$$

The interaction matrices have properties:

$$< \alpha\beta|v|\gamma\delta > \;=\; < \alpha\beta|v|\gamma\delta > \delta_{\Delta(\alpha)\Delta(\gamma)}\delta_{\Delta(\beta)\Delta(\delta)}; \tag{B.5}$$

$$\begin{aligned} < \alpha\beta|v|\gamma\delta >_A \;&=\; < \alpha\beta|v|\gamma\delta > \\ &\quad (\delta_{\Delta(\alpha)\Delta(\gamma)}\delta_{\Delta(\beta)\Delta(\delta)} - \delta_{\Delta(\alpha)\Delta(\delta)}\delta_{\Delta(\beta)\Delta(\gamma)}). \end{aligned} \tag{B.6}$$

For a set of orbital quantum number $(\alpha, \beta, \gamma, \delta)$ there may exit up to 4^4 correlation matrix elements due to the different spin-isospin assignment. The following are two of the correlation matrix elements having the same orbital quantum number but different spin and isospin (notice the different superscript they bear)

$$\begin{aligned} &C^I_{\alpha\beta\gamma\beta}, \quad \Delta(\alpha) = \Delta(\beta) = \Delta(\gamma) = \Delta(\delta); \\ &C^{II}_{\alpha\beta\gamma\delta}, \quad \Delta(\alpha) = \Delta(\gamma) \neq \Delta(\beta) = \Delta(\delta). \end{aligned} \tag{B.7}$$

Now we can write down the equation of motion for the above two elements without any spin-isospin content.

$$\begin{aligned} i\hbar\dot{C}^I_{\alpha\beta\gamma\delta} \;&=\; \sum_{\nu\tau}(< \alpha\beta|v|\nu\tau > C^I_{\nu\tau\gamma\delta} - C^I_{\alpha\beta\nu\tau} < \nu\tau|v|\gamma\delta >) \\ &\quad + {F^I}^*_{\gamma\delta\alpha\beta} - F^I_{\alpha\beta\gamma\delta} + {F^I}^*_{\delta\gamma\beta\alpha} - F^I_{\beta\alpha\delta\gamma}, \end{aligned} \tag{B.8}$$

$$\begin{aligned} F^I_{\alpha\beta\gamma\delta} \;&=\; \sum_{\lambda\mu\tau} < \lambda\mu|v|\gamma\tau > \{n_{\alpha\lambda}(C^I_{\beta\tau\delta\mu} + 3C^{II}_{\beta\tau\delta\mu}) \\ &\quad - n_{\beta\lambda}(C^I_{\alpha\tau\delta\mu} + 3C^{II}_{\alpha\tau\delta\mu}) \\ &\quad - n_{\alpha\mu}C^I_{\beta\tau\delta\lambda} - n_{\beta\mu}C^I_{\alpha\tau\lambda\delta} - n_{\tau\delta}C^I_{\alpha\beta\lambda\mu}\}; \end{aligned} \tag{B.9}$$

$$\begin{aligned} i\hbar\dot{C}^{II}_{\alpha\beta\gamma\delta} \;&=\; B_{\alpha\beta\gamma\delta} + \sum_{\nu\tau}(< \alpha\beta|v|\nu\tau > C^{II}_{\nu\tau\gamma\delta} - C^{II}_{\alpha\beta\nu\tau} < \nu\tau|v|\gamma\delta >) \\ &\quad + {F^{II}}^*_{\gamma\delta\alpha\beta} - F^{II}_{\alpha\beta\gamma\delta} + {F^{II}}^*_{\delta\gamma\beta\alpha} - F^{II}_{\beta\alpha\delta\gamma}, \end{aligned} \tag{B.10}$$

$$B_{\alpha\beta\gamma\delta} \;=\; \sum_{\lambda\mu\nu\tau} < \lambda\mu|v|\nu\tau > \{(\delta_{\alpha\lambda} - n_{\alpha\lambda})(\delta_{\beta\mu} - n_{\beta\mu})n_{\nu\gamma}n_{\tau\delta}$$

$$-n_{\alpha\lambda}n_{\beta\mu}(\delta_{\nu\gamma}-n_{\nu\gamma})(\delta_{\tau\delta}-n_{\tau\delta})\}, \tag{B.11}$$

$$F^{II}_{\alpha\beta\gamma\delta} = \sum_{\lambda\mu\tau} < \lambda\mu|v|\gamma\tau > \{n_{\alpha\lambda}(C^{I}_{\beta\tau\delta\mu}+3C^{II}_{\beta\tau\delta\mu})$$

$$-n_{\alpha\mu}C^{II}_{\beta\tau\delta\lambda}-n_{\beta\mu}C^{II}_{\alpha\tau\lambda\delta}-n_{\tau\delta}C^{II}_{\alpha\beta\lambda\mu}\}. \tag{B.12}$$

Now define a new quantity, (use the old symbol)

$$C_{\alpha\beta\gamma\delta} = C^{I}_{\alpha\beta\gamma\delta}+3C^{II}_{\alpha\beta\gamma\delta}. \tag{B.13}$$

For a spin-isospin saturation system, we can write down the equation of motion in term of the spin-isospin free quantities $n_{\alpha\beta}$ and $C_{\alpha\beta\gamma\delta}$ defined above.

$$i\hbar\dot{C}_{\alpha\beta\gamma\delta} = 3B_{\alpha\beta\gamma\delta}+\sum_{\nu\tau}(< \alpha\beta|v|\nu\tau > C_{\nu\tau\gamma\delta}-C_{\alpha\beta\nu\tau} < \nu\tau|v|\gamma\delta >)$$
$$+F^{*}_{\gamma\delta\alpha\beta}-F_{\alpha\beta\gamma\delta}+F^{*}_{\delta\gamma\beta\alpha}-F_{\beta\alpha\delta\gamma}, \tag{B.14}$$

$$F_{\alpha\beta\gamma\delta} = \sum_{\lambda\mu\tau} < \lambda\mu|v|\gamma\tau >$$
$$(3n_{\alpha\lambda}C_{\beta\tau\delta\mu}-n_{\beta\lambda}C_{\alpha\tau\delta\mu}-n_{\beta\mu}C_{\alpha\tau\lambda\delta}-n_{\tau\delta}C_{\alpha\beta\lambda\mu}). \tag{B.15}$$

$$i\hbar\dot{n}_{\alpha\beta} = \sum_{\gamma\delta\sigma}\{C_{\gamma\delta\beta\sigma} < \alpha\sigma|v|\gamma\delta > -C_{\alpha\sigma\gamma\delta} < \gamma\delta|v|\beta\sigma >\}. \tag{B.16}$$

The other quantities, such as correlation energy and mass dispersion, of this spin-isospin saturation system have the form

$$E_{\rm corr} = \frac{1}{2}\sum_{\alpha\beta\gamma\delta} 4C_{\alpha\beta\gamma\delta} < \gamma\delta|v|\alpha\beta >, \tag{B.17}$$

$$\sigma^2_R = 4\sum_{\alpha\beta} n_{\alpha\beta} < \beta|\alpha >_R$$
$$+4\sum_{\alpha\beta\alpha'\beta'} < \alpha'|\alpha >_R < \beta'|\beta >_R (C_{\alpha\beta\alpha'\beta'}-n_{\alpha\beta'}n_{\beta\alpha'}). \tag{B.18}$$

The above equations are the basic equations we used in the numerical calculation.

B.2 Spherical symmetry system

For the ground state or monopole giant resonance of double-shell nuclei, we always have a spherical system. In such system the wave function can be separated into

its radial function part and a spherical harmonic. Therefore, only the radial wave function need to be solved numerically and the numerical task is greatly reduced. The numerical effort of solving the equation of motion for the occupation and correlation matrix can also be reduced by eliminating the summation over the magnetic quantum numbers. In this section we will start from the formulae of spin-isospin saturation system derived in last section. Before we make any derivation we list some useful equations:

$$\frac{4\pi}{2l+1}\sum_m Y^*_{lm}(\hat{r})Y_{lm}(\hat{r}) = 1, \tag{B.19}$$

$$\begin{aligned} Y_{l_1m_1}(\hat{r})Y_{l_2m_2}(\hat{r}) &= \sum_{lm}\left[\frac{(2l_1+1)(2l_2+1)(2l+1)}{4\pi}\right]^{\frac{1}{2}} \\ &\quad \begin{pmatrix} l_1 & l_2 & l \\ m_1 & m_2 & m \end{pmatrix}\begin{pmatrix} l_1 & l_2 & l \\ 0 & 0 & 0 \end{pmatrix} Y_{lm}(\hat{r}), \end{aligned} \tag{B.20}$$

$$\begin{aligned} \int d\Omega Y_{l_1m_1}Y_{l_2m_2}Y^*_{l_3m_3}Y^*_{l_4m_4} &= \frac{[(2l_1+1)(2l_2+1)(2l_3+1)(2l_4+1)]^{1/2}}{4\pi} \\ &\quad \sum_{lm}(2l+1)\begin{pmatrix} l_1 & l_2 & l \\ 0 & 0 & 0 \end{pmatrix}\begin{pmatrix} l_3 & l_4 & l \\ 0 & 0 & 0 \end{pmatrix} \\ &\quad \begin{pmatrix} l_1 & l_2 & l \\ m_1 & m_2 & m \end{pmatrix}\begin{pmatrix} l_3 & l_4 & l \\ m_3 & m_4 & m \end{pmatrix}, \end{aligned} \tag{B.21}$$

$$\begin{aligned} &\sum_{m_3}\begin{pmatrix} j_1 & j_2 & j_3 \\ m_1 & m_2 & m_3 \end{pmatrix}\begin{pmatrix} l_1 & l_2 & j_3 \\ n_1 & n_2 & -m_3 \end{pmatrix} \\ &\quad = \sum_{l_3n_3}(-)^{j_3+l_3+m_1+n_1}(2l_3+1)\begin{Bmatrix} j_1 & j_2 & j_3 \\ l_1 & l_2 & l_3 \end{Bmatrix} \\ &\quad \begin{pmatrix} l_1 & j_2 & l_3 \\ n_1 & m_2 & n_3 \end{pmatrix}\begin{pmatrix} j_1 & l_2 & l_3 \\ m_1 & n_2 & -n_3 \end{pmatrix}, \end{aligned} \tag{B.22}$$

In order to have a spherical symmetric density distribution, the occupation matrix must have the following form

$$n_{\alpha\beta} = n_{l(\alpha)l(\beta)}\delta_{l(\alpha)l(\beta)}\delta_{m(\alpha)m(\beta)}. \tag{B.23}$$

With Eq. B.23 and identity Eq. B.19 the one-body density can be written as

$$\rho(r) = \frac{1}{4\pi r^2}\sum_{\alpha\beta}(2l+1)n_{l(\alpha)l(\beta)}\delta_{l(\alpha)l(\beta)}|R_{l(\alpha)}(r)|^2, \tag{B.24}$$

where the time dependence is implicit. Using Eq. B.21 the matrix element $<\alpha\beta|v|\gamma\delta>$ has the form

$$\begin{aligned} <\alpha\beta|v|\gamma\delta> &= <l(\alpha)l(\beta)|v|l(\gamma)l(\delta)> \\ &\sum_{lm}(2l+1)\begin{pmatrix} l(\alpha) & l(\beta) & l \\ 0 & 0 & 0 \end{pmatrix}\begin{pmatrix} l(\gamma) & l(\delta) & l \\ 0 & 0 & 0 \end{pmatrix} \\ &\begin{pmatrix} l(\alpha) & l(\beta) & l \\ m(\alpha) & m(\beta) & m \end{pmatrix}\begin{pmatrix} l(\gamma) & l(\delta) & l \\ m(\gamma) & m(\delta) & m \end{pmatrix}, \end{aligned} \tag{B.25}$$

$$\begin{aligned} <l(\alpha)l(\beta)|v|l(\gamma)l(\delta)> &= \frac{[(2l(\alpha)+1)(2l(\beta)+1)(2l(\gamma)+1)(2l(\delta)+1)]^{1/2}}{4\pi} \\ &v_0\int\frac{dr}{r^2}R^*_{l(\alpha)}R^*_{l(\beta)}R_{l(\gamma)}R_{l(\delta)}, \end{aligned} \tag{B.26}$$

To get rid of the magnetic quantum numbers we define a m-free two-body correlation matrix

$$C^l_{\alpha\beta\gamma\delta} = \sum_{m's} C_{\alpha\beta\gamma\delta}\begin{pmatrix} l(\alpha) & l(\beta) & l \\ m(\alpha) & m(\beta) & m \end{pmatrix}\begin{pmatrix} l(\gamma) & l(\delta) & l \\ m(\gamma) & m(\delta) & m \end{pmatrix}. \tag{B.27}$$

In the following all the indices no longer contain magnetic quantum number but the angular momentum and the radius quantum number (i.e. the nodes of the radial wave function). It is implicit that $n_{l(\alpha)l(\beta)} \neq 0$ only when $l(\alpha) = l(\beta)$. Now we again use the old expression, i.e. $n_{\alpha\beta}$.

$$i\hbar\dot{C}^l_{\alpha\beta\gamma\delta} =$$

$$3B^{l}_{\alpha\beta\gamma\delta}\begin{pmatrix} l(\alpha) & l(\beta) & l \\ 0 & 0 & 0 \end{pmatrix}\begin{pmatrix} l(\gamma) & l(\delta) & l \\ 0 & 0 & 0 \end{pmatrix}$$

$$+\sum_{\nu\tau}\Big[< l(\alpha)l(\beta)|v|l(\nu)l(\tau) > C^{l}_{\nu\tau\gamma\delta}\begin{pmatrix} l(\alpha) & l(\beta) & l \\ 0 & 0 & 0 \end{pmatrix}\begin{pmatrix} l(\nu) & l(\tau) & l \\ 0 & 0 & 0 \end{pmatrix}$$

$$- < l(\nu)l(\tau)|v|l(\gamma)l(\delta) > C^{l}_{\alpha\beta\nu\tau}\begin{pmatrix} l(\nu) & l(\tau) & l \\ 0 & 0 & 0 \end{pmatrix}\begin{pmatrix} l(\gamma) & l(\delta) & l \\ 0 & 0 & 0 \end{pmatrix}\Big]$$

$$+F^{l^*}{}_{\gamma\delta\alpha\beta} - F^{l}_{\alpha\beta\gamma\delta} + \left(F^{l^*}{}_{\delta\gamma\beta\alpha} - F^{l}_{\beta\alpha\delta\gamma}\right)(-)^{l(\alpha)+l(\beta)+l(\gamma)+l(\delta)}, \tag{B.28}$$

$$B^{l}_{\alpha\beta\gamma\delta} = \sum_{\lambda\mu\nu\tau} < l(\lambda)l(\mu)|v|l(\nu)l(\tau) >$$

$$\{(\delta_{\alpha\lambda} - n_{\alpha\lambda})(\delta_{\beta\mu} - n_{\beta\mu})n_{\nu\gamma}n_{\tau\delta} - n_{\alpha\lambda}n_{\beta\mu}(\delta_{\nu\gamma} - n_{\nu\gamma})(\delta_{\tau\delta} - n_{\tau\delta})\}, \tag{B.29}$$

$$F^{l}_{\alpha\beta\gamma\delta} = \sum_{\nu\tau l' l''}(2l'+1)(2l''+1)(-)^{l'+l(\beta)}$$

$$\Big[3\left(\sum_{\lambda} n_{\alpha\lambda} < l(\lambda)l(\nu)|v|l(\gamma)l(\tau) >\right) C^{l''}_{\beta\tau\delta\nu}(-)^{l+l''+l(\delta)}\begin{Bmatrix} l(\alpha) & l(\beta) & l \\ l(\delta) & l(\gamma) & l' \end{Bmatrix}$$

$$\begin{Bmatrix} l(\beta) & l(\delta) & l' \\ l(\nu) & l(\tau) & l'' \end{Bmatrix}\begin{pmatrix} l(\alpha) & l(\gamma) & l' \\ 0 & 0 & 0 \end{pmatrix}\begin{pmatrix} l(\nu) & l(\tau) & l' \\ 0 & 0 & 0 \end{pmatrix}$$

$$-\left(\sum_{\lambda} n_{\beta\lambda} < l(\lambda)l(\nu)|v|l(\gamma)l(\tau) >\right) C^{l''}_{\alpha\tau\delta\nu}(-)^{l''+l(\delta)}\begin{Bmatrix} l(\beta) & l(\alpha) & l \\ l(\delta) & l(\gamma) & l' \end{Bmatrix}$$

$$\begin{Bmatrix} l(\alpha) & l(\delta) & l' \\ l(\nu) & l(\tau) & l'' \end{Bmatrix}\begin{pmatrix} l(\beta) & l(\gamma) & l' \\ 0 & 0 & 0 \end{pmatrix}\begin{pmatrix} l(\nu) & l(\tau) & l' \\ 0 & 0 & 0 \end{pmatrix}$$

$$-\left(\sum_{\lambda} n_{\beta\lambda} < l(\nu)l(\lambda)|v|l(\gamma)l(\tau) >\right) C^{l''}_{\alpha\tau\nu\delta}(-)^{l(\nu)}\begin{Bmatrix} l(\alpha) & l(\beta) & l \\ l(\gamma) & l(\delta) & l' \end{Bmatrix}$$

$$\begin{Bmatrix} l(\nu) & l(\tau) & l' \\ l(\alpha) & l(\delta) & l'' \end{Bmatrix}\begin{pmatrix} l(\beta) & l(\gamma) & l' \\ 0 & 0 & 0 \end{pmatrix}\begin{pmatrix} l(\nu) & l(\tau) & l' \\ 0 & 0 & 0 \end{pmatrix}\Big]$$

$$-\sum_{\nu\tau\lambda} n_{\lambda\delta} < l(\nu)l(\tau)|v|l(\gamma)l(\lambda) > C^{l}_{\alpha\beta\nu\tau}$$

$$\begin{pmatrix} l(\nu) & l(\tau) & l \\ 0 & 0 & 0 \end{pmatrix}\begin{pmatrix} l(\gamma) & l(\delta) & l \\ 0 & 0 & 0 \end{pmatrix}. \tag{B.30}$$

The time derivative of occupation matrix is

$$
\begin{aligned}
i\hbar\dot{n}_{\alpha\beta} &= \frac{1}{2l(\alpha)+1}\sum_{\gamma\delta\sigma}\Big[< l(\alpha)l(\sigma)|v|l(\gamma)l(\delta) > \\
&\sum_{l}(2l+1)\begin{pmatrix} l(\alpha) & l(\sigma) & l \\ 0 & 0 & 0 \end{pmatrix}\begin{pmatrix} l(\gamma) & l(\delta) & l \\ 0 & 0 & 0 \end{pmatrix} C^{l}_{\gamma\delta\beta\sigma} \\
&- < l(\gamma)l(\delta)|v|l(\beta)l(\sigma) > \sum_{l}(2l+1) \\
&\begin{pmatrix} l(\gamma) & l(\delta) & l \\ 0 & 0 & 0 \end{pmatrix}\begin{pmatrix} l(\alpha) & l(\sigma) & l \\ 0 & 0 & 0 \end{pmatrix} C^{l}_{\alpha\sigma\gamma\delta}\Big].
\end{aligned}
\tag{B.31}
$$

The correlation energy

$$
\begin{aligned}
E_{\text{corr}} &= \frac{1}{2}\sum_{\alpha\beta\gamma\delta} < l(\gamma)l(\delta)|v|l(\alpha)l(\beta) > \\
&\sum_{l}(2l+1)\begin{pmatrix} l(\gamma) & l(\delta) & l \\ 0 & 0 & 0 \end{pmatrix}\begin{pmatrix} l(\alpha) & l(\beta) & l \\ 0 & 0 & 0 \end{pmatrix} C^{l}_{\alpha\beta\gamma\delta}.
\end{aligned}
\tag{B.32}
$$

Bibliography

Bibliography

[Alh 81] Y. Alhassid and S. E. Koonin, Phys. Rev. C**23**, 1590(1981).

[Ayi 80] S. Ayik, Z. Phys. A**298**, 83(1980).

[Ayi 85] S. Ayik and M. Dworzecka, Phys. Rev. Lett. **54**, 534(1985).

[Bal 81] R. Balian and M. Véneroni, Phys. Rev. Lett.,**47**,1353(1981).

[Ber 75] G. Bertsch and S. Tsai, Phys. Rep. C**18**, 125(1975).

[Ber 83] G. F. Bertsch, Supplement of the Progress of Theoretical Physics, Nos. **74&75**, 1983.

[Ber 83a] G. F. Bertsch, P.F. Bortignon, and R. A. Broglia, Rev. Mod. Phys. **55**, 287(1983).

[Ber 84] G. F. Bertsch, H. Kruse, and S. das Gupta, Phys. Rev. C**29**, 675(1984).

[Ber 88] G. F. Bertsch and S. Das Gupta, Phys. Rep. **160**, 190(1988).

[Blo 79] J. Blocki and H. Flocard, Phys. Lett. 85B, 163(1979).

[Bog 68] N. N. Bogoliubov, *Lectures on Quantum Statistics* **Vol 1** (MacDonald Technical and Scientific, London 1968).

[Boh 53] D. Bohm and D. Pines, Phys. Rev. **92**, 609(1953).

[Bon 76] P. Bonche, S. E. Koonin, and J. W. Negele, Phys. Rev. C**13**, 1226(1976).

[Bon 85] P. Bonche and H. Flocard, Nucl. Phys. **A437**, 189(1985).

[Buc 83] P. Buck, H. Feldmeier, Phys. Lett. **129**B, 172(1983).

[Cas 87] W. Cassing and S. J. Wang, Z. Phys. **A**328, 423(1987).

[Cas 87a] W. Cassing, Z. Phys. **A**327, 447(1987).

[Cho 87] Ph. Chomaz, Nguyen Van Giai and S. Stringari, Phys. Lett. **189**B, 375(1987).

[Dap 65] J. Da Providencia, Nucl. Phys. **61**, 87(1965).

[Das 79] C. H. Dasso, T. Dossing and H. C. Pauli, Z. Phys. A289, 395(1979).

[Dav 78] K. T. R. Davies, H. T. Feldmeier, H. Flocard and M. S. Weiss, Phys. Rev. C**18**, 2631(1978).

[Dav 80] K. T. R. Davies, H. Flocard, S. Krieger and M. S. Weiss, Nucl. Phys. **A**342, 111(1980).

[Dav 81] K. T. R. Davies and S. E. Koonin, Phys. Rev. C**32**, 2042(1981).

[Dav 85] K. T. R. Davies, K. R. S. Devi, S. E. Koonin and M. R. Strayer, *Treaties on Heavy Ion Science*, Vol **3** (Plenum, New York, 1985).

[Dro 86] S. Drozdz, V. Klemt, J. Speth and J. Wambach, Nucl. Phys. **A451**, 11(1986).

[Eng 75] Y. M. Engel, D. M. Brink, K. Goeke, S. J. Krieger and D. Vautherin, Nucl. Phys. **A**249, 215(1975).

[Fel 82] H. Feldmeire and P. Buck, in Lecture notes in physics, vol. 171 (Springer, Berlin 1982) p. 384

[Foc 30] V. Fock, Z. Phys. **61**, 126(1930).

[Goe 82] See, for example, the references cited in Time-Dependent Hartree-Fock and Beyond, Vol. **171** of Lecture Notes on Physics, edited by K. Goeke and P. G. Reinhard (Springer,Berlin,1982).

[Gon 88] M. Gong and M. Tohyama, to be published in Z. Phys.

[Gon 89] M. Gong, M. Tohyama and J. Randrup, submitted to Z. Phys.

[Gra 81] P. Grangé, H. A. Weidenmüller, G, Wolschin, Ann. Phys. **136**, 190(1981).

[Gri 80] J. J. Griffin, P. C. Lichtmer and M. Dworzecka, Phys. Rev. C**21**, 1351(1980).

[Har 27] D. Hartree, Proc. Camb. Phil. Soc. **24**, 89 and 111(1927).

[Hos 76] T. Hoshino, A. Arima, Phys. Rev. Lett. 37, 266(1976).

[Hos 88] T. Hoshino, H. Sagawa and A. Arima, Nucl.Phys. A**481**, 458(1988).

[Ike 86] H. Ikezoe, N. Shikazono, Y. Tomita, K. Ideno, Y. Sugiyama, E. Takekoshi, T. Tachikawa and T. Nomura, Nucl. Phys. **A456**, 298(1986).

[Jor 87] F. H. Jørgensen, T. Døssing, B. S. Nilsson and J. Randrup, Phys. lett. **191B**, 323(1987).

[Kad 62] L. P. Kadanoff and G. Baym, *Quantum Statistical Mechanics* (New York 1962).

[Kle 80] H. Kleinert and H. Reinhardt, Nucl Phys. **A332**, 331(1980).

[Kno 75] K. T. Knopfle et al. Phys. Rev. Lett. **35**, 779 (1975).

[Knu 76] W. Knüpfer and M. G. Huber, Phys. Rev. C**14**, 2254(1976).
Z. Phys. A**276**, 99(1976).

[Kox 80] S. Kox, A. J. Cole and R. Ost, Phys. Rev. Lett. **44**, 1204(1980).

[Kre 74] S. Krewald, J. Birkholz, A. Faessler and J. Speth, Phys. Rev. Lett.**33**, 1386(1974).

[Kre 77] S. Krewald, V. Klemt, J. Speth and A. Faessler, Nucl. Phys. **A**281, 166(1977).

[Laz 81] A. Lazzarini, H. Doubre, K. T. Lesko, V. Metag, A. Seamster, R. Vandenbosch and W. Merryfield, Phys. Rev. C**24**, 309(1981).

[Mar 85] J. B. Marston and S. E. Koonin, Phys. Rev. Lett. **54**, 1139(1985).

[Mos 75] J. M. Moss et al. Phys. Rev. Lett. **34**, 748 (1975).

[Neg 82] J. W. Negele, Rev. Mod. Phys. **54**, 913(1982).

[Nem 86] M. C. Nemes, A. F. R. De Toledo Piza, Phys. Lett. **172**B, 119(1986).

[Nor 74] W. Nörenberg, Phys. Lett. **53**B, 289(1974).

[Orl 79] H. Orland and R. Schaeffer, Z.Phys. A **290**, 191(1979).

[Pap 89] C. N. Papanicolas and V. Pandharipande, Physics Today, Jan. 1989, Page S-56.

[Ran 78] J. Randrup, Nucl. Phys. **A307** 319(1978).

[Ran 79] J. Randrup, Nucl. Phys. **A327** 490(1979).

[Ran 82] J. Randrup, Nucl. Phys. **A383** 468(1982).

[Rei 84] H. Reinhardt, R. Balian and Y. Alhassid, Nucl. Phys. A**422**, 349(1984).

[Rei 86] P.-G. Reinhard, M. Rufa, J. Maruhn, W. Greiner and J. Friedrich, Z. Phys. A323, 13(1986).

[Rin 80] P. Ring and P. Shuck, *The nuclear many-body problem*, (Springer-Verlag, 1980).

[Saw 62] J. Sawicki, Phys. Rev. **126**, 2231(1962).

[Sch 77] W. U. Schröder and J. R. Huizenga, Ann. Rev. Nucl. Sci. **27**, 465(1977).

[Sch 84] See for example, Wolfgang U. Schroder and John R. Huizenga, *Treaties on Heavy Ion Science*, Vol **2**(Plenum, New York, 1984).

[Spe 81] J. Speth and Adriaan van der Woude, Rep. Prog. Phys. Vol. **44**, 1981.

[Str 79] S. Stringari and D. Vautherin, Phys. Lett. 88**B**, 1(1979).

[Thi 86] M. Thies, Phys. Lett. 166B, 23(1986).

[Toh 85] M. Tohyama, Nucl. Phys. A**437**, 443(1985).

[Toh 87] M. Tohyama, Phys. Rev. C**36**, 187(1987).

[Toh 88] M. Tohyama, Phys. Rev. C**38**, 553(1988).

[Toh 89] M. Tohyama and M. Gong, Z. Phys. A**332**, 269(1989).

[Tol 81] A. Szanto de Toledo, T. M. Cormier, M. Herman, B. Lin, P. M. Stwertka, M. M. Coimdra and N. Carlin Filho, Phys. Rev. Lett. **47**, 1881(1981).

[Uma 86] A. S. Umar, M. R. Strayer and P. G. Reinhard, Phys. Rev. Lett. **56**, 2793(1986).

[Uma 86a] A. S. Umar and M. R. Strayer, Phys. Lett. B**171**, 353(1986).

[Vau 72] D. Vautherin and D. M. Brink, Phys. Rev. C**5**, 626(1972).

[Wan 85] S. J. Wang and W. Cassing, Ann. Phys. **159**, 328(1985).

[Won 78] C. Y. Wong and H. H. K. Tang, Phys. Rev. Lett. **40**, 1070 (1978).

[Won 79] C. Y. Wong and H. H. K. Tang, Phys. Rev. C**20**, 1419 (1979).

[Won 80] C. Y. Wong and K. T. R. Davies, Phys. Lett. **96B**, 258(1980).

[Won 83] C. Y. Wong and K. T. R. Davies, Phys. Rev. C**28**, 240(1983).

[Yam 84] M. Tohyama and S. Yamaji, Phys. Lett. **123**B, 16(1983);
S. Yamaji and M. Tohyama, Phys. Lett. **147**B, 339(1984).

[Yan 83] C. Yannouleas, M. Dworzecka and J. J. Griffin, Nucl. Phys. A**397**, 239(1983).